


**A STUDY OF THE EARLY CHANGES IN HEARTS FROM  
DIET-INDUCED OBESE RATS THAT MAY LEAD TO  
CARDIAC DYSFUNCTION**

**NICOLE JOY BEZUIDENHOUT**

**THESIS PRESENTED IN COMPLETE FULFILMENT OF THE  
REQUIREMENTS FOR THE DEGREE OF MASTER OF  
SCIENCE (MEDICAL PHYSIOLOGY) AT  
  
STELLENBOSCH UNIVERSITY**

**PROMOTER: PROF. BARBARA HUISAMEN**

**FACULTY OF HEALTH SCIENCES**

**DEPARTMENT OF BIOMEDICAL SCIENCES**

**MARCH 2011**

## DECLARATION

*By submitting this dissertation electronically, I declare that the entirety of the work contained therein is my own, original work, that I am the sole author thereof (save to the extent explicitly otherwise stated), that reproduction and publication thereof by Stellenbosch University will not infringe any third party rights and that I have not previously in its entirety or in part submitted it for obtaining any qualification.*

**Signature:**

**Date: March 2011**

---

**Copyright © 2011 Stellenbosch University**

**All rights reserved**

## ABSTRACT

**INTRODUCTION:** Obesity and its associated complications such as diabetes and cardiovascular disease are escalating worldwide. Cardiovascular mortality and the occurrence of heart failure following a myocardial infarction are increased among diabetics. A high caloric diet has been associated with specific metabolic alterations such as increased FA utilization and decreased glucose utilization. We therefore hypothesized that, in a rat model of diet-induced obesity, pathways involved in myocardial glucose utilization would be down regulated with simultaneous up regulation of FA utilization pathways and that this will lead to certain metabolic adaptations which will eventually become maladaptive. We **aimed** to elucidate mitochondrial oxidative capacity, biogenesis, and signaling pathways involved in substrate utilization and energy production in rats on the obesity inducing diet for a period of 8 or 16 weeks.

**METHODS:** The diet of male Wistar rats (180-200 g) was supplemented with sucrose and condensed milk for 8 or 16 weeks (DIO) and compared to age-matched controls. We determined the fasting blood glucose and serum insulin levels, which was used to calculate the HOMA index. Furthermore, (i) A set of hearts were removed and freeze-clamped immediately. (ii) Isolated hearts were perfused with Krebs-Henseleit buffer (10 mM glucose), subjected to regional ischaemia by ligating the left anterior descending artery (35 min). After 10 min reperfusion, the infarcted and non-infarcted zones were freeze-clamped separately. Isolated mitochondria prepared from fresh tissue were used to measure oxidative capacity using either glutamate or palmitoyl-L-carnitine as substrates and exposed to anoxia (20 min) /reperfusion and used in  $e^-$  transport chain complex analysis. Additionally we determined (i) ATP production (HPLC), (ii) citrate synthase activity and quantity as measure of active mitochondria per mg of protein and (iii) PDH complex expression and activity (ELISA). Levels of GLUT1, GLUT 4, PGC-1 $\alpha$ , PPAR $\alpha$ , PKB/Akt, GSK-3, PTEN, AMPK and PI3K

activity were measured via Western blotting and Real-time PCR was used to measure the expression of PDK 4 and FAT/CD36.

**RESULTS:** The blood glucose and serum insulin levels were significantly elevated in the diet group after 8 weeks of DIO. The PPAR $\alpha$ , PGC-1 $\alpha$  and PDK 4 levels were also significantly elevated in the diet group with no significant difference in the levels of any of the other proteins measured or the level of citrate synthase activity. After 16 weeks of DIO the citrate synthase, PTEN and p-PI3K activity was significantly reduced and the %recovery after anoxia/reperfusion when using palmitoyl was significantly increased in the diet group. There was no change in mitochondrial oxidative function in both groups after 8 and 16 weeks, as well as no difference in ATP production during state 3 respiration.

**CONCLUSION:** The increased blood glucose and serum insulin levels as well as the increase in the HOMA index in the diet group after 8 weeks of DIO indicates that these obese animals were insulin resistant. An increase in the level of PPAR $\alpha$  and PGC-1 $\alpha$  expression indicates an early compensatory effect which facilitates enhanced fatty acid utilization. This is underscored by elevated levels of PDK 4. We could find no significant difference in the quantity of the PDH enzyme but there was a significant increase in the level of PDH activity in the diet group after 16 weeks of DIO. Mitochondria from the 16 weeks DIO animals were able to withstand anoxia/reperfusion and showed no malfunctioning of the electron transport chain, despite a reduction in PI3K & PTEN activity and the presence of insulin resistance. Mitochondrial biogenesis does not seem to play a significant role in the heart's adaptive response as there was no increase in the citrate synthase activity in both groups. We conclude that the hearts from these obese and insulin resistant rats are coping well and have adapted metabolically to compensate for any reduction in glucose oxidation. It is plausible that this initial metabolic adaptation may become maladaptive as obesity progresses.

## OPSOMMING

**INLEIDING:** Vetsug en die geassosieerde komplikasies, naamlik diabetes en kardiovaskulêre siektes is besig om wêreldwyd toe te neem. Kardiovaskulêre sterftes en die voorkoms van hartversaking ná 'n miokardiale infarksie is verhoog onder diabete. 'n Dieet met 'n hoë vetinname word ook geassosieer met spesifieke metabolise veranderinge, soos verhoogde vetsuur gebruik en 'n afname in glukoseverbruik. Ons het dus vermoed dat seintransduksie paaie betrokke by miokardiale glukose verbruik afgereguleer sal wees met tesame opreguleering van seintransduksie paaie betrokke by vetsuur verbruik, en dat dit sal lei tot sekere metaboliese aanpassings wat uiteindelik wanaanpaslik sal word.

Ons **DOESTELLING** in hierdie studie was dus om meer lig te werp op mitokondriale oksidatiewe kapasiteit, biogenese, en seintransduksie betrokke by substraatverbruik en energieproduksie in rotte op die vetsugveroorsakende-dieet (vir 'n tydperk van 8 tot 16 weke).

**METODE:** Die dieet van die manlike Wistar rotte (180-200 g) is aangevul met sucrose en gekondenseerde melk vir 8 of 16 weke (DIO) en is dan vergelyk met kontrole rotte van dieselfde ouderdom. Die vastende bloedglukose- en insulienvlakke is bepaal en hierdie waardes is gebruik om die HOMA indeks te bereken. Verder is, (i) 'n stel harte verwyder en onmiddelik gevriesklamp (ii) geïsoleerde harte met Krebs-Henseleit buffer (10 mM glukose) geperfuseer en dan aan 35 min streeksiskemie en 10 min herperfusie blottgestel. Na 10 min herperfusie, is die infarct en nie-infarctsones apart gevriesklamp. Geïsoleerde mitokondrieë is voorberei van vars weefsel en is gebruik a) om oksidatiewe kapasiteit te meet met behulp van glutamaat of palmitoïel-L-karnitiese as substrate of b) blootgestel aan 20 min anoksie gevolg deur heroksigenasie of c) is gebruik in elektronvervoerkettingkompleks analise. Verder is die volgende ook bepaal: (i) ATP-produksie (HPLC), (ii) sitraatsintase aktiwiteit en hoeveelheid, gemeet as maatstaf van die aktiewe mitokondrieë per mg van proteïene en (iii) PDH-

komplekuitdrukking en aktiwiteit (ELISA). Vlakke van GLUT 1, GLUT 4, PGC-1 alpha, PPAR alpha, PKB/Akt, GSK-3, PTEN, AMPK, en PI 3 kinase is bepaal deur Western klad analise en “Real –time PCR” is gebruik om die uitdrukking van PDK 4 en FAT/CD 36 te bepaal.

**RESULTATE:** Die bloedglukose- en serum insulinvlakke was beduidend verhoog in die dieetgroep na 8 weke van DIO. Die PPAR alpha, PGC-1 alpha en PDK 4 vlakke was ook beduidend verhoog in die dieetgroep met geen beduidende verskil in die vlakke van enige van die ander proteïene gemeet of die vlakke van sitraat-sintase aktiwiteit nie. Na 16 weke van DIO het die vlakke van sitraat-sintase, PTEN en p-PI 3 kinase beduidend verlaag en die % herstel na anoksie/heroksigenering (met die gebruik van palmitoïel-L-karnitien) het beduidend toegeneem in die dieetgroep. Geen ander mitokondriale veranderinge kon waargeneem word nie. Ons kon geen verandering vind in die mitokondriale oksidatiewe funksie tussen die twee groepe na 8 en 16 weke van DIO. Daar was ook geen verandering in die hoeveelheid ATP geproduseer gedurende staat 3 respirasie.

**GEVOLGTREKKING:** Die verhoogde bloedglukose en serum insulienvlakke, sowel as die toename in die HOMA indeks in die dieetgroep na 8 weke van DIO, dui daarop dat hierdie oorgewig diere insulienweerstandig is. ‘n Toename in die vlak van PPAR alpha en PGC-1 alpha uitdrukking dui op ‘n vroeë kompenserende effek, wat die verhoogde verbruik van vetsure fasiliteer. Dit is beklemtoon deur verhoogde vlakke van PDK 4. Ons kon geen beduidende verskil in die hoeveelheid PDH-ensiem vind nie, maar daar was wel ‘n beduidende toename in die vlak van PDH aktiwiteit in die dieetgroep na 16 weke van DIO. Mitokondrieë van die 16 weke DIO diere kon anoksie/heroksigenering weestaan en het geen wanfunksionering van die elektronvervoerketting getoon nie, ten spyte van ‘n vermindering in PI 3 kinase en PTEN aktiwiteit en die teenwoordigheid van insulienweerstandigheid. Mitokondriale biogenese blyk nie ‘n beduidende rol te speel in die hart se aanpassingreaksie nie, want daar was

geen verhoging in die sitraat-sintase aktiwiteit in beide groepe nie. Na aanleiding van die resultate verkry met hierdie studie, maak ons ook die gevolgtrekking dat die harte van rotte na 16 weke se blootstelling aan 'n hoë vet omgewing, metabolies kon aanpas en goed funksioneer. Ons gevolgtrekking is dus dat die harte van diere wat lei aan vetsug en wat insulien weerstandig is die verlaaging in glukose metabolisme goed hanteer en metabolies aangepas het hierby. Dit is moontlik dat hierdie aanvanklike aanpassing wanaanpaslik kan word soos vetsug vorder.

## **ACKNOWLEDGMENTS**

Fistly, I would like to thank Prof Barbara Huisamen for her assistance and guidance throught this study. I would also like to thank, Prof Amanda Lochner, Dr John Lopez and all members of the Department of Medical Physiology for their ideas, suggestions and input into this study.

A special thanks to Rene Veikondis (from the sequencing facility) and Mart-mari Botha for their assistance.

For financial support I would like to thank the Department of Medical Physiology and the National Research Foundation.



<b>Declaration</b>	2
<b>Abstract</b>	3
<b>Opsomming</b>	5
<b>Acknowledgements</b>	8
<b>Table of content</b>	9
<b>List of Illustrations</b>	16
<b>Tables</b>	21
<b>List of abbreviations</b>	23
 <b>CHAPTER 1: LITERATURE REVIEW</b>	 31
 1.1 Obesity, cardiovascular disease: a “global epidemic”	 31
1.2 Insulin resistance	33
1.2.1 Overview of insulin action	33
1.2.2 The role of insulin in glucose homeostasis	34
1.2.3 The insulin signalling pathway	35
1.2.4 The pathophysiology of insulin resistance	36
1.2.4.1 The role of insulin resistance in obesity and cardiovascular disease	36
1.3 Myocardial substrate selection and utilization	38
1.3.1 The role of obesity, insulin resistance and ischaemia in the change of myocardial substrate selection and utilization	40
1.4 Cellular injury and myocardial infarction	40
1.4.1 The development of infarct size	41
1.4.1.1 Apoptosis and Necrosis	41
1.4.1.1.1 Apoptosis in ischaemia/reperfusion	42
1.5 Cardioprotective effects of the activation of PI3 kinase/PKB/Akt pathway during reperfusion	43
1.5.1 PI-3 kinase/PKB/Akt pathway	43

<b>1.5.1.1</b>	Activation of PKB/Akt	45
<b>1.5.1.2</b>	The role of PKB/Akt in the metabolism	46
<b>1.5.1.3</b>	The role of PKB/Akt in the regulation of apoptosis	46
<b>1.5.1.3.1</b>	Transcription factors involved in regulating apoptosis	47
<b>1.5.1.3.2</b>	Cell cycle regulators involved in regulating apoptosis	48
<b>1.6</b>	The regulators of the expression of metabolic genes in cardiomyocytes	48
<b>1.6.1</b>	Peroxisome proliferator-activated receptors	50
<b>1.6.1.1</b>	PPAR isoforms	51
<b>1.6.2</b>	Peroxisome proliferator-activated receptor- $\gamma$ coactivator (PGC)-1 $\alpha$	51
<b>1.6.3</b>	The role of PPAR $\alpha$ and PGC-1 $\alpha$ in cardiomyocytes	51
<b>1.6.3.1</b>	Transcriptional regulation of cardiac mitochondrial biogenesis and respiratory function	52
<b>1.6.3.2</b>	The role of PGC-1 $\alpha$ in the activation of PPAR $\alpha$	53
<b>1.6.3.3</b>	Perturbations in PGC-1/PPAR signalling in the insulin resistant and diabetic heart	54
<b>1.6.3.4</b>	Myocardial fuel shifts and heart failure in the insulin resistant and diabetic heart	55
<b>1.7</b>	Proteins implicated in cardiomyocytes metabolism	57
<b>1.7.1</b>	Glucose metabolism	58
<b>1.7.1.1</b>	Glucose transporters	58
<b>1.7.1.1.1</b>	Glucose transporter 1	58
<b>1.7.1.1.2</b>	Glucose transporter 4	59
<b>1.7.1.2</b>	Pyruvate dehydrogenase complex (PDC)	60
<b>1.7.1.3</b>	Pyruvate dehydrogenase kinase 4 (PDK-4)	62
<b>1.7.1.4</b>	Phosphoinositide-3 kinase (PI3 kinase)	63
<b>1.7.1.5</b>	Phosphatase and tensin homolog on chromosome ten (PTEN)	64
<b>1.7.1.6</b>	Glycogen synthase kinase 3 (GSK-3)	65

<b>1.7.2</b>	Fatty acid metabolism	67
<b>1.7.2.1</b>	Fatty acid translocase/CD36 (FAT/CD36)	68
<b>1.7.2.2</b>	Carnitine palmitoyl transferase-1 (CPT-1)	69
<b>1.7.2.3</b>	5'Adenosine monophosphate – activated protein kinase (AMPK)	69
<b>1.7.2.3.1</b>	AMPK and glucose uptake during ischaemia	70
<b>1.7.2.3.1.1</b>	Control of FA oxidation by malonyl-CoA	71
<b>1.7.2.3.1.1.1</b>	Synthesis of malonyl-CoA	72
<b>1.7.2.3.1.1.2</b>	Degradation of malonyl-CoA	72
<b>1.7.2.3.1.2</b>	The role of AMPK in the regulation of malonyl-CoA levels	73
<b>1.7.2.3.1.3</b>	The role of AMPK during ischaemia/reperfusion	74
<b>1.8</b>	The role of mitochondria in myocardium	77
<b>1.8.1</b>	Mitochondrial ATP production	77
<b>1.8.1.1</b>	Pyruvate decarboxylation	78
<b>1.8.1.2</b>	Citric acid cycle	78
<b>1.8.1.3</b>	Oxidative phosphorylation	79
<b>1.8.1.4</b>	Electron transport chain complexes I-IV	82
<b>1.8.1.4.1</b>	The production of ATP by the electron transport chain	82
<b>1.8.1.4.1.1</b>	Complex I	84
<b>1.8.1.4.1.2</b>	Complex II	84
<b>1.8.1.4.1.3</b>	Complex III	84
<b>1.8.2</b>	Pathophysiology associated with impaired mitochondrial ATP production	85
<b>1.9</b>	Cardioprotection	86
<b>1.9.1</b>	The role of mitochondrial biogenesis in cardioprotection	86
<b>1.10</b>	Adaptive and maladaptive responses of the heart	88
<b>1.10.1</b>	Metabolic adaptation	89
<b>1.10.1.1</b>	Metabolic adaptation in the diabetic heart	90
<b>1.10.2</b>	Metabolic maladaptation	91

1.10.2.1	Lipotoxicity	91
1.10.3	Mitochondrial dysfunction and insulin resistance	92
1.11	Motivation for study	93
1.12	Aims	94
<b>CHAPTER 2: METHODS</b>		95
2.1	Animals	95
2.1.1	Study design	95
2.1.2	Diet	98
2.2	Blood glucose determination	98
2.3	Measurement of serum insulin levels	99
2.3.1	Experimental procedure	99
2.3.2	HOMA index	100
2.4	Pilot study	101
2.4.1	Perfusion protocol	101
2.5	Biochemical analysis	102
2.5.1	Infarcted vs. Non-infarcted zones	102
2.5.2	Preparation of lysates	102
2.5.2.1	The Bradford protein determination method	103
2.5.2.1.1	Bradford procedure	103
2.5.3	Immuno blotting	105
2.5.3.1	Separation of proteins	105
2.6	Preparation and analysis of mitochondrial function	109
2.6.1	Preparation of mitochondria from fresh heart tissue	109
2.6.1.1	Lowry's protein determination method	109
2.6.1.1.1	Sample preparation	109
2.6.1.1.2	Procedure	110
2.6.2	Analysis of mitochondrial function	110
2.6.2.1	Anoxia/Reperfusion of isolated cardiac mitochondria	112

<b>2.6.3</b>	Mitochondrial electron transport chain complex analysis	112
<b>2.6.3.1</b>	Experimental procedure	113
<b>2.6.4</b>	Quantification of mitochondrial ATP production	116
<b>2.6.4.1</b>	Experimental procedure	116
<b>2.6.4.2</b>	High performance liquid chromatography	116
<b>2.6.4.2.1</b>	Principle of experiment	116
<b>2.6.4.2.2</b>	Preparation of samples for HPLC	118
<b>2.6.5</b>	Citrate synthase assay	119
<b>2.6.5.1</b>	Principle of experiment	119
<b>2.6.5.2</b>	Sample preparation	120
<b>2.6.5.3</b>	Experimental procedure	121
<b>2.6.6</b>	Pyruvate dehydrogenase (PDH) Combo (Activity + Quantity) microplate assay	121
<b>2.6.6.1</b>	Principle of MSP 18	122
<b>2.6.6.2</b>	Experimental procedure	122
<b>2.6.6.3</b>	Principle of MSP 19	123
<b>2.6.6.4</b>	Experimental procedure	123
<b>2.7</b>	Quantitative RT-PCR (real time-polymerase chain reaction) analysis	124
<b>2.7.1</b>	mRNA isolation	124
<b>2.7.1.1</b>	Experimental procedure	125
<b>2.7.2</b>	TURBO DNA-free™	125
<b>2.7.2.1</b>	Procedural overview	126
<b>2.7.3</b>	Quantitation of RNA	127
<b>2.7.4</b>	Purity of RNA	127
<b>2.7.5</b>	Integrity of RNA	127
<b>2.7.6</b>	Formaldehyde agarose gel electrophoresis	128
<b>2.7.7</b>	cDNA synthesis	129
<b>2.7.7.1</b>	cDNA reaction preparation	129
<b>2.7.8</b>	Taqman gene expression assays	132

2.7.8.1	About the kit	133
2.7.8.2	Preparing the PCR reaction mix	135
2.7.8.2.1	Analysis of results	137
2.8	Statistical analysis	137
<b>CHAPTER 3: RESULTS</b>		<b>139</b>
3.1	Characteristics of the diet-induced obesity model	139
3.1.1	Body weight	139
3.1.2	Intra-peritoneal fat weight (g)	140
3.1.3	Fasting blood glucose and insulin levels	141
3.1.4	HOMA index	142
3.2	PKB/Akt expression and activation between non-infarcted and infarcted zones compared between DIO and control groups	143
3.3	The expression of the regulators of metabolic genes	146
3.4	The expression of metabolic proteins	148
3.4.1	GLUT 4	148
3.4.2	GLUT 1	149
3.4.3	Glycogen synthase kinase expression	150
3.4.4	PI-3 kinase expression	152
3.4.5	PTEN expression	154
3.4.6	AMPK expression	156
3.5	Mitochondrial function	157
3.5.1	Oxidative phosphorylation potential	157
3.5.2	Anoxia/reperfusion of isolated cardiac mitochondria	161
3.5.3	Quantification of ATP production	162
3.6	Electron transport chain complex analysis	164
3.7	Citrate synthase activity	165
3.8	Pyruvate dehydrogenase enzyme quantity and activity	166
3.9	Expression of protein levels measured by RT-PCR	168

<b>3.9.1</b>	PDK 4 expression	168
<b>3.9.2</b>	FAT/CD36 expression	170
<b>CHAPTER 4: DISCUSSION</b>		<b>172</b>
<b>4.1</b>	Early and progressed metabolic remodelling in response to obesity	173
<b>4.2</b>	The role of mitochondria in the myocardial adaptive response	182
<b>CHAPTER 5: CONCLUSION</b>		<b>186</b>
<b>REFERENCES</b>		<b>187</b>

## LIST OF ILLUSTRATIONS

<b>Figure 1:</b>	An overview of myocardial metabolism	39
<b>Figure 2:</b>	A schematic representation of the role of the PI-3 kinase/PKB/Akt pathway in cell survival	44
<b>Figure 3:</b>	Schematic representation of PKB/Akt activation	45
<b>Figure 4:</b>	PPAR alpha and PGC-1 alpha	50
<b>Figure 5:</b>	Dynamic regulation of myocardial energy metabolism by developmental, dietary, and pathophysiological changes	56
<b>Figure 6:</b>	Overview of the major energy producing pathways – Glucose oxidation and Fatty acid oxidation	57
<b>Figure 7:</b>	Insulin-stimulated translocation of GLUT 4-containing vesicles to the plasma membrane to facilitate the transport of glucose into the cell	60
<b>Figure 8:</b>	Regulation of the PDH complex	61
<b>Figure 9:</b>	An overview of the role of key proteins such as PPAR alpha, PDK 4 and PDC in obesity (i.e. in response to increased plasma free FAs)	63
<b>Figure 10:</b>	Schematic representation of the negative regulation of PI-3 kinase through the dephosphorylation of PIP3 to PIP2 by PTEN	65
<b>Figure 11:</b>	The regulation of GSK-3 by the insulin signal-transduction pathway	66
<b>Figure 12:</b>	An overview of the key role players involved in FA oxidation	67
<b>Figure 13:</b>	AMPK as a cellular energy sensor that controls metabolic pathways	70
<b>Figure 14:</b>	Schematic representation of the inhibition of CPT-1 by malonyl-CoA	72
<b>Figure 15:</b>	AMPK activation and subsequent phosphorylation of ACC and possible MCD leads to an alteration in the levels of malonyl-CoA and subsequently increases FA oxidation	74



<b>Figure 16:</b>	Activation of AMPK in response to ischaemia	76
<b>Figure 17:</b>	Schematic representation of the conversion of pyruvate to acetyl-CoA by the pyruvate dehydrogenase complex enzyme	78
<b>Figure 18:</b>	Schematic representation of the citric acid cycle	79
<b>Figure 19:</b>	Overview of mitochondrial oxidative phosphorylation	81
<b>Figure 20:</b>	Overview of the electron transport chain	82
<b>Figure 21:</b>	Metabolic adaptation and maladaptation of the heart	88
<b>Figure 22:</b>	(A) and (B) Study design for the respective groups after 8 and 16 weeks of diet	97
<b>Figure 23:</b>	Retrograde perfusion protocol	101
<b>Figure 24:</b>	Typical respiration graph generated by an oxygraph	111
<b>Figure 25:</b>	Citric acid cycle	119
<b>Figure 26:</b>	Polymerization reaction	134
<b>Figure 27:</b>	Strand displacement	134
<b>Figure 28:</b>	Cleavage	134
<b>Figure 29:</b>	Completion of polymerization	134
<b>Figure 30:</b>	Whisker-box plot	138
<b>Figure 31:</b>	Mean weight (g) after 8 weeks of DIO	139
<b>Figure 32:</b>	Mean weight (g) after 16 weeks of DIO	139
<b>Figure 33:</b>	Mean intra-peritoneal fat weight (g) after 8 weeks of DIO	140
<b>Figure 34:</b>	Mean intra-peritoneal fat weight (g) after 16 weeks of DIO	140
<b>Figure 35:</b>	Fasting blood glucose levels after 8 weeks of DIO	141
<b>Figure 36:</b>	Insulin levels after 8 weeks of DIO	141
<b>Figure 37:</b>	HOMA index	142
<b>Figure 38:</b>	Phosphorylated PKB/Akt levels in the infarcted and non-infarcted zones in both the diet and control group after 8 weeks of DIO	143
<b>Figure 39:</b>	Total PKB/Akt expression in the infarcted and non-infarcted zones in both the diet and control group after 8 weeks of DIO	144

<b>Figure 40:</b>	Phospho/Total ratios for PKB/Akt	145
<b>Figure 41:</b>	PPAR alpha expression in control and diet group after 8 weeks of DIO	146
<b>Figure 42:</b>	PPAR alpha expression in control and diet group after 16 weeks of DIO	146
<b>Figure 43:</b>	PGC-1 alpha expression in control and diet group after 8 weeks of DIO	147
<b>Figure 44:</b>	PGC-1 alpha expression in control and diet group after 16 weeks of DIO	147
<b>Figure 45:</b>	GLUT 4 expression in control and diet group after 8 weeks of DIO	148
<b>Figure 46:</b>	GLUT 4 expression in control and diet group after 16 weeks of DIO	148
<b>Figure 47:</b>	GLUT 1 expression in control and diet group after 8 weeks of DIO	149
<b>Figure 48:</b>	GLUT 1 expression in control and diet group after 16 weeks of DIO	149
<b>Figure 49:</b>	Phosphorylated GSK-3 in control and diet group after 8 weeks of DIO	150
<b>Figure 50:</b>	Phosphorylated GSK-3 in control and diet group after 16 weeks of DIO	150
<b>Figure 51:</b>	Total GSK-3 expression in control and diet group after 8 weeks of DIO	151
<b>Figure 52:</b>	Total GSK-3 expression in control and diet group after 16 weeks of DIO	151
<b>Figure 53:</b>	Phosphorylated PI-3 kinase in control and diet group after 8 weeks of DIO	152
<b>Figure 54:</b>	Phosphorylated PI-3 kinase in control and diet group after 16 weeks of DIO	152
<b>Figure 55:</b>	Total PI-3 kinase expression in control and diet group after 8 weeks of DIO	153

<b>Figure 56:</b>	Total PI-3 kinase expression in control and diet group after 16 weeks of DIO	153
<b>Figure 57:</b>	Phosphorylated PTEN in control and diet group after 8 weeks of DIO	154
<b>Figure 58:</b>	Phosphorylated PTEN in control and diet group after 16 weeks of DIO	154
<b>Figure 59:</b>	Total PTEN expression in control and diet group after 8 weeks of DIO	155
<b>Figure 60:</b>	Total PTEN expression in control and diet group after 16 weeks of DIO	155
<b>Figure 61:</b>	AMPK expression in control and diet group after 8 weeks of DIO	156
<b>Figure 62:</b>	AMPK expression in control and diet group after 16 weeks of DIO	156
<b>Figure 63:</b>	Oxidative phosphorylation potential after 8 weeks of DIO with glutamate as a substrate	157
<b>Figure 64:</b>	Oxidative phosphorylation potential after 8 weeks of DIO with palmitoyl-L-carnitine as a substrate	157
<b>Figure 65:</b>	Oxidative phosphorylation potential after 16 weeks of DIO with glutamate as a substrate	158
<b>Figure 66:</b>	Oxidative phosphorylation potential after 16 weeks of DIO with palmitoyl-L-carnitine as a substrate	158
<b>Figure 67:</b>	The percentage recovery after 20 minutes of anoxia in control and diet groups using glutamate as a substrate	161
<b>Figure 68:</b>	The percentage recovery after 20 minutes of anoxia in control and diet groups using palmitoyl-L-carnitine as a substrate	161
<b>Figure 69:</b>	Amount of ATP produced during state 3 respiration	162
<b>Figure 70:</b>	Amount of ATP produced during state 3 respiration by the control group when using either glutamate or palmitoyl-L-carnitine as substrates	162

<b>Figure 71:</b>	Amount of ATP produced during state 3 respiration by the diet group when using either glutamate or palmitoyl-L-carnitine as substrates	163
<b>Figure 72:</b>	The level of citrate synthase activity ( $\mu\text{mol}/\text{mgprot}/\text{min}$ ) in both the control and diet group after 8 weeks of DIO	165
<b>Figure 73:</b>	The level of citrate synthase activity ( $\mu\text{mol}/\text{mgprot}/\text{min}$ ) in both the control and diet group after 16 weeks of DIO	165
<b>Figure 74:</b>	The level of PDH enzyme quantity after 8 weeks of DIO	166
<b>Figure 75:</b>	The level of PDH enzyme quantity after 16 weeks of DIO	166
<b>Figure 76:</b>	The level of PDH enzyme activity measured after 8 weeks of DIO	167
<b>Figure 77:</b>	The level of PDH enzyme activity measured after 16 weeks of DIO	167
<b>Figure 78:</b>	PDK 4 expression after 8 weeks of DIO	168
<b>Figure 79:</b>	PDK 4 expression after 16 weeks of DIO	169
<b>Figure 80:</b>	FAT/CD36 expression after 8 weeks of DIO	170
<b>Figure 81:</b>	FAT/CD36 expression after 16 weeks of DIO	171
<b>Figure 82:</b>	Uptake of glucose and fatty acids by GLUT 4 and FAT/CD36	178
<b>Figure 83:</b>	Schematic representation of FAT/CD36 and GLUT 4 translocation in healthy and insulin resistant cardiac muscle	179

## TABLES

<b>Table 1:</b>	Composition of diet for control and DIO group	98
<b>Table 2:</b>	Protocol for stack gel	105
<b>Table 3:</b>	Protocol for separation gel	105
<b>Table 4:</b>	Western blotting protocol for PPAR alpha and PGC-1 alpha	106
<b>Table 5:</b>	Western blotting protocol for GLUT 1 and GLUT 4	106
<b>Table 6:</b>	Western blotting protocol for total and phospho GSK-3	106
<b>Table 7:</b>	Western blotting protocol for total and phospho PI-3 kinase	107
<b>Table 8:</b>	Western blotting protocol for total and phospho PTEN	107
<b>Table 9:</b>	Western blotting protocol for total and phospho PKB/Akt	107
<b>Table 10:</b>	Western blotting protocol for total AMPK	108
<b>Table 11:</b>	Reaction scheme for citrate synthase assay	121
<b>Table 12:</b>	Instructions by the manufacturer to prepare the 2x RT master mix (per 20 µl reaction)	130
<b>Table 13:</b>	Instructions from the manufacturer to prepare the cDNA reverse transcriptase reactions	131
<b>Table 14:</b>	Instructions to program the thermal cycling conditions	132
<b>Table 15:</b>	Components (Multiplex: Target + Control reactions)	136
<b>Table 16:</b>	Setting thermal cycler conditions	137
<b>Table 17:</b>	ADP/O ratio, State 3, State 4, RCI and oxidative phosphorylation rates of control and diet groups measured after 8 weeks DIO using glutamate as a substrate	159

<b>Table 18:</b>	ADP/O ratio, State 3, State 4, RCI and oxidative phosphorylation rates of control and diet groups measured after 8 weeks DIO using palmitoyl-L-carnitine as a substrate	159
<b>Table 19:</b>	ADP/O ratio, State 3, State 4, RCI and oxidative phosphorylation rates of control and diet groups measured after 16 weeks of DIO using glutamate as a substrate	160
<b>Table 20:</b>	ADP/O ratio, State 3, State 4, RCI and oxidative phosphorylation rates of control and diet groups measured after 16 weeks of DIO using palmitoyl-L-carnitine as a substrate	160
<b>Table 21:</b>	State 3 respiration (natoms O <sub>2</sub> /mg prot/min): succinate rotenone, oligomycin and CCCP when using glutamate as a substrate	164
<b>Table 22:</b>	State 3 respiration (natoms O <sub>2</sub> /mg prot/min): succinate, rotenone, oligomycin, and CCCP when using palmitoyl-L-carnitine as a substrate	164
<b>Table 23:</b>	Summary of results	181

## LIST OF ABBREVIATIONS

### Units of Measurement

- %: percentage
- °C: degrees Celsius
- AU: arbitrary units
- Ci: curie
- g: grams
- g: gravity
- IU: international units
- M: molar
- mg: milligrams
- mg/kg: milligrams per kilogram
- mg/ml: milligrams per millilitre
- min: minutes
- ml: millilitre
- mM: millimolar
- mm<sup>2</sup>: cubic millimetres
- N: normal
- nm: nanometer
- p: pico
- rpm: revolutions per minute
- sec: seconds
- μ: micro
- μg/ml: micrograms per millilitre
- μM: micromolar
- μm: micrometer

## Molecular & Chemical Compounds

WHO	World health organisation
6-PF2-K	6-phosphofructo-2-kinase
ACC	Acetyl-CoA carboxylase
AcCoA	Acetyl-CoA
ADP	Adenosine diphosphate
AMP	Adenosine monophosphate
AMPK	5' Adenosine monophosphate-activated protein kinase
AMPKK	AMPK kinase
ANOVA	Analysis of variance
APS	AmMonium persulfate
AR	Androgen receptor
ATP	Adenosine triphosphate
ATPase	Adenosine triphosphatase
BAD	Bcl-2/Bcl-X antagonist
BAT	Brown adipose tissue
Bcl-2	B-cell lymphoma 2
Bcl-X	Bcl-2 related gene
Bim	Bcl-2 interacting mediator of cell death
BMI	Body mass index
BSA	Bovine serum albumin
Ca <sup>2+</sup>	Calcium
CaCl <sub>2</sub>	Calcium chloride
cAMP	Cyclic adenosine monophosphate
CCCP	Carbonyl cyanide 3-chlorophenylhydrazone
CDC	Centres for disease control and prevention
Cdk	Cyclin dependent kinase
cDNA	Complementary deoxyribonucleic acid
cGMP	Cyclic guanosine monophosphate
CO <sub>2</sub>	Carbon dioxide



CoA	Coenzyme A
CoASH	Coenzyme A
COO <sup>-</sup>	Carboxyl group
CoQH <sub>2</sub>	Ubiquinol
CPT-1	Carnitine palmitoyl transferase 1
CREB	Cyclic AMP response element binding protein
CrP	Creatine phosphate
CuSO <sub>4</sub>	Copper sulphate
CVD	Cardiovascular disease
DEPC	Diethylpyrocarbonate
DIO	Diet-induced obesity
DNA	Deoxyribonucleic acid
DNase	Deoxyribonuclease
dNTP	Deoxynucleotide triphosphate
DTNB	5,5'-Dithiobis-(2-nitrobenzoic acid)
e.g.	Example
E1	Pyruvate dehydrogenase
E2	Dihydrolipoamide acetyltransferase
E3	Dihydrolipoamide dehydrogenase
ECL	Enhanced chemiluminescence
EDTA	Ethylenediaminetetraacetic acid
EGTA	ethylene glycol tetraacetic acid
eiF	Eukaryotic initiation factor
ERRs	Estrogen-related receptors
FA	Fatty acid
FABP	Fatty acid binding protein
FAD	Flavin adenine dinucleotide
FAT	Fatty acid translocase
FAT/CD36	Fatty acid translocase/cluster of differentiation 36
FeS	Iron sulphide
FH	Forkhead

FMN	Flavin mononucleotide
F <sub>0</sub> F <sub>1</sub> ATP synthase	ATP synthase
FoxO	Forkhead box
GLUT 1	Glucose transporter 1
GLUT 4	Glucose transporter 4
GSK-3	Glycogen synthase kinase 3
GSK-3 $\alpha$	Glycogen synthase kinase 3 alpha
GSK-3 $\beta$	Glycogen synthase kinase 3 beta
H <sub>2</sub> O	Water
H <sub>3</sub> PO <sub>4</sub>	Phosphoric acid
HCl	Hydrochloric acid
HDL	High density lipoprotein
HEP	High energy phosphates
HOMA	Homeostasis model assessment
HPLC	High performance liquid chromatography
HRP	Horseradish peroxidase
i.e.	that is
IGF-1	Insulin-like growth factor I
IKK	I $\kappa$ B kinase
IL-1 $\alpha$	Interleukin 1 alpha
ILK	Integrin-linked kinase
iNOS	Inducible nitric oxide synthase
IRS	Insulin receptor substrate
I $\kappa$ B	I $\kappa$ B
K <sub>2</sub> HPO <sub>4</sub>	Dipotassium phosphate
KCl	Potassium chloride
KH <sub>2</sub> PO <sub>4</sub>	Monopotassium phosphate
LCAD	Long-chain acyl-CoA dehydrogenase
L-CPT-1	Liver isoform of CPT-1
LKB 1	Serine/threonine kinase 11
MCAD	Mitochondrial acyl-CoA dehydrogenase

MCD	Malonyl-CoA decarboxylase
M-CPT-1	Heart/muscle isoform of CPT-1
MDM2	Murine double minute 2
Mg Cl <sub>2</sub>	Magnesium chloride
Mg <sup>2+</sup>	Magnesium
MGB	Minor groove binder
MgSO <sub>4</sub>	Magnesium sulphate
MOPS	3-[N-morpholino]propanesulfonic acid
mRNA	Messenger ribosomal nucleic acid
N	Normal
Na <sub>2</sub> CO <sub>3</sub>	Sodium carbonate
Na <sub>2</sub> HPO <sub>4</sub>	Disodium phosphate
Na <sub>2</sub> SO <sub>4</sub>	Sodium sulphate
Na <sub>3</sub> VO <sub>4</sub>	Sodium orthovanadate
NaCl	Sodium Chloride
NAD	Nicotinamide adenine dinucleotide
NADH	Reduced nicotinamide adenine dinucleotide
NaHCO <sub>3</sub>	Sodium bicarbonate
NaK-tartrate	Sodium potassium tartrate
NaOH	Sodium hydroxide
NFQ	Nonfluorescent quencher
NFκB	Nuclear factor-kappa B
NH <sub>2</sub>	Amine group
-NH <sub>3</sub> <sup>+</sup>	Amino group
NO	Nitric oxide
NRF-1	Nuclear respiratory factor 1
NRF-2	Nuclear respiratory factor 2
O <sub>2</sub>	Oxygen
OAA	Oxaloacetate
OD	Optical density
-OH	Hydroxide

p110	Protein 110
p85	Protein 85
PCA	Perchloric acid
PCR	Polymerase chain reaction
PDC	Pyruvate dehydrogenase complex
PDE3B	Phosphodiesterase 3B
PDH	Pyruvate dehydrogenase
PDK 1	3'phosphoinositide-dependent kinase-1
PDK 4	Pyruvate dehydrogenase kinase 4
PDP	Pyruvate dehydrogenase phosphatases
PED/PEA-15	Protein phosphoprotein enriched in diabetes/astrocytes-15
PERC	PGC-1 related estrogen receptor coactivator
PFK	Phosphofructokinase
PGC-1 alpha	Peroxisome proliferator-activated receptor gamma coactivator alpha
pH	Potential of Hydrogen
Phospho	Phosphorylated
PI	Phosphoinositide
PI 3 kinase	Phosphatidylinositol 3 kinase
PIP2	Phosphatidylinositol 4,5-bisphosphate
PIP3	Phosphatidylinositol (3,4,5)-trisphosphate
PKB/Akt	Protein kinase B/Akt
PKB $\beta$	Protein kinase B beta
PKC	Protein kinase C
PMSF	Phenylmethanesulfonylfluoride
PPAR alpha	Peroxisome proliferator-activated receptor alpha
PRC	PGC-1 related coactivator
PTEN	Phosphatase and tensin homolog on chromosome ten
PTP	Permeability transition pore
Q	Ubiquinone

QH	Ubiquinol
QH <sub>2</sub>	Cytochrome c reductase
Ras	Rat sarcoma
RCF	Relative centrifugal force
REST	Relative expression software tool
RISK	Reperfusion injury salvage kinase
RNA	Ribonucleic acid
RNase	Ribonuclease
ROS	Reactive oxygen species
RPC	Reverse phase chromatography
Rpm	Revolutions per minute
RT	Reverse transcription
RXR	Retinoid X receptor
SANS	South African national standard
SDS	Sodium dodecyl sulfate
SDS-PAGE	Sodium dodecyl sulfate polyacrylamide gel electrophoresis
SEM	Standard error of the mean
Ser473	Serine 473
SH2	Src homology 2
Shc	Src homologous and collagen-like protein
SIRP	Single regulatory protein
Src	Sarcoma
SSO	Sulfo-N-succinimidyl oleate
STD	Standard
TBAP	Tetrabutylammoniumphosphate
TBS	Tris buffered saline
TBST	Tris buffered saline with Tween
TCA	Tricarboxylic acid cycle
TCA	Trichloroacetic acid
TEMED	Tetramethylethylenediamine

Tfam	Mitochondrial transcription factor A
Thr308	Threonine 308
TNB	5-thio-2-nitrobenzoic acid
TNF	Tumour necrosis factor
TRADD	TNF receptor type 1 associated death domain
TRAIL	TNF-related apoptosis-inducing ligand
TRI-reagent	Trizol-reagent
Tris	2-Amino-2-hydroxymethyl-propane-1,3-diol
UCP 3	Uncoupling protein 3
USA	United states of America
UV	Ultra violet
YAP	Yes-associated protein
ZDF	Zucker diabetic fatty
ZL	Zucker lean
ZO	Zucker obese

## **CHAPTER 1: LITERATURE REVIEW**

### **1.1 OBESITY, CARDIOVASCULAR DISEASE: A “GLOBAL EPIDEMIC”**

The World health organisation (WHO) estimated that within the next few years, dietary associated chronic non-communicable diseases such as ischaemic heart disease, diabetes, stroke and hypertension will be responsible for the bulk of the global burden of disease [Hennekens CH 2007]. Currently these global epidemics include obesity, diabetes and cardiovascular disease [Chopra et al. 2002]. It is suggested that the progressive increase in the prevalence of these diseases can be attributed to an increase in the adoption of the so-called Western lifestyle which involves the over consumption of inexpensive high energy/caloric foods and reduced physical activity [Hossain et al. 2007].

Cardiovascular disease (CVD) can be defined as a non-communicable disease affecting both the heart and the vasculature. The four most common types of heart disease are 1) coronary heart disease (which includes heart attack and angina), 2) stroke, 3) high blood pressure and 4) heart failure [American Heart Association March 18 2010, Learn and Live].

The prevalence of CVD is increasing at an alarming rate to the extent where CVD has been labelled the leading cause of death and disability in the industrialized world [Katz 2000] with ischaemic heart disease (a form of coronary heart disease) being the leading cause of death in developed countries (WHO 2002). In the United States of America, cardiovascular related diseases are the leading cause of death surpassing cancer linked mortalities (National Center of Health Statistics 2002/3). Furthermore cardiovascular diseases are responsible for 41% of all deaths in North America with ischaemic heart disease leading all of the cardiovascular diseases (American Heart Association. Heart and stroke statistical update. Dallas, TX: American Heart Association; 2001).

South Africa is one of the many developing countries that have shown a similar progression to that of developed countries such as the USA, where the poor have become the most vulnerable to CVD [Reddy and Yusuf 1998] . It is therefore crucial to elucidate the causes and mechanisms of cardiovascular disease.

In previous years, CVD was rife in developed countries such as North America. However this is no longer the case as CVD has become more prevalent in developing countries as well. This is mainly due to the increase in the incidence of overweight and obese individuals in lower income regions [Chopra et al. 2002].

Obesity is defined as a condition where the accumulation of excess body fat has reached the point where it may have adverse effects on an individual's health which leads to a reduction in life expectancy and/or an increase in health problems [Haslam et al. 2005]. According to the Centers for Disease Control and Prevention (CDC) the terms overweight and obese are both labels for ranges of weight that are greater than what is generally considered healthy for a given height. For adults these ranges (overweight- BMI between 25 and 29; obese – BMI of 30 or higher) are determined by a number called the “body mass index” (BMI). BMI is defined as weight in kilograms divided by height in meters squared, and is used because for most individuals it correlates with their amount of body fat [Eckel 1997]. It is important to remember that even though there is a correlation between BMI and the amount of body fat, BMI does not directly measure the amount of body fat. Therefore the definition of obesity still remains a controversial topic.

The epidemic of obesity is no longer confined to developed countries. The prevalence of obesity is spreading to the developing world as well [He et al. 2005; Gu et al. 2007; Kearney et al. 2005]. This is greatly due to dietary and lifestyle changes that accompany economic development [Folake et al. 2008]. Obesity is associated with numerous co-morbidities of which heart disease is the most common. The increase in the prevalence of obesity can be attributed to a



number of factors, however it has been suggested that environmental factors such as a high fat diet and reduced physical activity are probably the most likely culprits [Eckel 1997; Folake et al. 2008].

Obesity is one of the most common risk factors associated with the development of heart disease and greatly increases an individual's probability of developing cardiovascular disease [McLellan 2002].

A variety of risk factors associated with obesity such as hypertension, dyslipidemia, reductions in HDL cholesterol and impaired glucose tolerance or non-insulin-dependent diabetes mellitus appear to play a role in coronary heart disease risk [Eckel 1997]. The prevalence of insulin resistance as well as compensatory hyperinsulinemia is increased in obese individuals [Reaven et al. 2004]. In addition CVD is considered to be the leading cause of death in the diabetic population [Duncan et al. 2007].

However, the interaction between obesity, insulin resistance and cardiovascular disease remain not fully understood. To better understand these interactions, the mechanism of obesity-induced insulin resistance and cardiovascular abnormalities is reviewed in the following section.

## **1.2 INSULIN RESISTANCE**

### **1.2.1 Overview of insulin action**

Insulin is a polypeptide hormone secreted by the beta cells in the islets of Langerhans in the pancreas. It plays an important role in the regulation of the metabolism of carbohydrates and fats, especially the conversion of glucose to glycogen, which lowers the blood glucose level. Insulin acts on insulin sensitive tissue such as brain, fat, muscle and liver tissue to allow the transport of glucose into cells [Ebeling P et al. 1998]. Insulin is released by the pancreas in response

to various stimuli. However the transport of insulin from the beta-cells is mainly determined by the plasma glucose levels and the concentrations of amino acids and fatty acids [Waselle et al. 2005].

Although the main role of insulin is to regulate glucose homeostasis, it is also involved in the regulation of a wide range of vital metabolic pathways and cellular functions [Saltiel et al. 2001]. A few of these vital metabolic and cellular processes include: glycolysis, glycogenesis, transport of ions and amino acids, lipid metabolism, DNA synthesis, gene transcription, mRNA turnover, protein synthesis and degradation as well as having a role in cellular growth and differentiation. A deficiency in insulin can lead to the development of type 1 diabetes and related disorders [Gupta 1997].

### **1.2.2 The role of insulin in glucose homeostasis:**

Insulin is the main role player in the regulation of glucose homeostasis [Khan et al. 2002]. It is of great importance that blood glucose levels remain constant as persistently high blood sugar concentrations over many years can lead to the development of a variety of clinical complications such as retinopathy, nephropathy and cardiovascular disease. All of these diseases play a role in increasing an individual's chances of morbidity and mortality [Khan et al. 2002].

Insulin plays a crucial role in the uptake of glucose into cells by stimulating the translocation of the main glucose transporter in muscle and fat cells GLUT4, to the plasma membrane where it facilitates the transport of glucose into the cell thereby normalising the increased post-prandial glucose levels [Watson et al. 2001]. The GLUT4 transporter relies largely on insulin stimulation for its translocation and this mechanism involves the activation of phosphatidylinositol 3-kinase (PI 3 kinase) together with specific serine/threonine phosphorylation events [Miura et al. 2001]. The involvement of the classic insulin signalling

pathway and specifically PI 3 kinase in the translocation of GLUT4 transporters to the plasma membrane has been established [Khan et al. 2002].

Another key role player in the regulation of glucose homeostasis is protein kinase B (PKB/Akt). Its involvement in insulin signalling and the regulation of glucose homeostasis have been studied extensively using knockout mouse models as one of the approaches. The PKB $\beta$  isoform appears to be the main isoform present in insulin-responsive tissues and is strongly associated with the maintenance of glucose homeostasis [Dummler et al. 2007].

### **1.2.3 The insulin signalling pathway:**

In order for insulin to exert its effects it has to bind to its cell-surface receptor. The insulin receptor consists of two alpha subunits and two beta subunits which are linked to form a  $\alpha_2\beta_2$  heterotetrametric complex [Khan et al. 2002]. Following the binding of insulin to the extracellular alpha subunits, a signal is transmitted across the plasma membrane which activates the intracellular tyrosine kinase domain of the beta subunit. This allows the receptor to undergo a series of intramolecular transphosphorylation reactions in which one beta subunit phosphorylates its adjoining partner on specific tyrosine residues. Once the insulin receptor has been activated, it phosphorylates a variety of important proximal substrates on tyrosine, such as members of the insulin receptor substrate family (IRS1/2/3/4), Shc adapter protein isoforms and single regulatory protein (SIRP) family members. The tyrosine phosphorylation of the IRS proteins creates recognition sites for additional effector molecules containing Src homology 2 (SH2) domains e.g. the p85 regulatory subunit of the type 1A PI 3-kinase. [Pessin et al. 2000]. This regulatory subunit resides in the cytosol bound to a catalytic p110 subunit forming a dimer which, upon recruitment of the p85 subunit brings the catalytic subunit, to the plasma membrane in order to catalyze the phosphorylation of the 3' position in the inositol ring of phosphoinositide (PI) lipids. In the case of insulin signalling this specifically involves the formation of PI

(3, 4, 5)- triphosphate from PI (4, 5) –biphosphate, and PI(3, 4)-biphosphate from PI (4)-phosphate which, in each instance, is catalyzed by the Type IA PI 3 kinase. The phosphorylated and activated 3'position of these PI lipids recruits and activates the 3'phosphoinositide-dependent kinase-1 (PDK-1). The phosphorylated PDK-1 then activates certain downstream effectors such as the two classes of serine/threonine kinases Akt (also known as protein kinase B) and protein kinase C (PKC $\zeta/\lambda$ ). These two effectors in turn induce the translocation of GLUT 4 to the plasma membrane. [Khan et al. 2002].

#### **1.2.4 The pathophysiology of Insulin resistance**

Insulin resistance encompasses defective insulin signalling and glucose transport into cells [Ginsberg 2000]. Insulin resistance is strongly correlated to the development of heart disease as can be seen in the diabetic community where cardiovascular mortality has been found to be the leading cause of death and disability [Duncan et al. 2007].

Generally insulin resistance can be the result of a pre-receptor or post-receptor abnormality [McFarlane SI et al. 2001]. In this regard insulin resistance will occur if PI 3-kinase activation is diminished. The insulin-PI 3 kinase pathway, once activated plays an important role in stimulating vascular nitric oxide (NO) production, cardiovascular cation transport mechanisms and glucose transport in cardiovascular tissue as well as the conventional insulin-sensitive tissues fat, muscle and liver [McFarlane SI et al. 2001] .

##### **1.2.4.1 The role of insulin resistance in obesity and cardiovascular disease:**

As previously mentioned, insulin resistance generally refers to the resistance to the effects of insulin on particularly glucose uptake, metabolism, or storage [Khan et al. 2000]. Insulin resistance in obesity and type 2 diabetes is characterised by

reduced insulin-stimulated glucose transport and metabolism in specifically adipocytes and skeletal muscle [Reaven 1995]. Another functional defect that plays a role in insulin resistance in obesity and type 2 diabetes is impaired suppression of hepatic glucose output [Reaven 1995]. It is speculated that these defects may occur as a result of impaired insulin signalling in the respective target tissues. [Kahn et al. 2000]

Obesity, especially visceral obesity, contributes greatly to impaired glucose tolerance, hyperinsulinemia, type 2 diabetes, dyslipidemia, hypertension and premature cardiovascular disease. In addition visceral obesity and assisting risk factors are closely correlated with an increased risk for the development of cardiovascular disease as illustrated by data obtained from the Quebec cardiovascular study [Tchernof et al. 1996]. This study revealed that visceral obesity is associated with two of the strongest independent risk factors for ischaemic heart disease. These two factors are fasting hyperinsulinemia and increased apolipoprotein B concentrations. Visceral fat cells, when compared with peripheral fat cells, tend to be more resistant to the metabolic effects of insulin and more sensitive to lipolytic hormones. As a result, the elevated release of free fatty acids into the portal system supplies increased substrate for hepatic triglyceride synthesis. This leads to increased production of apolipoprotein B, increases in the proportion of small dense low density lipoprotein particles, decreased HDL cholesterol, and increased triglycerides, all of which can act to impair the metabolism of insulin [McFarlane SI et al. 2001]. Additionally, the insulin resistant and diabetic heart is also more susceptible to impaired mitochondrial function which seems to play a very important role in the development of cardiovascular disease [Madrazo and Kelly 2008].

### **1.3 MYOCARDIAL SUBSTRATE SELECTION AND UTILIZATION**

The heart consumes a tremendous amount of energy (ATP) and must therefore continuously produce large amounts of ATP in response to physiological demands and fuel delivery [Tian and Barger 2006]. Generally myocardium can take up and utilize a variety of substrates. Under so-called “normal” conditions i.e. sufficient nutrient and oxygen supply to the myocardium, the heart derives the most of its energy from the oxidation of fatty acids (60-70%), glucose (30-40%) and lactate (10%) [van den Brom et al. 2009]. The heart preferentially utilizes fatty acids as a substrate for energy production, as it produces more ATP per molecule than glucose [Wallhaus et al. 2001]. However under ischaemic conditions, when the supply of nutrients and oxygen to the myocardium is very limited, the heart switches from the oxygen consuming utilization of FAs to a more oxygen efficient, anaerobic energy producing process known as glycolysis.

It has been shown that at the end stages of heart failure, the myocardium has low ATP content due to a decreased ability to generate ATP by oxidative metabolism, and thus is unable to effectively utilize fatty acids for the production of energy for contractile work [Ashrafian 2002; Dzeja et al. 2000; Katz 1993; Peyton et al. 1982]. Under these circumstances utilizing carbon fuel for the production of ATP via glycolysis, instead of fatty acid and glucose oxidation, would prove to be more beneficial for the heart.

However it is of great importance to remember that heart failure is not an isolated or specific disease, but rather a complex syndrome that is dependent on a number of things, including etiology, duration, underlying coronary artery disease and ischaemia, endothelial dysfunction, and the co-occurrence of disorders such as diabetes, hypertension, and obesity [Stanley et al. 2005]. Thus myocardial substrate selection and utilization will adjust accordingly to ensure the optimal production of energy (ATP) under any given circumstance to protect the heart.

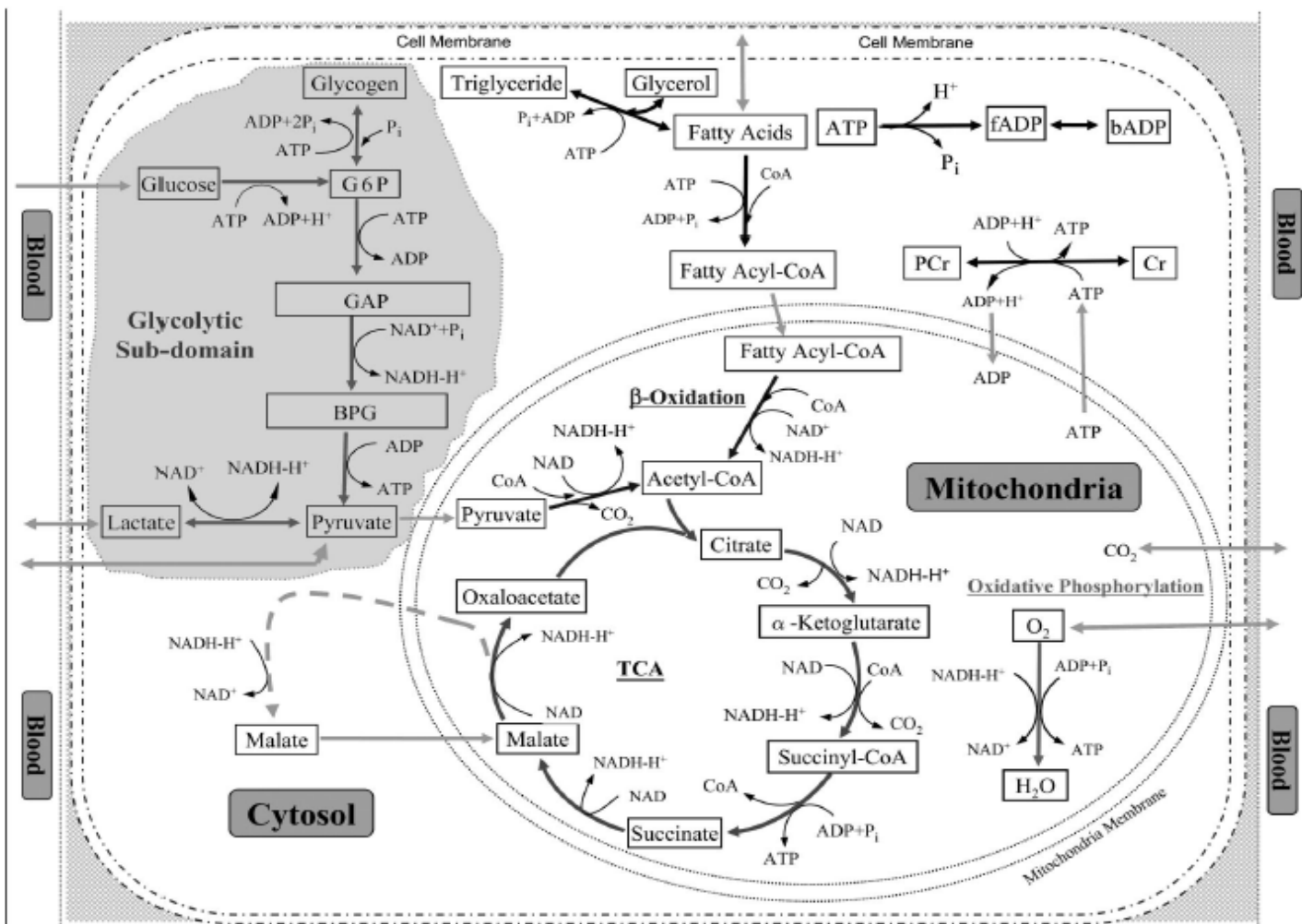


Figure 1: An overview of myocardial metabolism [Zhou et al. 2005]

### **1.3.1 The role of obesity, insulin resistance and ischaemia in the change of myocardial substrate selection and utilization**

Metabolic stressors such as ischaemia and diabetes, specifically type 2 diabetes is accompanied by increased lipolysis and hypertriglyceridemia. Reduced insulin-mediated myocardial glucose uptake and utilization alter myocardial substrate metabolism to further favour fatty acid oxidation [van den Brom et al. 2009]. The elevation in plasma free acid levels ensuing from obesity results in an increase in fatty acid oxidation, leading to the overproduction of fatty acid metabolites which act to interfere with insulin signalling, at the insulin receptor substrate level, effectively reducing the transport of glucose into the cell [Boden and Shulman 2002]. When a cell becomes insulin resistant in response to obesity, myocardial substrate selection and utilization changes to favour and enhance fatty acid metabolism and reduce glucose metabolism due to a decrease in the availability of glucose as a substrate. However this is not very beneficial or sought after under ischaemic conditions as the reduced oxygen levels will result in the inability of the cell to effectively utilize both glucose and the increasing levels of free fatty acids for the production of ATP. This inability of the cell to produce sufficient energy will have damaging effects on the myocardium i.e. it will result in the activation of detrimental processes such as apoptosis, necrosis and subsequent cell death [Gill et al. 2002].

## **1.4 CELLULAR INJURY AND MYOCARDIAL INFARCTION**

Ischaemic heart disease commonly presents itself as a myocardial infarction. A myocardial infarction, more commonly known as a heart attack, is primarily due to reduced blood supply to cardiac tissue. This is usually as a result of a coronary occlusion caused by the rupturing of an atherosclerotic plaque in the wall of an artery.



### **1.4.1 The development of infarct size**

Infarct size is a measure of the amount of cell death that occurred as a result of apoptosis, as it has been suggested that the inhibition of apoptosis during reperfusion could possibly play a role in a reduction in infarct size [Zhao Z et al. 2003]. Necrosis and apoptosis represent two distinct types of cell death in myocardium, and has been associated with reperfusion induced myocardial injury after reversible coronary occlusion [Buja et al. 1998]. It has also previously been shown in rabbit, rat and dog models of regional ischaemia and reperfusion, that myocardial apoptosis is primarily triggered during reperfusion [Zhao et al. 2000; Gottlieb et al. 1994; Freude et al. 2000].

#### **1.4.1.1 Apoptosis and Necrosis**

A myocardial infarction can induce cell death by both necrosis and apoptosis [Barr et al. 1994]. Necrosis is a passive process which occurs in response to lethal injury and involves the rupturing of the cell membrane, cell swelling, plasma membrane breakdown, clumping of nuclear chromatin, swelling and disruption of sarcoplasmic reticulum and mitochondria as well as the manifestation of the granular densities in the matrix of mitochondria [Maulik et al. 1998]. The rupturing of the sarcoplasmic reticulum in necrotic cardiomyocytes results in calcium overloading which causes disturbances in other electrolytes [Jennings et al. 1964]. Whereas apoptosis is an active, highly regulated, energy-requiring process that takes place without the rupturing of the cell membrane and is characterized by internucleosomal cleavage of DNA by a  $\text{Ca}^{2+}$  and  $\text{Mg}^{2+}$  dependent endonuclease [Maulik et al. 1998]. Additionally segregation of nuclear chromatin and condensation of the cytoplasm are some of the ultra structural features presented by apoptosis [Maulik et al. 1998].

#### **1.4.1.1.1 Apoptosis in ischaemia/reperfusion**

Evidence exists that suggests that reperfusion of ischaemic myocardial tissue leads to reperfusion injury, a term used to describe a specific type of cellular injury [Maulik et al. 1998]. The generation of oxygen-derived free radicals, intracellular  $\text{Ca}^{2+}$  overloading and the redistribution of membrane phospholipids are all features associated with reperfusion injury and hallmarks of apoptosis [Richter 1993; Greenlund et al. 1995]. So it appears as though reperfusion and not ischaemia induces apoptosis in cardiomyocytes. Maulik et al. found no evidence of apoptosis in rat hearts subjected to 2 hours of ischaemia, however apoptosis became evident when these hearts were subjected to 15 min of ischaemia followed by 90 min of reperfusion [Maulik et al. 1998 (a); Maulik et al. 1998 (b)].

The development of a myocardial infarction and the initiation of apoptosis can be triggered by a variety of stimuli. The overproduction of reactive oxygen species (ROS) by mitochondria, in response to an increase in oxidative phosphorylation, can act as a stimulus for the initiation of apoptosis, as ROS is capable of damaging certain cellular components such as proteins, lipids and DNA [Halliwell et al. 1999].

It is important to note however that there are other role players in the development of an infarct during an ischaemic insult. The onset of intracellular acidosis via the inhibition of the vacuolar ATPase has been associated with the initiation of apoptosis in cardiac myocytes [Karwatowska-Prokopczuk et al. 1998; Long et al. 1998]. Elevated intracellular calcium levels observed during ischaemia and early reperfusion [Karmazyn and Moffat 1993] appears to play an important role in ischaemia/reperfusion injury, and high mitochondrial calcium levels have been implicated in the induction of the permeability transition pore (PTP) opening, allowing the release of calcium, cytochrome c, NAD and apoptogenic

factors into the cytosol [Crompton et al. 1999; Di Lisa et al. 2001; Heiskanen et al. 1999].

## **1.5 CARDIOPROTECTIVE EFFECTS OF THE ACTIVATION OF PI 3-KINASE/PKB/AKT PATHWAY DURING REPERFUSION**

### **1.5.1 PI3 kinase/PKB/Akt pathway**

As discussed previously insulin is a polypeptide hormone secreted by the beta cells in the islets of Langerhans in the pancreas and functioning in the regulation of the metabolism of carbohydrates and fats, especially the conversion of glucose to glycogen, which lowers the blood glucose level. Insulin acts on insulin sensitive tissues such as brain, fat, muscle and liver tissue to allow the transport of glucose into cells. Insulin binds to specific tyrosine kinase receptors on its target cells which leads to amongst others the downstream activation of the PI 3-kinase/PKB/Akt pathway [Burgering and Coffer 1995; Franke et al. 1995]. PKB/Akt has been implicated as a key role player in growth factor-mediated cell survival and inhibition of apoptosis in response to various stimuli [Fayard et al. 2005].

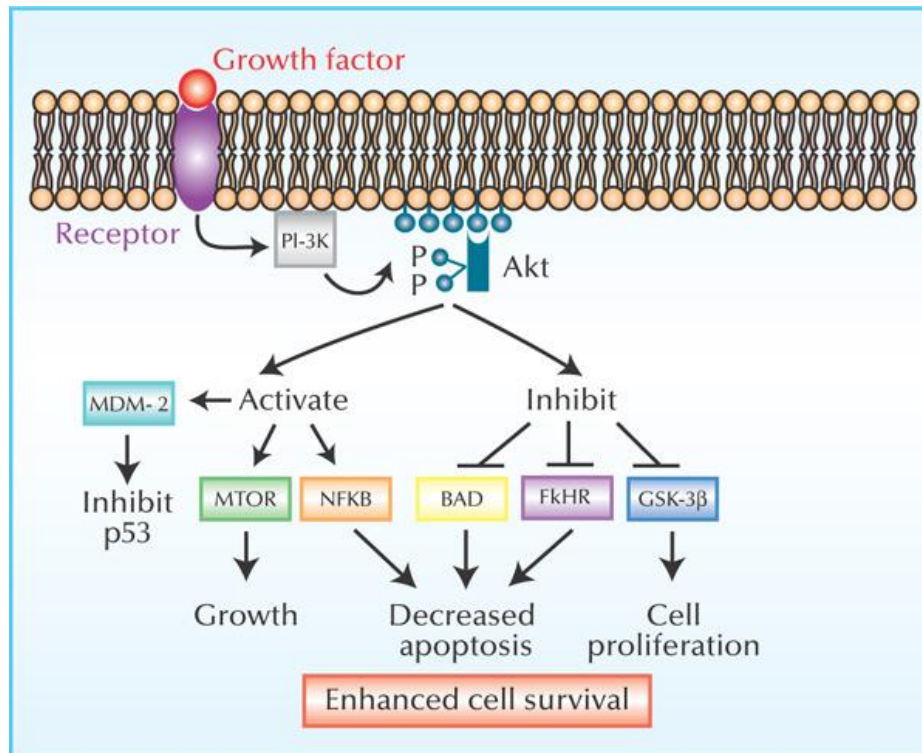


**Figure 2: A schematic representation of the role of the PI 3 kinase/PKB/Akt pathway in cell survival [ref - <http://www.ncbi.nlm.nih.gov/>]**

The PI 3-kinase/PKB/Akt pathway is one of the survival pathways known to protect the heart against ischaemic damage during myocardial reperfusion [Hausenloy and Yellon 2004; Yellon and Baxter 1999]. PKB/Akt is not only involved in the direct and indirect negative regulation of apoptosis but PKB/Akt also plays a crucial role in the translocation and recruitment of GLUT 4-containing vesicles to the membrane [Le Roith and Zick. 2001] for insertion in order to facilitate glucose uptake and utilization which plays a critical part in compensating for the increase in energy expenditure and decrease in its energy (ATP) producing capacity experienced during ischaemia.

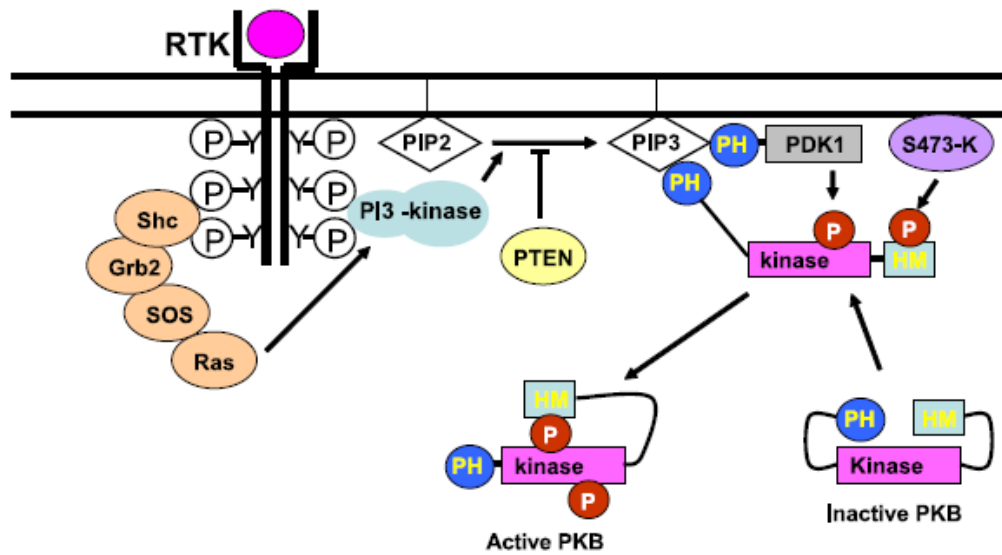


**Figure 3: Schematic representation of PKB/Akt activation**  
[Hanada et al. 2004]

#### 1.5.1.1 Activation of PKB/Akt:

PKB/Akt is activated by receptor tyrosine kinases such as insulin and Insulin-like growth factor I (IGF-I). It has been shown that activation of PKB/Akt by these ligands is blocked by the PI 3 kinase inhibitors wortmannin and LY294002 thus implicating PI 3 kinase as one of the key role players in the activation of PKB/Akt [Franke et al. 1995, Burgering and Coffey 1995, Cross et al. 1995, Kohn et al. 1995, Chan et al. 1999, Chan et al. 2003]. Phosphorylation of the threonine308 (Thr308) and serine473 (Ser473) sites located on PKB/Akt is essential for its phosphorylation and subsequent activation [Alessi et al. 1996]. The Thr308 and Ser473 sites are phosphorylated by a Thr308 kinase, pyruvate dehydrogenase kinase 1 (PDK 1) [Alessi et al. 1997; Stephens et al. 1998], and a Ser473 kinase, which may be integrin-linked kinase (ILK) 1 [DelcomMenne et al. 1998].

#### **1.5.1.2 The role of PKB/Akt in the metabolism**

Glycogen synthase kinase-3 (GSK-3) is a physiological substrate for PKB/Akt and phosphorylates and inactivates glycogen synthase in response to insulin stimulation [Burgering and Coffey 1995]. PKB/Akt phosphorylates and inactivates both isoforms of GSK-3 (alpha and beta) in a PI 3 kinase-dependent manner [Hanada et al. 2004]. PKB/Akt in addition to inactivating GSK-3 is also responsible for the phosphorylation and activation of phosphodiesterase 3B (PDE3B), contributing to the regulation of the intracellular level of cAMP and cGMP in response to insulin [Kitamura et al. 1999], and a cardiac-specific isoform of 6-phosphofructo-2-kinase (6-PF2-K) resulting in the activation of this enzyme and the promotion of glycolysis [Gold 2003].

#### **1.5.1.3 The role of PKB/Akt in the regulation of apoptosis**

Bcl-2/Bcl-X antagonist (BAD) is a member of the Bcl-2 family of proteins. BAD inhibits the anti-apoptotic potential of Bcl-2 and Bcl-X by binding to them [Downward 1999]. However when BAD is phosphorylated by PKB/Akt it does not demonstrate proapoptotic activity but rather promotes cell survival by forming complexes with other proteins. When phosphorylated, BAD is released from the Bcl-2/Bcl-X complex that is localized on the mitochondrial membrane and instead forms a complex with 14-3-3 [del Paso et al. 1997, Datta et al. 1997].

PKB/Akt also interacts with and phosphorylates a cytosolic protein, phosphoprotein enriched in diabetes/astrocytes-15 (PED/PEA-15) in a PI 3 kinase-dependent manner. This protein exhibits anti-apoptotic potential by inhibiting caspase 3 activity downstream of the death domain-containing receptors, Fas and tumour necrosis factor (TNF)-receptor family members [Trencia et al. 2003].

In addition PKB/Akt can phosphorylate caspase 9 in a Ras-dependent manner. Caspase 9 acts as an initiator as well as an effector of apoptosis [Donepudi and Grutter 2002], and phosphorylation of this protein results in the inhibition of cytochrome c-induced cleavage of this pro-caspase 9 which is required for the enzymatic action of caspase 9 [Hanada et al. 2004].

#### **1.5.1.3.1 Transcription factors involved in regulating apoptosis**

PKB/Akt has been shown to regulate apoptosis through transcription factors that are responsible for the activation of both pro and anti-apoptotic genes [Hanada et al. 2004].

A role for PKB/Akt in the regulation of the Forkhead (FH or FoxO) family of transcription factors was first identified by findings from the genetic analysis of *C. elegans* [Paradis et al. 1998, Paradis et al. 1999]. The phosphorylation sites for PKB/Akt are highly conserved among FH isoforms and are phosphorylated directly by PKB/Akt [Rena et al. 1999, Biggs et al. 1999, Wolfrum et al. 2003, Brunet et al. 1999, Kops et al. 1999]. This phosphorylation of FH results in the exclusion of FH from the nucleus leading to decreased transcriptional activity required for promoting apoptosis. Target genes for the FH family include, extracellular ligands e.g. Fas ligand, TNF-related apoptosis-inducing ligand (TRAIL) and TNF receptor type 1 associated death domain (TRADD), and intracellular components for apoptosis such as bcl-2 interacting mediator of cell death (Bim), a proapoptotic Bcl-2 member and Bcl-6 [Burgering and Medema 2003].

Another important transcription factor that is phosphorylated by PKB/Akt is the nuclear factor- $\kappa$ B (NF $\kappa$ B). NF $\kappa$ B is a key regulator of the immune response and deregulation of its activity is implicated in the development of autoimmune disease and cancer [Li and Verma 2000]. NF $\kappa$ B is phosphorylated and activated in response to the phosphorylation and subsequent degradation of I $\kappa$ B, an

inhibitor of NF $\kappa$ B, by the Ik B kinase (IKK) complex and PKB/Akt has been implicated in the direct and indirect regulation of IKK activity [Hanada et al. 2004]. PKB/Akt has been reported to inactivate NF $\kappa$ B in numerous ways including phosphorylating IKK $\alpha$  in a PI 3 kinase –dependent manner that is required for NF $\kappa$ B activation in response to TNF $\alpha$  (primary cytokine involved in the regulation of the imMune system and key regulator of apoptosis) stimulation [Ozes et al. 1999]. A few other transcription factors have also been shown to play a role in the regulation of apoptosis by PKB/Akt including, cyclic AMP (cAMP)-response element binding protein (CREB) [Du et al. 1998], the orphan nuclear receptor Nurr77 [He 2002, Pekarsky et al. 2001, Masuyama et al. 2001], androgen receptor (AR) [Lin et al. 2001], and yes-associated protein (YAP) [Basu et al. 2003].

#### **1.5.1.3.2 Cell cycle regulators involved in regulating apoptosis**

A number of cell cycle regulators have been shown to be phosphorylated by PKB/Akt in order to inhibit the activation of apoptosis. Murine double minute 2 (MDM2) is one such cell cycle regulator and is a protein product of the tumour suppressor gene p53 [Shimizu et al. 2003]. Another is the cyclin/Cdk inhibitor (p21/cip1/waf1). p21 plays a crucial role in maintaining cell cycle progression and has been reported as a direct substrate for PKB/Akt [Coqueret 2003]. The phosphorylation of this protein results in the inhibition of its potential to arrest the cell cycle and inhibit cell growth [Zhou BP et al. 2001].

### **1.6 THE REGULATORS OF THE EXPRESSION OF METABOLIC GENES IN CARDIOMYOCYTES**

Under non-ischaemic conditions, the heart produces almost all of its energy (>95%) via oxidative phosphorylation in the mitochondria, and the overall oxidative capacity of a cell greatly depends on the volume density and



composition of its mitochondria. As previously mentioned, mitochondria preferentially utilize fatty acids for ATP production, but mitochondrial substrate selection can be altered following an alteration in the expression of specific metabolic enzymes involved in these processes [Stanley et al. 2005]. Both nuclear and mitochondrial transcription alterations play a role in the metabolic changes observed in heart failure [Garnier et al. 2003]. Two regulators of the expression of metabolic genes can be found in cardiomyocytes. The first is peroxisome proliferator-activated receptor alpha (PPAR alpha) a transcription factor activated by the binding of endogenous Long-chain fatty acids and the second peroxisome proliferator-activated receptor-  $\gamma$  coactivator alpha (PGC-1 alpha) a co-activator of PPAR alpha.

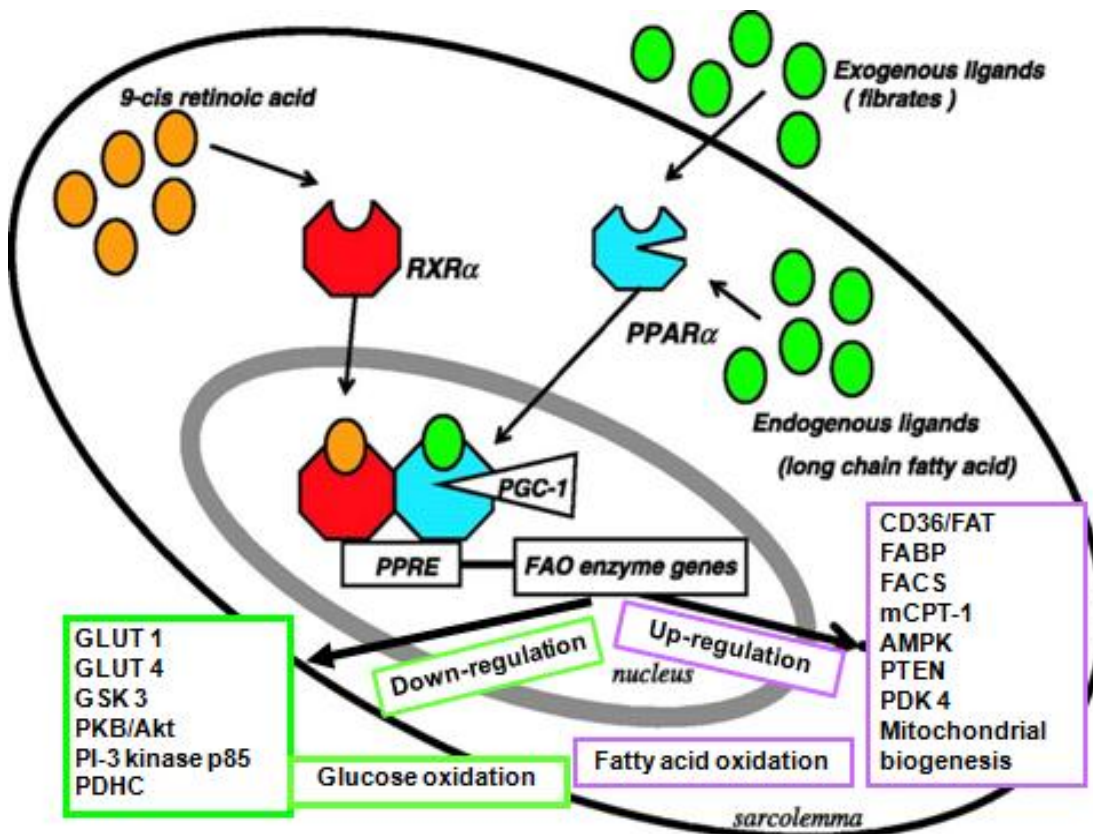


**Figure 4:** PPAR alpha and PGC-1 alpha are two regulators of the expression of metabolic genes in cardiomyocytes and are involved in the up and down regulation of an array of proteins involved in both FA oxidation and glucose oxidation.

### 1.6.1 Peroxisome proliferator-activated receptors

PPARs (peroxisome proliferator-activated receptors) are a group of nuclear receptor proteins that function as transcription factors regulating the expression of genes involved in myocardial mitochondrial fatty acid as well as glucose oxidation [Berger and Moller 2002; Huss and Kelly 2004]. PPARs play essential roles in the regulation of cellular differentiation, development and metabolism (carbohydrate, lipid and protein) [Berger 2005]

#### **1.6.1.1 PPAR isoforms**

There are three isoforms of PPARs, alpha, gamma and delta, expressed throughout the body (Berger and Moller 2002; Gilde et al. 2003; Huss and Kelly and Scarpulla 2004; Lehman and Kelly 2002). All PPARs heterodimerize with the retinoid X receptor (RXR-) and bind to specific regions of DNA of target genes called peroxisome proliferators hormone response elements, generally present in the promoter region of the gene of interest. PPAR alpha is highly expressed in tissues that have high rates of fatty acid oxidation such as the heart, liver, brown fat and kidney [Stanley et al. 2005]. Activation of PPAR alpha in the heart results in an increase in the expression of fatty acid oxidation enzymes as well as an increase in the rate of fatty acid oxidation in cardiomyocytes [Gilde et al. 2003] as it has been shown that PPAR-alpha knockout mice have decreased expression of fatty acid oxidation enzymes and suppressed fatty acid oxidation [Campbell et al. 2002].

#### **1.6.2 Peroxisome proliferator-activated receptor-γ coactivator (PGC)-1 alpha**

Peroxisome proliferator-activated receptor-γ coactivator (PGC)-1 alpha is a member of a family of transcription coactivators that plays a central role in the regulation of cellular energy metabolism. PGC-1 alpha has also been implicated as a key role player in a process known as mitochondrial biogenesis, as it has been shown that the overexpression of PGC-1 alpha in the heart results in an increase in the mRNA of numerous mitochondrial genes [Lehman et al. 2000].

#### **1.6.3 The role of PPAR alpha and PGC-1 alpha in cardiomyocytes**

Mitochondrial enzymes involved in cardiac energy metabolism are encoded by both nuclear and mitochondrial genes [Kelly and Scarpulla 2004]. This includes all of the enzymes involved in β-oxidation and the TCA cycle, most of the

electron transport subunits [Anderson et al. 1981], and mitochondrial number. These two sets of genes are tightly regulated in order to determine the overall cardiac oxidative capacity [Huss and Kelly 2005].

#### **1.6.3.1 Transcriptional regulation of cardiac mitochondrial biogenesis and respiratory function**

The PGC-1 family of transcriptional coactivators are involved in the regulation of mitochondrial metabolism and biogenesis. PGC-1 alpha was the first member to be discovered through its functional interaction with the nuclear receptor PPAR gamma in brown adipose tissue (BAT) [Puigserver et al. 1998], and has two related coactivators PGC-1 beta (PERC) and PGC-1-related coactivator (PRC) [Andersson and Scarpulla 2001, Lin et al. 2002, Kressler et al. 2002]. PRC is ubiquitously expressed and coactivates transcription factors involved in mitochondrial biogenesis [Andersson and Scarpulla 2001, Savagner et al. 2003]. PGC-1 alpha and PGC-1 beta are both preferentially expressed in tissues with a high oxidative capacity such as the heart where they provide critical regulatory functions with regard to mitochondrial functional capacity [Puigserver et al. 1998, Lin et al. 2002, Wu et al. 1999, Kamei et al. 2003, St-Pierre et al. 2003]. PGC-1 alpha is distinct from the other PGC-1 family members because of its broad responsiveness to developmental alterations in energy metabolism and physiological and pathological signals at the level of expression and transactivation [Huss and Kelly 2005]. This is evident in the heart at birth as the expression of PGC-1 alpha increases in response to an increase in cardiac oxidative capacity and a perinatal shift from reliance on glucose metabolism to FA oxidation for energy [Lehman et al. 2000]. PGC-1 alpha can be induced by certain physiological stimuli, such as cold exposure, fasting and exercise, that increase ATP demand and stimulate mitochondrial oxidation [Puigserver et al. 1998, Lehman et al. 2000, Baar et al. 2002, Wu et al. 2002, Goto et al. 2000]. In the heart specifically activation of PGC-1 alpha increases cardiac mitochondrial oxidative capacity and in cardiac myocytes in culture, PGC-1 alpha has been

shown to increase mitochondrial number as well as upregulate the expression of mitochondrial enzymes and increase the rates of FA oxidation and coupled respiration [Lehman et al. 2000, Huss et al. 2004]. More specifically PGC-1 alpha activates the expression of nuclear respiratory factor-1 (NRF-1) and NRF-2 and is responsible for the direct coactivation of NRF-1 on its target gene promoters [Wu et al. 1999 (b)]. NRF-1 and NRF-2 are responsible for the regulation of the expression of mitochondrial transcription factor A (Tfam), which is a nuclear-encoded transcription factor that binds to the regulatory sites on mitochondrial DNA and is essential for replication, maintenance, and transcription of the mitochondrial genome [Fisher et al. 1992, Garesse et al 2001, Larsson et al 1998]. Additionally, NRF-1 and NRF-2 also regulate the expression of nuclear genes encoding respiratory chain subunits and other proteins essential for mitochondrial function [Scarpulla 2002, Virbasius et al. 1993].

#### **1.6.3.2 The role of PGC-1 alpha in the activation of PPAR alpha**

PGC-1 alpha is not only involved in regulating mitochondrial biogenesis and function at the transcriptional level but is also involved in the regulation of genes involved in the cellular uptake and mitochondrial oxidation of FAs by direct coactivation of PPARs as well as estrogen-related receptors (ERRs) [Vega et al. 2000, Dressel et al. 2003, Huss et al. 2002, Schreiber et al. 2003].

As previously mentioned PPARs are FA-activated members of the nuclear receptors superfamily of transcription factors and serve as central regulators of cardiac FA metabolism [Huss and Kelly 2005]. The isoforms PPAR alpha and PPAR beta are the primary regulators of FA metabolism in the heart and function by binding as obligate heterodimers with the RXR alpha and recruiting coactivators, including PGC-1 alpha, in response to direct binding and activation by FAs and their derivatives. PPAR alpha is responsible for the regulation of almost every step of cardiac FA utilization [Desvergne and Wahli 1999], which has been shown in studies where PPAR alpha –null mice have reduced cardiac expression of genes that are involved in the cellular uptake, mitochondrial

transport, and mitochondrial oxidation of FAs [Lee et al. 1995, Djouadi et al. 1999]. It has also been shown that the uptake of myocardial FAs and oxidation rates are decreased in these mice, whereas glucose oxidation rates are increased [Campbell et al. 2002] and that PPAR alpha serves a homeostatic function during physiological and dietary stressors [Kersten et al. 1999, Leone et al. 1999].

#### **1.6.3.3        Perturbations in PGC-1/PPAR signalling in the insulin resistant and diabetic heart**

The diabetic cardiomyopathy that develops in the context of insulin resistance and diabetes is associated with increased cardiac reliance on FAs as the primary energy substrate [Wall and Lopaschuk 1989, Saddik et al. 1994, Belke et al. 2000, Neitzel et al. 2003]. This phenomenon of enhanced FA oxidation and diminished glucose oxidation is linked to the combined effects of myocyte insulin resistance and high-circulating free FAs [Huss and Kelly 2005]. It has been found that the expression as well as the activity of PPAR alpha, PGC-1 alpha and the enzymes involved in mitochondrial FA oxidation are induced in insulin-deficient and insulin-resistant forms of diabetes in mouse models [Finck et al. 2003, Finck et al. 2002]. Although the direct mechanism involved in the activation of PPAR alpha signalling in the diabetic heart is unknown it has been suggested that the increase in the cellular import of FAs is most likely the culprit, serving as ligands for this nuclear receptor [Huss and Kelly 2005]. Other studies have however shown a reduction in the level of transcription by PPAR alpha in diabetic myocardium [Depre et al. 2000, Young et al. 2001], but this could be due to temporal-dependent regulatory events during the progression of diabetic myocardial disease.

#### **1.6.3.4 Myocardial fuel shifts and heart failure in the insulin resistant and diabetic heart**

As previously described, the insulin resistant and diabetic heart is characterized by an increase in the FA oxidation rates, possibly as a result of the chronic activation of the PPAR alpha gene regulatory pathway [Huss and Kelly 2005]. Studies using mice with a cardiac-specific overexpression of PPAR alpha (MHC-PPAR alpha mice) exhibit increased expression of PPAR alpha target genes involved in cellular FA import and peroxisomal and mitochondrial FA oxidation, concurrent with lipid accumulation and increased FA oxidation rates [Finck et al. 2002, Hopkins et al. 2003 (a)], while myocardial glucose uptake and oxidation rates are reciprocally decreased suggesting that the chronic increased reliance on FAs for energy in the diabetic heart leads to pathological signatures that match the metabolic phenotype of the diabetic heart and that a primary drive on the PPAR alpha gene regulatory pathway triggers cross-talk suppression of glucose utilization pathways [Huss and Kelly 2005].

These two regulators of the expression of metabolic genes in cardiomyocytes therefore play an important role in the up-regulation of the expression of an array of proteins involved in fatty acid metabolism, some of which include, fatty acid-binding protein (FABP), pyruvate dehydrogenase kinase 4 (PDK4), acetyl-CoA carboxylase (ACC), Malonyl-CoA decarboxylase (MCD) as well as mitochondrial biogenesis. They are also responsible for the down-regulation of the expression of an array of proteins involved in glucose metabolism some of which include glucose transporters 1 (GLUT 1) and 4 (GLUT 4) and glycogen synthase kinase 3 (GSK-3).

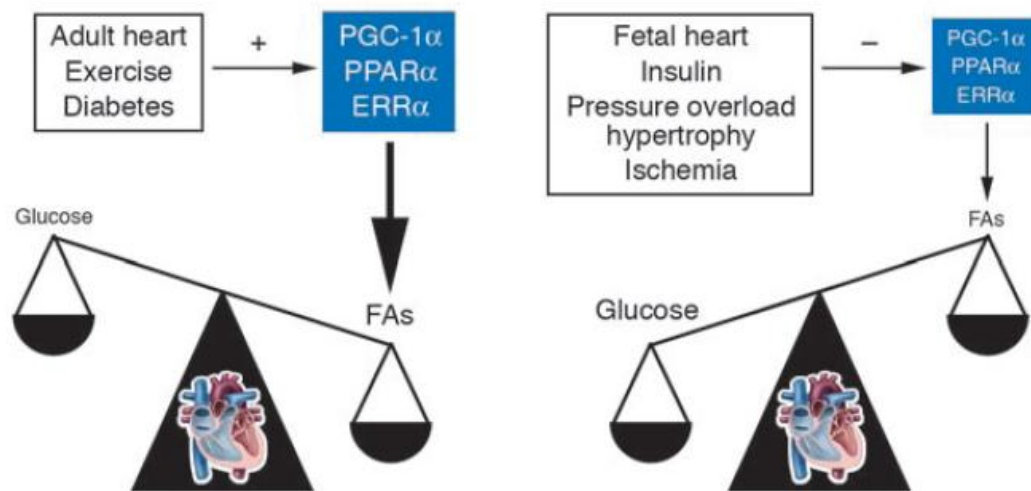


**Figure 5: Dynamic regulation of myocardial energy metabolism by developmental, dietary, and pathophysiological changes [Huss and Kelly 2005].**



## 1.7 PROTEINS IMPLICATED IN CARDIOMYOCYTE METABOLISM

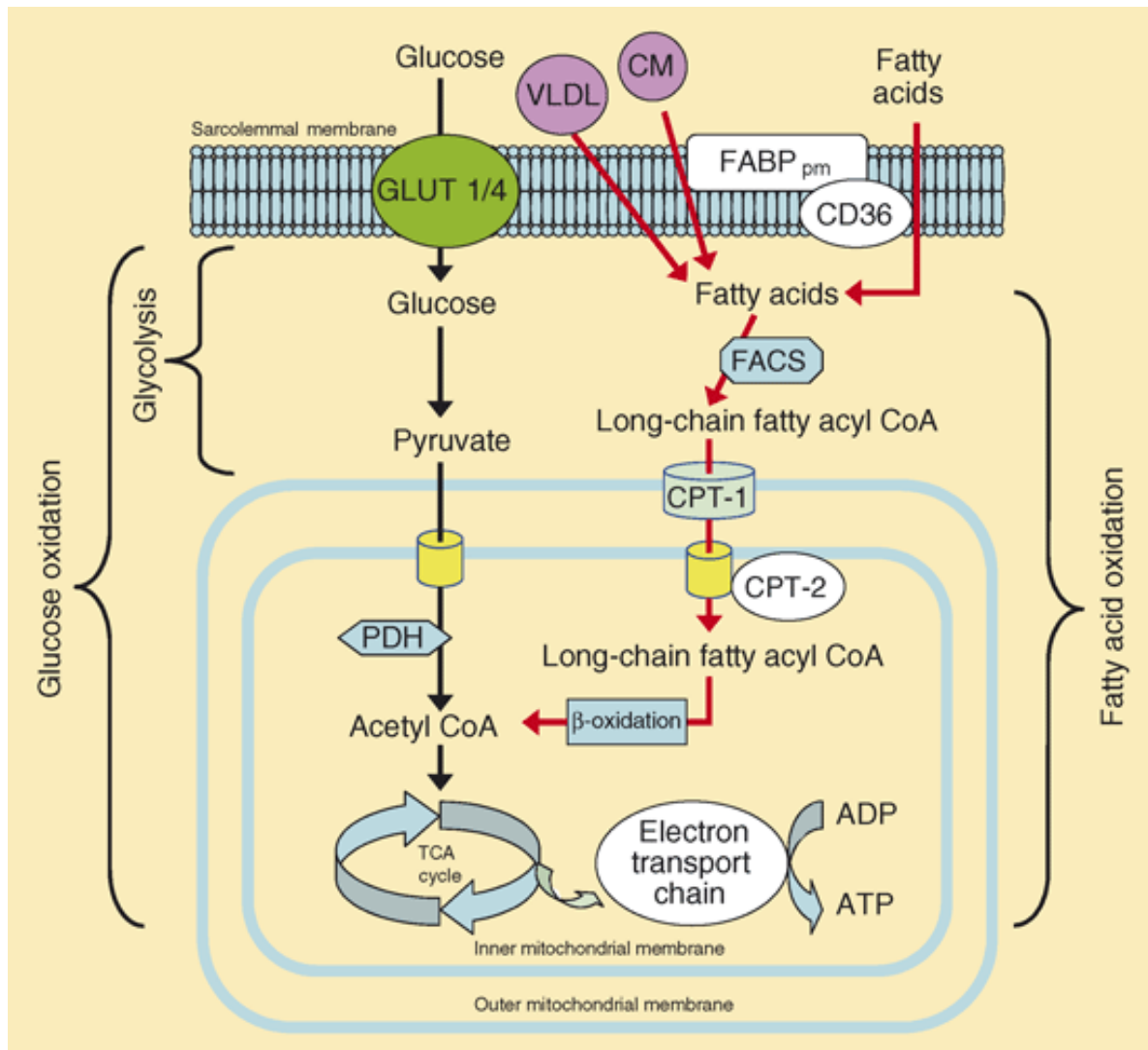


Figure 6: Overview of the major energy producing pathways – Glucose oxidation and Fatty acid oxidation [Ussher et al. 2006]

### **1.7.1 Glucose metabolism**

#### **1.7.1.1 Glucose transporters**

Glucose is removed from the blood by a family of facilitative transporters also known as GLUTs. These transporters catalyze the transport of glucose down its concentration gradient into primarily striated muscle and adipose tissue. There are twelve known glucose transporter isoforms. These GLUT isoforms can be categorised into three classes: (1) Class I comprises GLUT 1-4, (2) Class II comprises GLUT 6, 8, 10 and 12 and (3) Class III comprises GLUT 5, 7, 9 and 11 [Uldry and Thorens 2004].

##### **1.7.1.1.1 Glucose transporter 1**

Glucose transporter 1 (GLUT 1) is a ubiquitously and constitutively expressed membrane spanning protein [Khan and Pessin 2002]. GLUT 1 transporters are insulin-independent glucose transporters, functioning mainly as regulators of basal glucose transport in cardiac myocytes [Kodde et al. 2007]. GLUT 1 transporters are expressed in different levels in almost every kind of tissue but expressed in high levels in especially human erythrocytes and endothelial cells lining the blood vessels of the brain [Maher et al. 1994]. GLUT 1 with the help of GLUT 3, another glucose transporter primarily expressed in neurons facilitate the transport of glucose across the blood-brain barrier and into neurons. [Watson and Pessin 2001].

The transport of glucose by GLUT 1 has been described as an alternating conformer model in which the transporter has mutually exclusive binding sites located on the extracellular and on the intracellular face of the transporter. The binding of glucose to the extracellular/ import site induces the transporter to switch to the opposite conformation allowing glucose to be transported across the plasma membrane and into the cell [Uldry and Thorens 2004]. GLUT 1 in addition to transporting glucose, with a  $K_m$  of  $\sim 3\text{mM}$ , also transports galactose, mannose

and glucosamine [Uldry et al. 2002]. GLUT 1 is sensitive to several inhibitors and the transport activity of this glucose transporter can be inhibited by the intracellular binding of cytochalasin B and forskolin (diterpene toxin) [Baldwin and Lienhard 1989, Morris et al. 1991] and the extracellular binding of  $\text{HgCl}_2$ , phloretin, phlorizin and 4,6-O-ethylidene-D-glucose [Mueckler et al. 1994].

#### **1.7.1.1.2 Glucose transporter 4**

Glucose transporter 4 (GLUT 4) is the main glucose transporter whose translocation is reliant on insulin stimulation and is predominantly found in striated muscle (heart tissue), skeletal muscle and adipose tissue. Under basal conditions, GLUT 4 transporters are sequestered into vesicles in the interior of the cell. Post-prandially, as blood glucose levels rise, the released insulin activates a series of intracellular signalling cascades which results in the translocation of GLUT 4 to the plasma membrane. This process is completely reversible and, as circulating insulin levels reduce, so these glucose transporters are removed from the plasma membrane by a process known as endocytosis and recycled back to their intracellular storage compartments. [Watson and Pessin 2001]

PKB/Akt has been implicated in regulating the translocation of GLUT 4-containing vesicles to the plasma membrane, however PKB/Akt may not be the only downstream kinase involved in this regulation [Le Roith and Zick 2000]. Protein kinase C isoforms  $\zeta$  (zeta) and  $\lambda$  (lambda) are also activated by PI 3-kinase and PDK-1 (phosphatidylinositol dependent kinase -1) and is also involved in the regulation of GLUT 4 translocation [Czech and Corvera 1999]

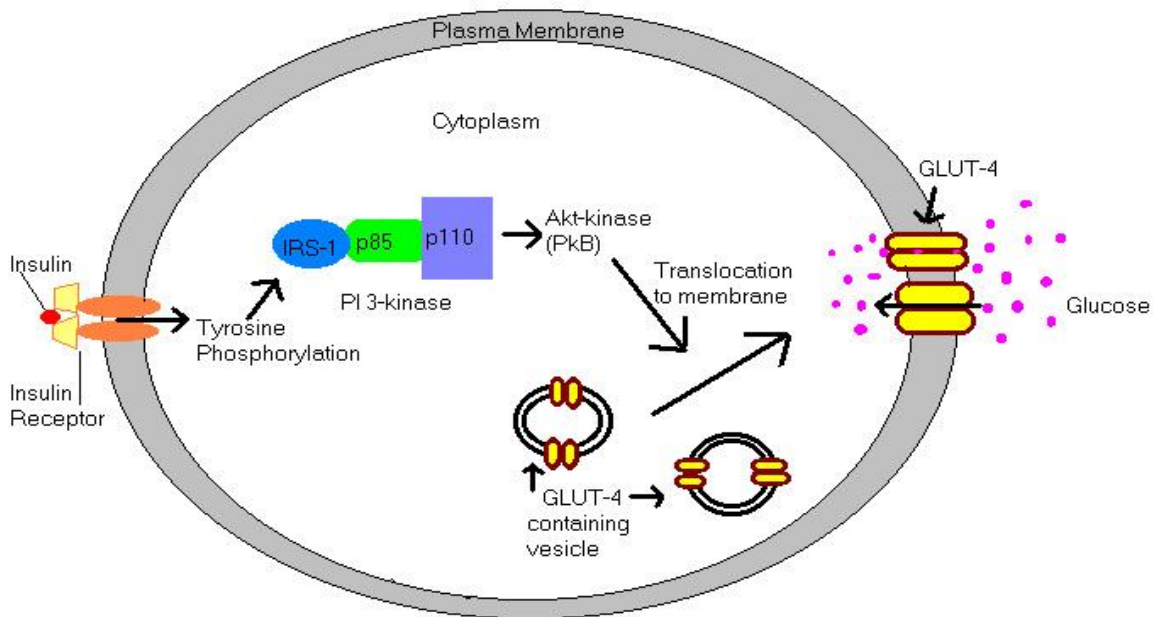


**Figure 7: Insulin-stimulated translocation of GLUT 4-containing vesicles to the plasma membrane to facilitate the transport of glucose into the cell** [<http://student.biology.arizona.edu/honors2003/group05/bg.html>]

#### 1.7.1.2 Pyruvate dehydrogenase complex (PDC)

The PDC is an intramitochondrial enzyme complex [Steinbeck et al. 1986] and is regulated by a phosphorylation/dephosphorylation cycle that is catalyzed by specific pyruvate dehydrogenase kinases (PDKs) and pyruvate dehydrogenase phosphatases (PDPs) [Harris et al. 2001]. The pyruvate dehydrogenase complex

is composed of three enzymes: E1 (pyruvate dehydrogenase), E2 (dihydrolipoamide acetyltransferase) and E3 (dihydrolipoamide dehydrogenase) [Sugden et al. 1995]. PDC plays a very important role in the glucose oxidation pathway by catalyzing the irreversible decarboxylation of pyruvate to acetyl-CoA [SchumMer et al. 2008]. The products, acetyl-CoA and NADH, of this decarboxlation reaction inhibits PDC activity directly as well as by increasing PDK activity [Roche et al. 2001].

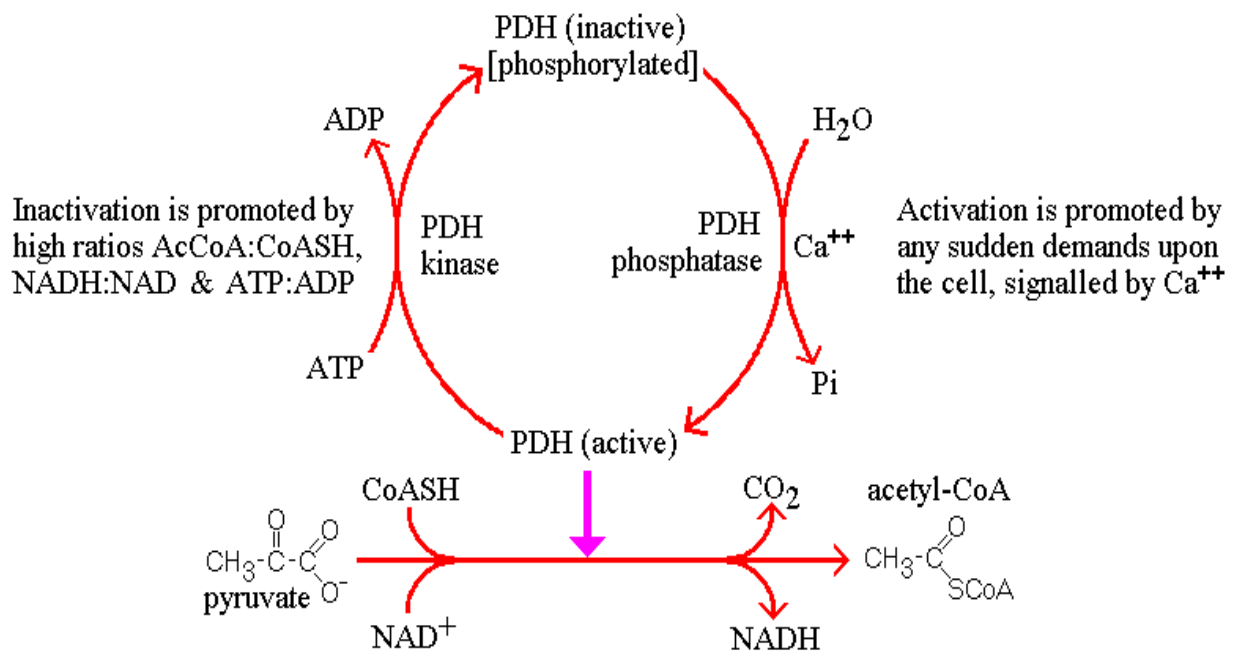


**Figure 8: Regulation of the PDH complex** - is tightly regulated by PDH kinases (PDK 4 specifically in the heart) and PDH phosphatases allowing it to switch between an inactive/phosphorylated and an active/unphosphorylated state. This switch between the inactive and active state is promoted by high ratios of AcCoA, CoASH, NADH:NAD, ATP:ADP and sudden demands upon the cell, signalled by Ca<sup>2+</sup> respectively

[<http://www.bmb.leeds.ac.uk/illingworth/metabol/2120lec3.htm>]

#### **1.7.1.3 Pyruvate dehydrogenase kinase 4 (PDK-4)**

Pyruvate dehydrogenase kinase (PDK) 4 is one of the four isoforms of pyruvate dehydrogenase kinases and is the predominant form of PDKs in the heart and its expression is rapidly induced by peroxisome proliferator activated receptor- $\alpha$  ligands [Bowker-Kinley et al. 1998; Harris RA et al. 2001]. PDK-4 is responsible for the phosphorylation and inactivation of the pyruvate dehydrogenase (PDH), a multienzyme complex located in the mitochondrial matrix responsible for the conversion of pyruvate (the end-product of glycolysis) to acetyl-CoA and NADH, which enters the citric acid cycle and the electron transport chain respectively for the production of ATP. The activity of pyruvate dehydrogenase is regulated by specific pyruvate dehydrogenase kinases (PDKs) and pyruvate dehydrogenase phosphatases.

PDK 4 activity is inhibited by  $\text{NAD}^+$ , CoA, ADP and pyruvate and stimulated by NADH, acetyl-CoA and ATP. In obesity, PDK-4 activity is increased in response to elevated plasma fatty acid levels as an increase in fatty acid  $\beta$ -oxidation results in an increase in PDK-4's stimulants (NADH and Acetyl-CoA) [Stanley et al. 2005].

The resulting decrease in the activity of pyruvate dehydrogenase leads to an increase in the conversion of pyruvate to lactate and eventually to acidosis, which can be very detrimental to the heart.

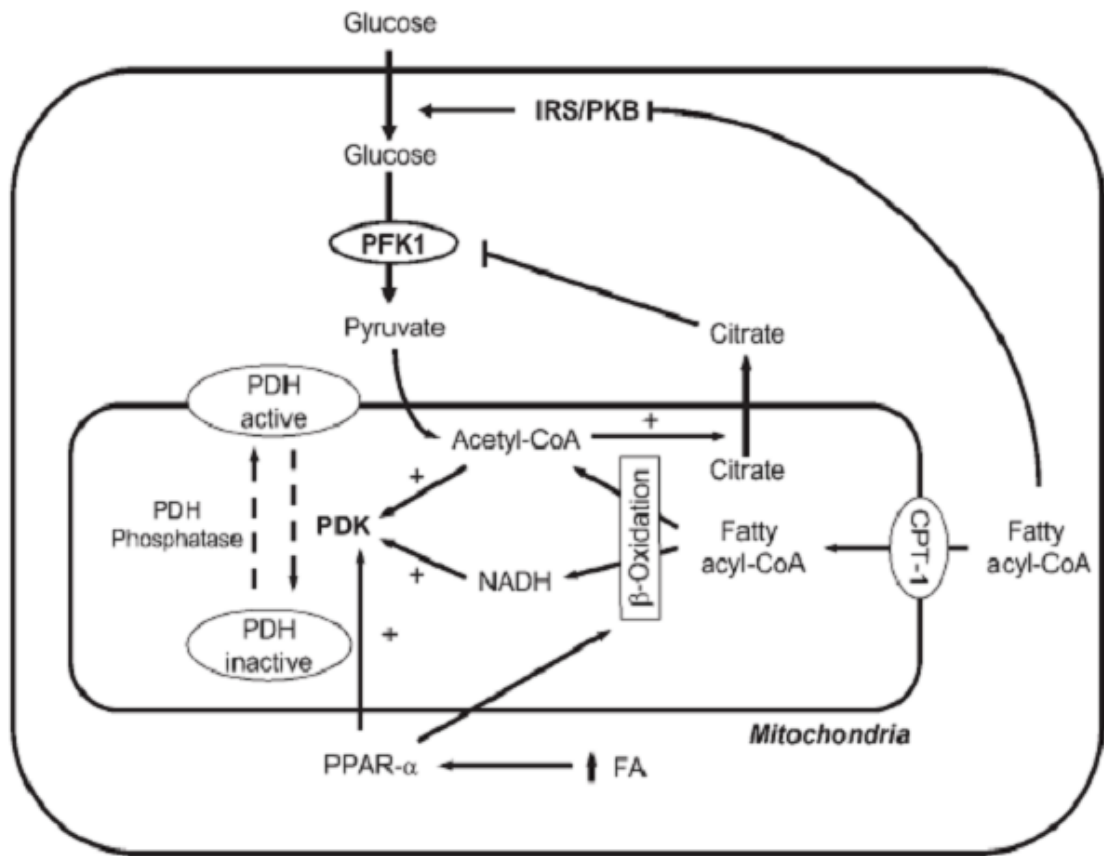


**Figure 9:** An overview of the role of key proteins such as PPAR alpha, PDK 4 and PDC in obesity (i.e. in response to increased plasma free FAs) [An and Rodrigues 2006].

#### 1.7.1.4 Phosphoinositide- 3 kinase (PI3K)

Phosphoinositide 3-kinase plays a key role in the regulation of cell growth and survival, and based on evidence from extensive in vivo and in vitro studies PI3 kinase has also been implicated as a key regulator of cardiac hypertrophy and cell survival and growth [Oudit et al. 2008; Oudit et al. 2004; Alloatti et al. 2004]. There are three classes of PI 3 kinases [Stephens et al. 1993]. Class I PI3 kinases are heterodimeric enzymes composed of a regulatory subunit p85 and a catalytic subunit p110 [Oudit et al. 2004].

PI3 kinase activation by specific insulin receptor substrates leads to the phosphorylation of the phosphatidyl-inositol PtdIns (4,5)P<sub>2</sub> (PIP<sub>2</sub>) to the secondary messenger PtdIns (3,4,5)P<sub>3</sub> (PIP<sub>3</sub>). PIP<sub>3</sub> in turn recruits and activates PDK-1 (phosphatidylinositol dependent kinase 1) which leads to the phosphorylation and activation of PKB/Akt. It has been demonstrated that PKB/Akt has the ability to phosphorylate multiple targets, some of which lead to the activation of pro-survival substrates, such as the prosurvival kinase (RISK) pathways [Hausenloy and Yellon 2004] and the inhibition of specific pro-apoptotic effectors [Mocanu et al. 2006].

#### **1.7.1.5 Phosphatase and tensin homolog on chromosome ten (PTEN)**

PTEN also known as the phosphatase and tensin homologue on chromosome 10 is a dual protein and lipid phosphatase, which negatively regulates the PI3 kinase pathway [Hlobilkova et al. 2003]. It is ubiquitously expressed in all cells and its activity is reflected by its cellular level [Mocanu et al. 2006]. PTEN dephosphorylates PIP<sub>3</sub> back into PIP<sub>2</sub>, thereby promoting the inhibition of pro-survival substrates and activating specific pro-apoptotic effectors.

Not much is known about the role of PTEN in the pathology of the ischaemic myocardium; however it has been shown that PTEN down regulation may be one of the mechanisms responsible for ischaemic preconditioning protection in normal hearts [Cai and Semenza 2005]. Levels of PTEN are increased in diabetic rat hearts [Mocanu et al. 2006] and it has been demonstrated that the inhibition of PTEN in diabetic mice can be associated with a decrease in blood glucose [Butler et al. 2002].



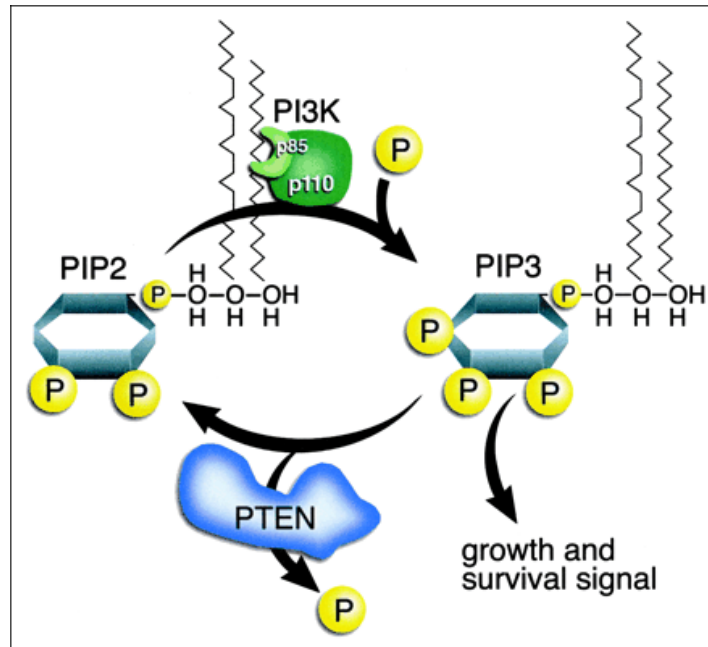


**Figure 10: Schematic representation of the negative regulation of PI 3 kinase through the dephosphorylation of PIP3 to PIP2 by PTEN [Sansel et al. 2004]**

#### 1.7.1.6 Glycogen synthase kinase 3 (GSK-3)

Glycogen synthase kinase 3 is a serine/threonine protein kinase involved in the phosphorylation and inactivation of glycogen synthase [Doble et al. 2003]. GSK-3 has two isoforms namely GSK-3 $\alpha$  and GSK-3 $\beta$  both of which are expressed in the heart [Crackower et al. 2002, Doble and Woodgett 2003, Toker and Cantley 1997, Gross et al. 2004]. Phosphorylation of GSK-3 $\beta$  by PKB/Akt results in the inhibition of GSK-3  $\beta$  which leads to improved cell survival and hypertrophy [Doble and Woodgett 2003, Haq et al. 2000, Antos et al. 2002]. Activation of PKB/Akt by insulin results in the phosphorylation and inactivation of GSK-3, rendering it incapable of inhibiting glycogen synthase activity thereby stimulating glycogen synthesis [Cross et al. 1995]. GSK-3 also inactivates the protein synthesis eukaryotic initiation factor (eIF)-2B (the guanine nucleotide exchange

factor) by phosphorylation. Insulin-mediated activation of PKB/Akt reverses these processes, thereby enhancing protein synthesis [Welsh and Proud. 1993].

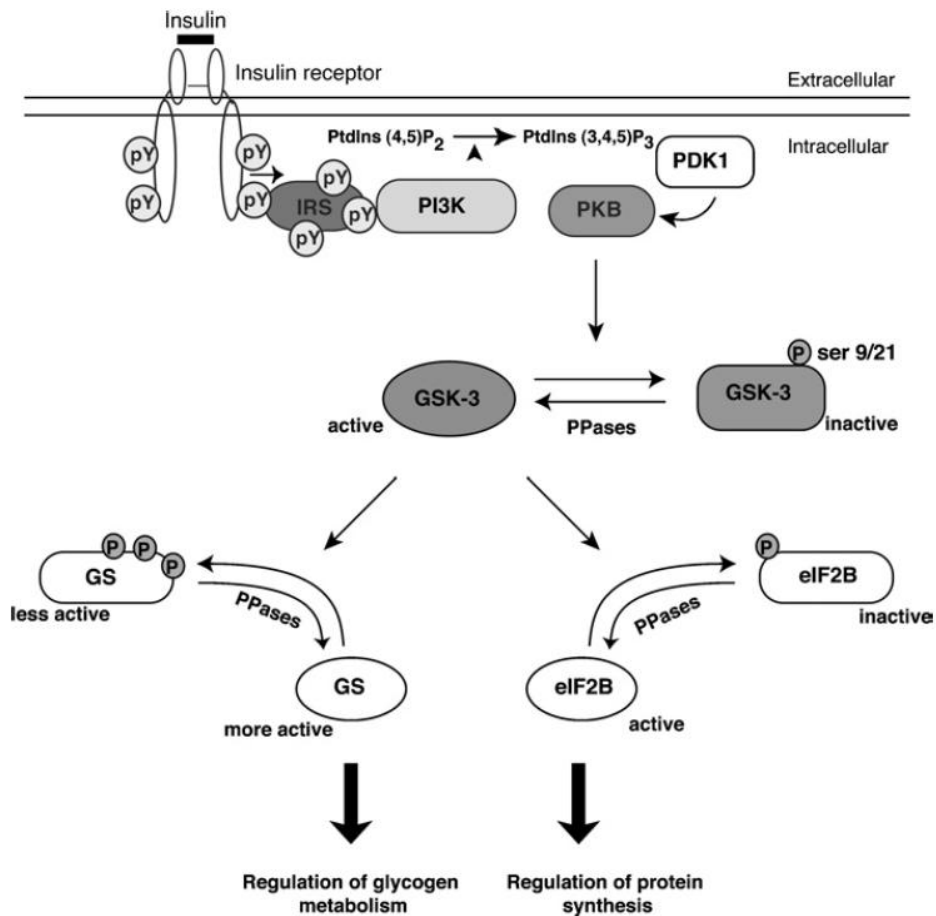


**Figure 11: The regulation of GSK-3 by the insulin signal-transduction pathway** – The binding of insulin to its cell-surface receptor triggers the recruitment and activation of PI 3-kinase. At the plasma membrane PI 3-kinase stimulates the formation of PIP3, which triggers the co-localization of PDK 1 and PKB/Akt, allowing PDK 1 to activate PKB/Akt. Upon activation, PKB phosphorylates and inactivates GSK-3, resulting in the dephosphorylation of glycogen synthase and eIF2B, two substrates of GSK-3 that control the rates of glycogen metabolism and protein synthesis respectively [Patel et al. 2004]

### 1.7.2 Fatty acid metabolism

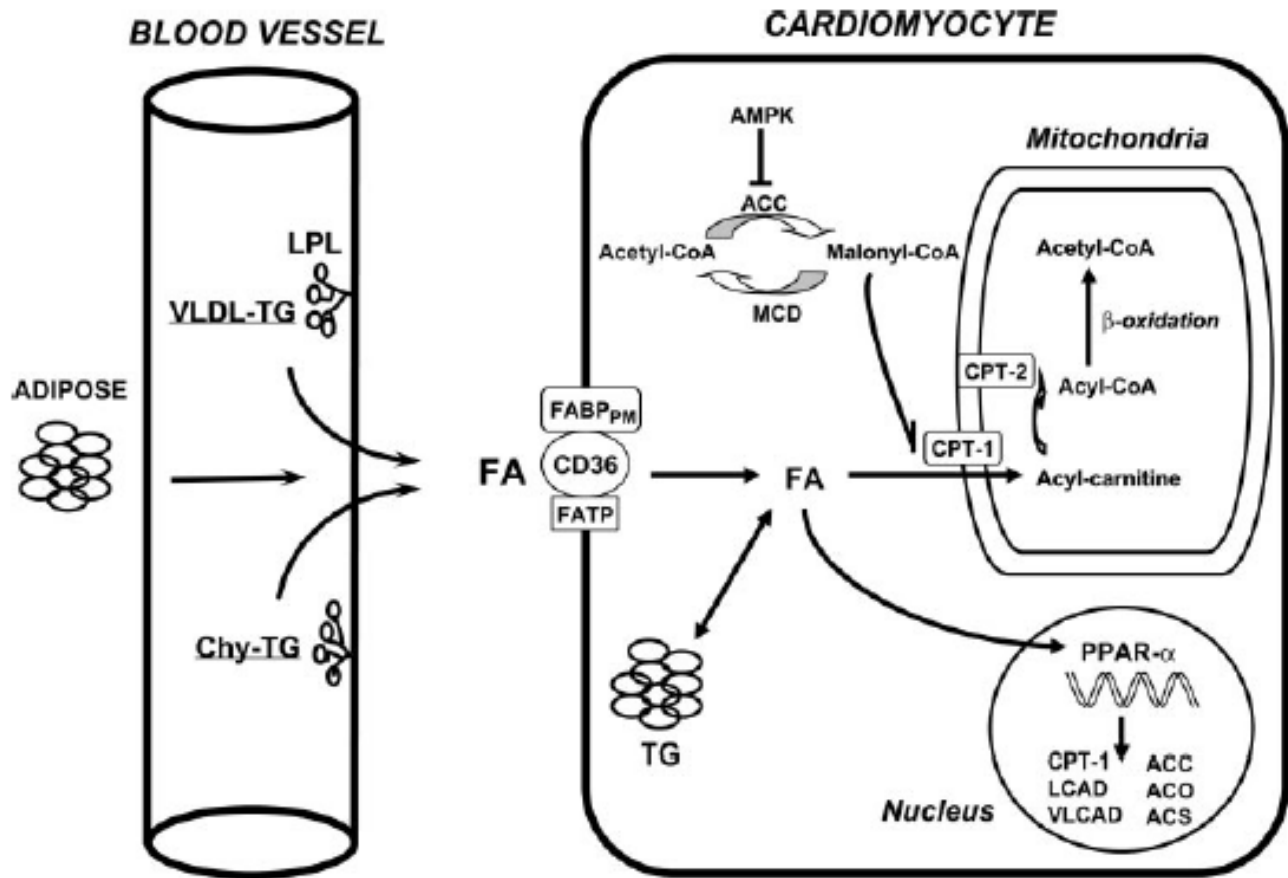


Figure 12: An overview of the key role players involved in FA oxidation [An and Rodrigues 2006].

### **1.7.2.1 Fatty acid translocase/CD 36 (FAT/CD36)**

Under normal/physiological conditions the heart predominantly utilizes long-chain fatty acids for the production of ATP [Glatz et al. 1995; Van der Vusse et al. 1992]. However, before these Long-chain fatty acids can be oxidized it has to be transported across the sarcolemma and into the cardiomyocytes via a protein-mediated transport system [Luiken et al. 1997; Luiken et al. 1999].

Several transport proteins are involved in this process but the exact molecular mechanism of their action is not yet fully understood [Bonen et al. 2002]. One of these transport proteins is the 88 kDa FAT/CD36 protein [Brinkmann et al. 2002]. FAT/CD36, just like the glucose transporter GLUT 4 is present both at the sarcolemma and in intracellular storage compartments [Glatz et al. 2001]. Long-chain fatty acid uptake was significantly inhibited when using the FAT/CD36 blocker sulfo-N-succinimidyl oleate (SSO) [Coort et al. 2002] which demonstrates the involvement of FAT/CD36 in the transport of long-chain fatty acids into the cell. Insulin has been implicated in the translocation of FAT/CD36 to the sarcolemma of cardiac myocytes. Furthermore, Coort et al. 2007 was able to demonstrate that an increased AMPK activity in cardio myocytes is involved in the translocation of FAT/CD36 from its intracellular storage compartments to the sarcolemma [Luiken et al. 2003]. PPAR alpha is a member of the nuclear receptor superfamily and functions as a ligand activated transcription factor [Francis et al. 2003 (a)]. PPAR alpha is highly expressed in the heart [Francis et al. 2003] and FAT/CD36 is one of its target genes [Carley and Severson 2005]. Fatty acids act as endogenous ligands for cardiac PPAR alpha, therefore in obese and diabetic hearts, the increase in fatty acids/ligands for this transcription factor leads to an increase in PPAR alpha expression and the transcription of its target genes such as FAT/CD36 [Barger et al. 2000; Finck 2004, Carley and Severson 2005].

#### **1.7.2.2 Carnitine palmitoyl transferase-1 (CPT-1)**

CPT-1 is an important membrane protein located in the outer mitochondrial membrane [Woldegiorgis et al. 2000]. CPT-1 is involved in the conversion of long-chain fatty acyl-CoA to acylcarnitines, which facilitates the transport of long-chain fatty acids from the cytosol to the mitochondrial matrix for  $\beta$ -oxidation [Bieber 1988, McGarry et al. 1989]. CPT-1 also catalyzes the rate-limiting step in fatty acid-oxidation and is tightly regulated by Malonyl-CoA [Woldegiorgis et al. 2000]. Two isoforms of CPT-1 are expressed in mammalian tissues; a liver isoform (L-CPT1) and a heart/muscle isoform (M-CPT-1) [Woldegiorgis et al. 2000]. The heart expresses both the liver and the M-CPT-1 isoforms [Adams et al. 1998, Zhu et al. 1997]. The L- and M-CPT1 genes are subject to transcriptional activation by PPAR alpha in response to high levels of long-chain fatty acids thereby enhancing fatty acid oxidation, and making long-chain fatty acids regulators of their own metabolism [Brandt et al. 1998].

#### **1.7.2.3 5' Adenosine monophosphate – activated protein kinase (AMPK)**

AMP-activated protein kinase is a heterotrimeric complex composed of catalytic  $\alpha$ -subunits and regulatory  $\beta$ - and  $\gamma$ -subunits and plays a pivotal role in regulating energy balance at the cellular and whole-body level [Hardie 2008]. AMPK activation occurs through phosphorylation of threonine 172 in the catalytic domain by one or more upstream AMPK kinases, one such AMPKK is the recently discovered LKB 1 [Woods et al. 2003].

AMPK is considered to be a “metabolic master switch” [Winder et al. 1999; Hardie and Hawley 2001] and is rapidly activated during myocardial ischaemia [Kudo et al. 1995; Kudo et al. 1996; Marsin et al. 2000] and could potentially be an essential mediator in controlling fatty acid and glucose metabolism during and following ischaemia by shutting down energy consuming processes and

facilitating energy producing processes [Hardie and Hawley 2001]. During ischaemia the increased breakdown of ATP results in an increase in AMP levels [Hardie and Hawley 2001]. As the AMP/ATP ratio increase so does the AMPK activity [Kudo et al. 1995; Kudo et al. 1996].

Myocardial ischaemia incites the heart to rapidly adapt to the restricted oxygen supply and nutrients by switching from aerobic to anaerobic metabolism to maintain the level of ATP necessary for contractile function, ion channel activity and cell integrity [Sambandam and Lopaschuk 2003].

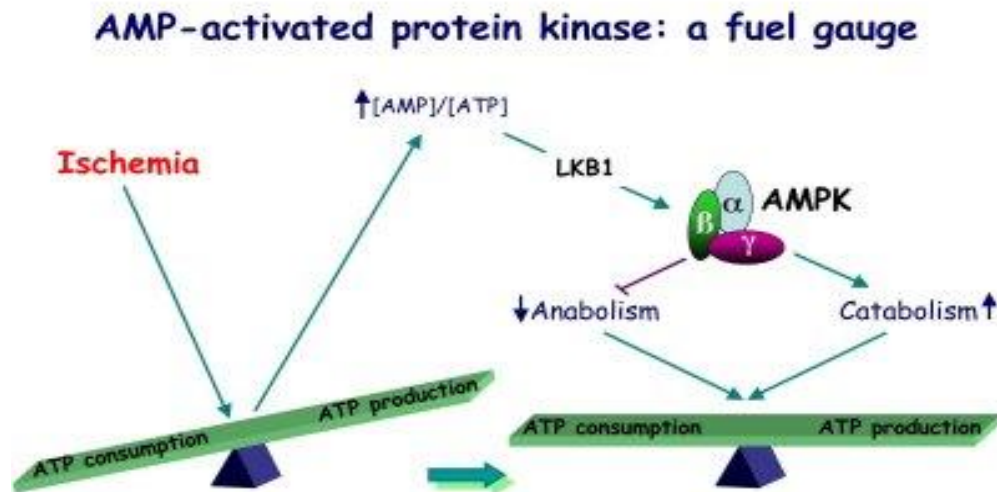


**Figure 13: AMPK as a cellular energy sensor that controls metabolic pathways [http://www.card.ucl.ac.be/BasicResearchP1.html]**

#### **1.7.2.3.1 AMPK and glucose uptake during ischaemia**

Following an ischaemic insult the heart becomes less efficient at converting energy into contractile function [Lopaschuk and Stanley 1997], because FA oxidation dominates over glucose oxidation as the main source of mitochondrial metabolism and overall ATP production. However, during ischaemia the uptake of glucose as well as glycolysis increase which results in an increase in proton

production [Dennis et al. 1991, Hochachka and Mommsen 1983] as a consequence of the uncoupling of glycolysis and glucose oxidation. Energy dedicated to contractile function is then used to re-establish ionic homeostasis.

The preferential use of FAs as a source of fuel during and following ischaemia is the result of two factors including 1) an increase in the levels of circulating FAs [Mueller et al. 1978, Lopaschuk et al. 1994] and 2) decreased control of FA metabolism as a result of subcellular changes in the heart [Kudo et al. 1995, Kudo et al. 1996, Saddik et al. 1993]. One such important subcellular change is the decrease in malonyl-CoA (an endogenous inhibitor of FA oxidation) levels which leads to the dysregulation of FA oxidation [Kudo et al. 1995, Kudo et al. 1996, Saddik et al. 1993, Dyck et al. 1998]. Malonyl-CoA levels are regulated by the rates of two enzymes, acetyl-CoA carboxylase (ACC) and malonyl-CoA decarboxylase (MCD). ACC and MCD are involved in the synthesis and degradation of malonyl-CoA respectively and the activity of these two enzymes are controlled by AMPK which is activated during ischaemia. This activation of AMPK results in a decrease in malonyl-CoA levels which subsequently leads to a loss in mitochondrial FA uptake control [Hopkins et al. 2003 (b)].

#### **1.7.2.3.1.1 Control of FA oxidation by malonyl-CoA**

Malonyl-CoA regulates FA oxidation by the inhibition of CPT-1, which leads to a reduction in mitochondrial FA oxidation rates. As previously mentioned, malonyl-CoA is synthesized from acetyl-CoA by ACC [Saddik et al. 1993, Bianchi et al. 1990], and degraded through decarboxylation by the MCD enzyme [Dyck et al. 1998, Dyck et al. 2000]. Malonyl-CoA plays an important metabolic signalling role in the heart and therefore it has to be degraded rapidly with a half-life of only 1.25 min [Reszko et al. 2001].

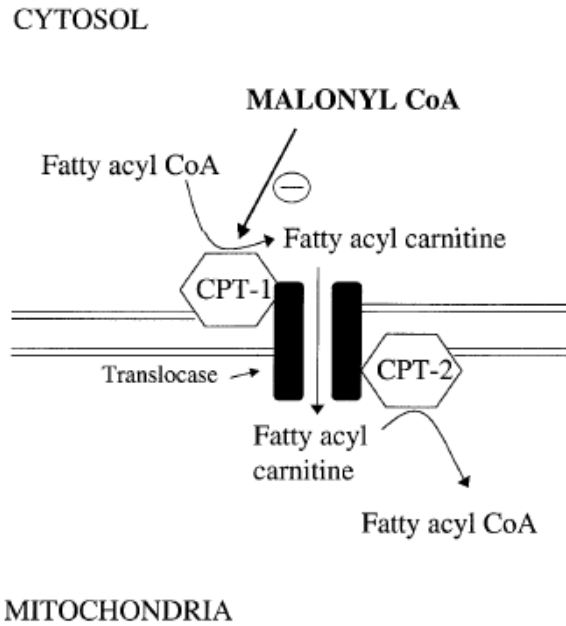


**Figure 14: Schematic representation of the inhibition of CPT-1 by malonyl-CoA [Hopkins et al. 2003 (b)]**

#### **1.7.2.3.1.1.1 Synthesis of malonyl-CoA**

Two isoforms of ACC, ACC alpha and ACC beta, are present in the heart [Abu-Elheiga et al. 1997] of which ACC beta is directly involved in the regulation of FA oxidation [Abu-Elheiga et al. 2000], allowing the synthesis of malonyl-CoA to occur in close physical proximity to CPT-1 to enable the direct inhibition of this mitochondrial transporter. Additionally, evidence from various studies suggests that ACC beta is an important regulator of FA oxidation in cardiac myocytes [Makinde et al. 1997], and that it plays an important role in the regulation of FA oxidation rates in the heart.

#### **1.7.2.3.1.1.2 Degradation of malonyl-CoA**

MCD is the enzyme responsible for the degradation of malonyl-CoA to acetyl-CoA and an increase in the activity of this enzyme has been shown to decrease malonyl-CoA levels and increase FA oxidation in the reperfused ischaemic heart



[Dyck et al. 1998]. Studies using a streptozotocin-induced diabetic rat heart model have shown an increase in the activity and expression of MCD [Sakamoto et al. 2000], as well as an increase in mRNA expression during high-fat feeding, fasting and streptozotocin-induced diabetes [Young et al. 2001]. This suggests a role for MCD in altering energy metabolism.

#### **1.7.2.3.1.2 The role of AMPK in the regulation of malonyl-CoA levels**

As previously mentioned the activity of ACC and MCD in the heart are both under phosphorylation control of AMPK [Hopkins et al. 2002 (b)], making AMPK a key role player in the regulation of malonyl-CoA levels as well as FA oxidation in the heart.

AMPK is activated by the AMP/ATP ratio and the creatine/phosphocreatine ratio [Ponticos et al. 1998]. However, in the heart, the activity of AMPK can be altered under conditions where significant alterations in the AMP/ATP ratio do not occur [Beauloye et al. 2001], such as in the case of where insulin has been shown to inhibit AMPK kinase (a kinase known to phosphorylate and significantly increase the activity of AMPK [Hardie and Carling 1997]) activity in isolated perfused hearts, specifically under conditions where the AMP/ATP and creatine/phosphocreatine ratios did not change [Beauloye et al. 2001].

In the heart AMPK acts as a metabolic sensor which is activated during metabolic stress such as hypoxia when ATP levels are low [Hopkins et al. 2003 (b)]. AMPK is also a key role player in the regulation of FA oxidation in myocardium by increasing the rates of FA oxidation when ATP levels are low, and decreasing FA oxidation when ATP levels are high. This regulation is accomplished through the modulation of ACC and MCD [Hopkins et al. 2003 (b)].

Various studies have shown a close correlation between the phosphorylation and inactivation of ACC which leads to decreased synthesis of malonyl-CoA, relieving the inhibition of CPT-1-mediated uptake of mitochondrial FAs [Park et al. 2002].

Studies have shown that AMPK activation in cardiac cells results in the translocation of overexpressed MCD from the cytoplasm to the mitochondria [Hopkins et al. 2003 (b)]. Whether or not AMPK is responsible for the direct phosphorylation of cardiac MCD remains unclear [Hopkins et al. 2003 (b)].

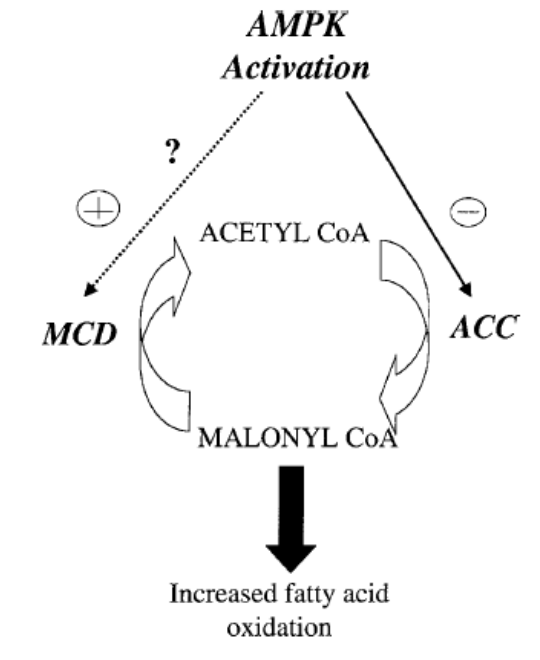


**Figure 15: AMPK activation and subsequent phosphorylation of ACC and possibly MCD leads to an alteration in the levels of malonyl-CoA and subsequently increases FA oxidation [Hopkins et al. 2003 (b)]**

#### **1.7.2.3.1.3 The role of AMPK during ischaemia/reperfusion**

AMPK is responsible for the increase in both FA oxidation and glycolysis during ischaemia/reperfusion to increase the production of energy in response to the high energy demand under these conditions [Hopkins et al. 2003 (b)]. Ischaemia has been shown to cause a rapid increase in the phosphorylation and activity of AMPK [Kudo et al. 1995]. Increased phosphorylation and activation of AMPK may increase myocyte glucose utilization by increasing the uptake of glucose, through increased translocation of GLUT 4 to the sarcolemma of the myocyte

[Russel RR 3<sup>rd</sup> et al. 1999], or by increasing the rate of glycolysis through increased phosphorylation and activation of phosphofructokinase-2 which produces fructose 2, 6-bisphosphate (potent activator of glycolysis) [Marsin et al. 2000]. Additionally AMPK also increase FA oxidation rates [Hopkins et al. 2003 (b)]. The activation of AMPK during ischaemia leads to the preferential use of FAs as a substrate of residual oxidative metabolism, and an increase in the production of lactate and protons (deleterious glycolytic by-products) as a result of FA-inhibition of glucose oxidation [Hopkins et al. 2003 (b)].

Increased AMPK activity continues during reperfusion of the myocardium [Kudo et al. 1995], continuing the exposure to high levels of circulating FAs. The rates of FA oxidation recovers [Lerch et al. 1992] and glycolytic rates remain elevated [McVeigh and Lopaschuk 1990]. This results in a greater uncoupling between glycolysis and glucose oxidation and subsequent proton production [Liu et al. 1996], and reduced recovery of the pH level post reperfusion [Liu et al. 2002]. ACC activity is reduced and malonyl-CoA levels reduced [Kudo et al. 1995]. The reduction in malonyl-CoA levels could explain the high rates of FA oxidation that occurs during reperfusion [Kudo et al. 1995]. The levels of MCD however are maintained [Dyck et al. 1998], resulting in a net decrease in steady-state malonyl-CoA levels. During this time the balance between the synthesis of malonyl-CoA and its degradation is shifted towards its breakdown which may relieve the inhibition of CPT-1. This increase in the transport of FAs into the mitochondria together with higher levels of circulating FAs may lead to enhanced ischaemic damage of the myocardium [Hopkins et al. 2003 (b)].

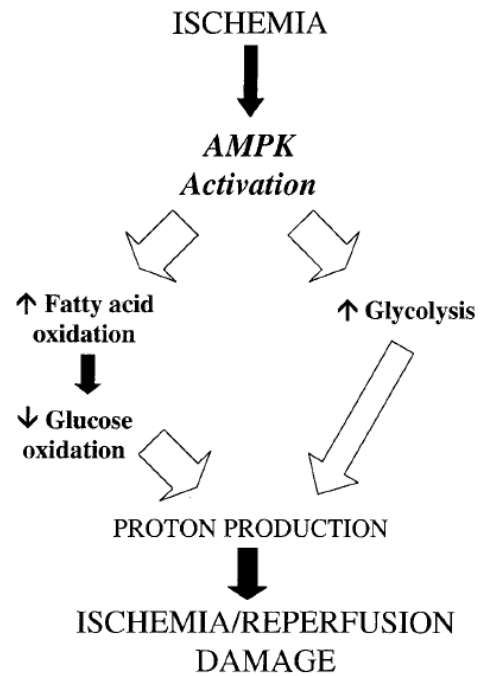


**Figure 16: Activation of AMPK in response to ischaemia which leads to ischaemia/reperfusion damage through increased FA oxidation and glycolysis and reduced glucose oxidation [Hopkins et al. 2003 (b)]**

## **1.8 THE ROLE OF MITOCHONDRIA IN MYOCARDIUM**

### **1.8.1 Mitochondrial ATP production**

Mitochondria are membrane-enclosed organelles distributed throughout the cytosol of most eukaryotic cells [Henze and Martin 2003]. In muscle cells the mitochondria are situated underneath the cell membrane and in between the myofibrils [Palmer et al. 1977]. Mitochondria are responsible for producing the majority of the energy (ATP) in the cell [Bindoff 2003]. The process of aerobic respiration occurs in the mitochondria in the presence of oxygen and relies on processes such as pyruvate decarboxylation, the citric acid cycle, the electron transport chain and oxidative phosphorylation for the production of ATP.

### 1.8.1.1 Pyruvate decarboxylation:

Pyruvate decarboxylation is a reaction, generally catalyzed by the pyruvate dehydrogenase complex, which uses pyruvate to form acetyl-CoA, releasing NADH and carbon dioxide via decarboxylation. This reaction takes place in the mitochondrial matrix and usually acts as an important link between the anaerobic metabolic pathway, glycolysis, and the aerobic citric acid cycle [Molecular Biology of the Cell, 4<sup>th</sup> Edition, Alberts B, Johnson A, Lewis J, Raff M, Roberts K, Walter P 2002].

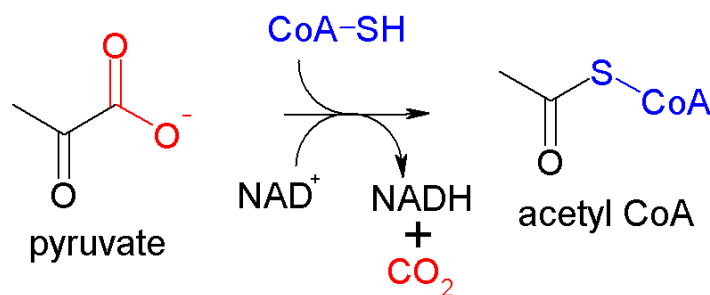


**Figure 17: Schematic representation of the conversion of pyruvate to acetyl-CoA by the pyruvate dehydrogenase complex enzyme [http://comMons.wikimedia.org]**

### 1.8.1.2 Citric acid cycle

The citric acid cycle is composed of a series of enzyme-catalysed chemical reactions that occur in the matrix of the mitochondrion. Acetyl-CoA produced from pyruvate decarboxylation is used by the citric acid cycle to ultimately produce two molecules of ATP, six molecules of NADH, two molecules of QH<sub>2</sub> (Q-electron acceptor), and four molecules of CO<sub>2</sub> per glucose molecule. [Wolfe and Farook 1990]

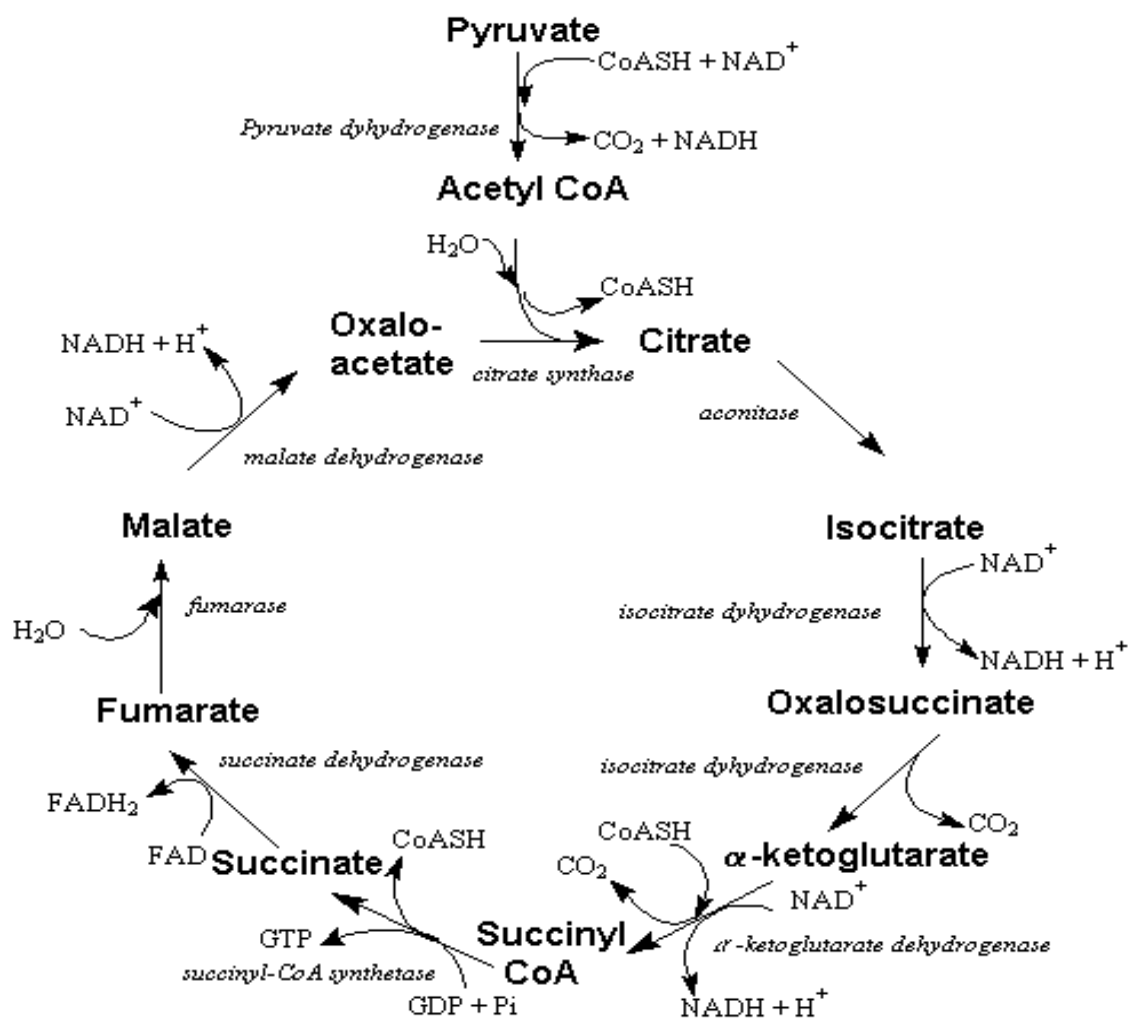


**Figure 18: Schematic representation of the citric acid cycle** [[http://www.uic.edu/classes/phar/phar332/Clinical\\_Cases/vitamin%20cases/thiamin/thiamin\\_pyrophosphate.htm](http://www.uic.edu/classes/phar/phar332/Clinical_Cases/vitamin%20cases/thiamin/thiamin_pyrophosphate.htm)]

### 1.8.1.3 Oxidative phosphorylation:

The electron transport chain is the site of oxidative phosphorylation, where the  $\text{NADH}$  and succinate generated in the citric acid cycle are oxidized [Schultz and Chan 2001]. The energy released from this process is used to power the ATP synthase enzyme. During oxidative phosphorylation, electrons are transferred

from electron donors to electron acceptors such as oxygen. These reactions are called redox reactions [Matthews 1985].

The electron transport chain is a series of five protein complexes linked together in the mitochondrial inner membrane. The energy released by the flow of electrons through the chain, or redox reactions, is used to create a proton gradient across the inner mitochondrial membrane in a process called chemiosmosis [Mitchell and Moyle 1967]. Chemiosmosis creates potential energy in the form of a pH gradient and an electrical potential across this membrane. The flow of protons back across the membrane down this gradient through the ATP synthase enzyme uses this energy to generate ATP [Mitchell and Moyle 1967].



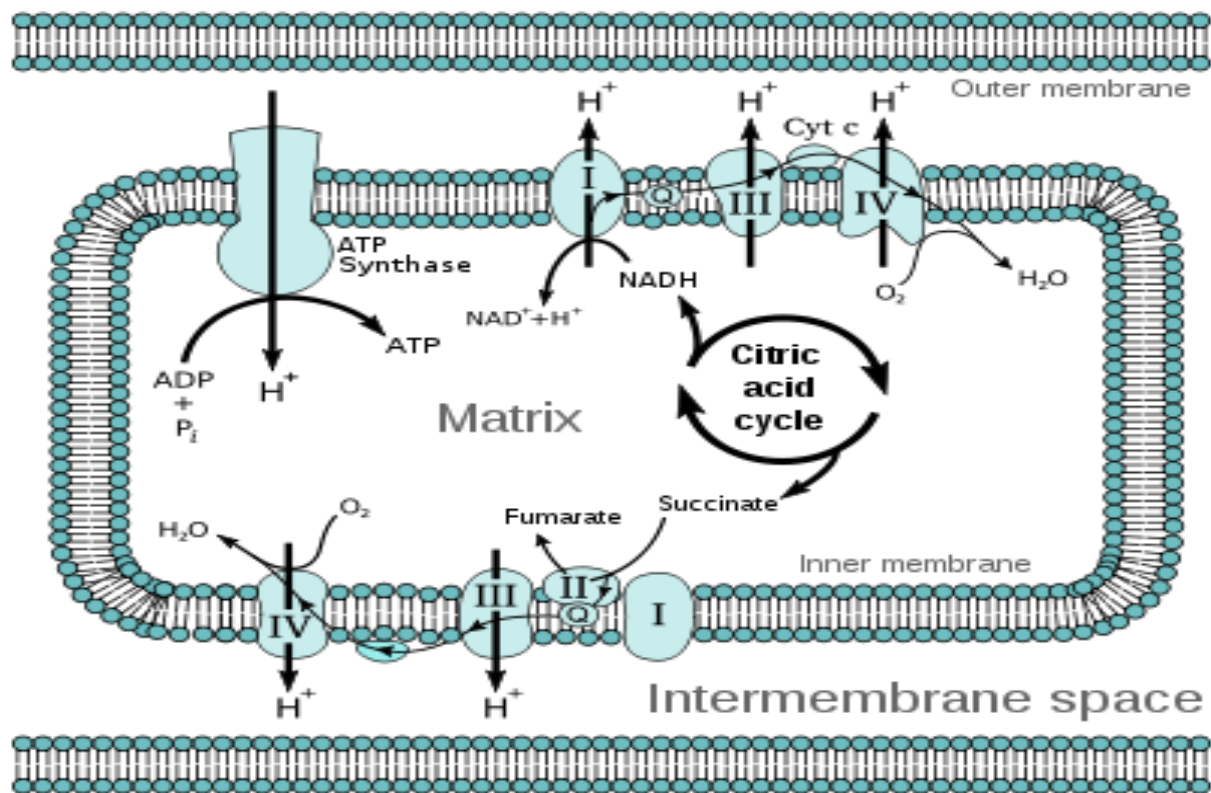


**Figure 19: This schematic represents an overview of mitochondrial oxidative phosphorylation.** The phosphorylation of ADP to ATP at complex V (ATP synthase) is driven by a proton gradient across the inner mitochondrial membrane. The oxidation of carbon substrate in the TCA cycle generates reducing equivalents that subsequently provide electron flow to the electron transport system. Electrons are transferred from NADH through complex I (NADH dehydrogenase) and oxidation of succinate by complex II (succinate dehydrogenase). Electron flow from other sources such as electron transferring flavoprotein is not shown.

[[http://flaggedrevs.labs.wikimedia.org/wiki/Oxidative\\_phosphorylation](http://flaggedrevs.labs.wikimedia.org/wiki/Oxidative_phosphorylation)]

#### 1.8.1.4 Electron transport chain complexes I-IV:

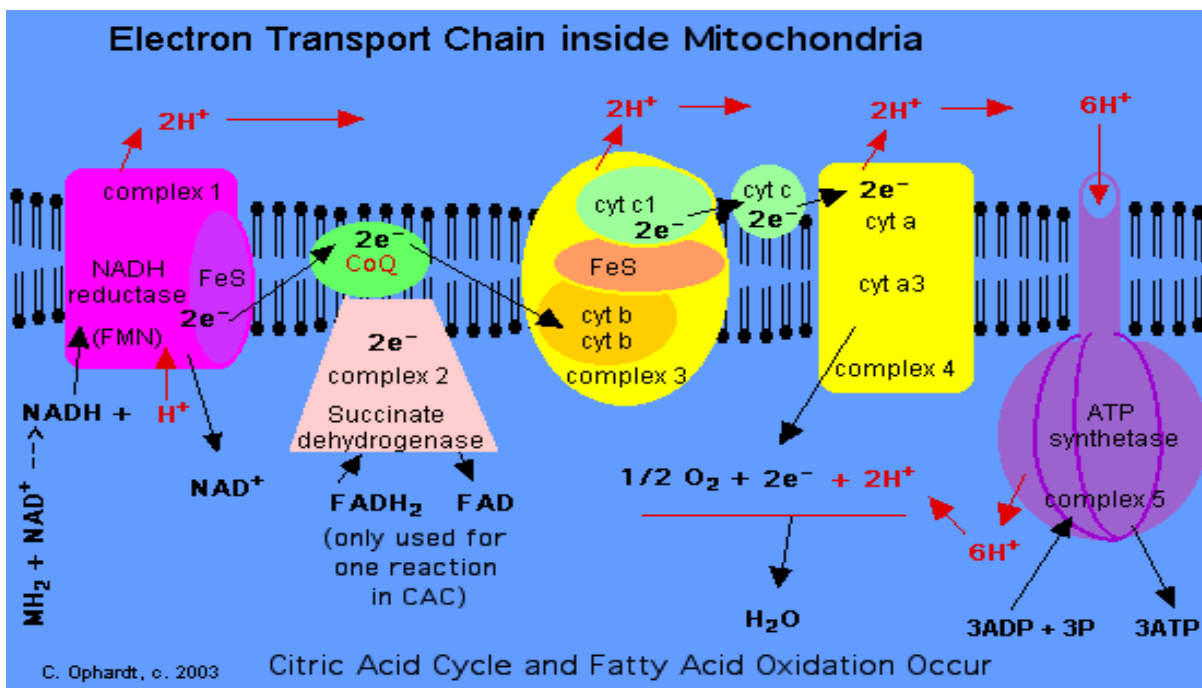


Figure 20: Overview of the electron transport chain. [http://www.elmhurst.edu/~chm/vchembook/596electransport.html]

#### 1.8.1.4.1 The production of ATP by the electron transport chain

NADH and another hydrogen ion enter complex I and pass along the 2 hydrogen ions to the interspace in the mitochondria. These 2 hydrogen ions act as a proton pump and are utilized by ATP synthetase to produce an ATP for every two hydrogen ions produced. Complex 3 and 4 also act in this manner, producing 2 hydrogen ions each thus generating 3 molecules of ATP for every use of the complete electron transport chain. In addition NADH passes along 2 electrons to first FMN, then to an iron-sulfur protein FeS and finally to coenzyme Q. The net effects of these reactions are to regenerate coenzyme  $\text{NAD}^+$  which is ready to react with metabolites in the citric acid cycle creating a cycling effect.

Coenzyme Q picks up an additional 3 hydrogen ions in order to produce  $\text{CoQH}_2$ . Coenzyme Q is also lipid soluble and can therefore move through the membrane to come into contact with enzyme complex III. Coenzyme  $\text{QH}_2$  carrying an extra 2 electrons and 2 hydrogen ions now starts a cascade of events through enzyme complex III (cytochrome reductase bc).

Cytochromes contain a heme structure which contains iron ions. These iron ions, initially present in the +3 state, are changed to the +2 state by the addition of an electron. The Coenzyme  $\text{QH}_2$  passes along the 2 electrons first to cytochrome b1 heme, then b2 heme, then to an iron-sulfur protein, then to cytochrome c1 and finally cytochrome c, while releasing another two hydrogen ions into the mitochondrial interspace. Cytochrome c is also capable of moving through the lipid membrane layer and diffusing toward complex IV which is also known as cytochrome c oxidase. This complex is responsible for the removal of two electrons from two molecules of cytochrome c and transferring them to molecular oxygen, producing a molecule of water while simultaneously moving two protons across the membrane producing a proton gradient. These final hydrogen ions are then used together with the previously released four hydrogen ions to ultimately produce ATP. The final step towards the production of ATP is the ATP synthetase enzyme which can be found at numerous locations in the bilayer membrane of the mitochondria. The proton gradient created by the efflux of hydrogen ions into the mitochondrial interspace is used by the  $\text{F}_0\text{F}_1$  ATP synthase complex to produce ATP via oxidative phosphorylation. The  $\text{F}_0$  component of the ATP synthase acts as an ion channel for return of protons back to the mitochondrial matrix, during which free energy, produced during the generation of the oxidized forms of the electron carriers  $\text{NAD}^+$  and Q, is released. This free energy is then used to drive ATP synthesis by the  $\text{F}_1$  component of the ATP synthase.

#### **1.8.1.4.1.1 Complex I:**

Complex I, also known as NADH reductase contains a coenzyme flavin mononucleotide (FMN) which is similar to FAD. NADH is a metabolite produced by the citric acid cycle which interacts with the complex I enzyme of the electron transport chain. Complex I is responsible for removing 2 electrons from NADH and transferring them to a lipid-soluble carrier known as ubiquinone (Q). This reduced product, ubiquinol (QH) is free to diffuse within the membrane while Complex I is simultaneously moving 4 protons across the membrane, producing a proton gradient. Complex I produces a lot of harmful free radicals due to the high incidence of premature electron leakage to oxygen.

#### **1.8.1.4.1.2 Complex II:**

Complex II, unlike complex I, is not a proton pump but a succinate dehydrogenase enzyme which funnels additional electrons in to the quinine pool (Q) by removing electrons from succinate and transferring them via FAD to Q. Other electron donors such as fatty acids also funnel electrons into Q via FAD, also without creating a proton gradient.

#### **1.8.1.4.1.3 Complex III:**

Complex III or the cytochrome bc1 complex is responsible for the stepwise removal of two electrons from QH<sub>2</sub> at the Q<sub>o</sub> site and the sequential transfer of these two electrons to two molecules of cytochrome c. Cytochrome c is a water-soluble electron carrier located within the intermembrane space. Complex III like complex I may leak electrons to oxygen resulting in the formation of reactive oxygen species.

Therefore although oxidative phosphorylation plays a crucial role in the production of ATP, which is a vital part of the metabolism, it also produces large

amounts of reactive oxygen species such as superoxide and hydrogen peroxide which may cause damage to cells and can ultimately lead to cell death [Gill et al. 2002].

Although mitochondria are the main site for ATP generation in most tissues, mitochondria also participate in a number of alternative activities such as intracellular calcium regulation, thermogenesis and the control of apoptosis [Kowaltowski 2000].

### **1.8.2 Pathophysiology associated with impaired mitochondrial ATP production**

Mitochondria play a critical role in cellular function. They are responsible for the majority of the ATP production of the cell and play a number of other important roles such as the regulation of energy expenditure, apoptosis signaling, and the production of reactive oxygen species [Lanza et al. 2009]. Mitochondria are the main site for the generation of reactive oxygen species (ROS), such as hydrogen peroxide, with complex III of the electron transport chain being the dominant site for its production [Chen et al. 2007].

Cardiac ischaemia causes damage to the mitochondrial electron transport chain [Lesnefsky et al. 2001 (b); Lesnefsky et al. 1997; Rouslin 1983], and mitochondrial dysfunction contributes to myocardial injury during ischaemia and reperfusion [Lesnefsky et al. 2001 (b); Chen et al. 2007].

An alteration in mitochondrial function has also been implicated as the underlying cause of several pathological states, such as mitochondrial disorders [Gardner and Boles 2005], cardiac dysfunction [Lesnefsky et al. 2001 (b)] as well as the aging process [Lanza et al. 2009]. Therefore it is of great importance to understand their involvement in these disorders. The implementation of direct

measurements of mitochondrial function and oxidative capacity of isolated mitochondria will provide valuable information in the pursuit to this understanding.

A lot of controversy exists surrounding the relationship between insulin resistance and mitochondrial function. To elucidate this relationship Asmann and his colleagues investigated this relationship and found that insulin is a key regulator of mitochondrial function and impaired insulin signalling is a potential mechanism by which mitochondrial dysfunction manifests in insulin resistant individuals [Asmann et al. 2006]. Furthermore it was demonstrated that insulin stimulates mitochondrial ATP production rates in healthy controls but not in insulin resistant individuals [Stump et al. 2003].

## **1.9 CARDIOPROTECTION**

Type 2 diabetes mellitus is closely correlated with the malfunctioning of the intracellular insulin signalling pathway [Kondo and Kahn 2004]. It has been demonstrated that the PI3 kinase/Akt pathway, plays an important role in cardioprotection when activated during ischemia/reperfusion [Hausenloy and Yellon 2004].

### **1.9.1 The role of mitochondrial biogenesis in cardioprotection**

Recent evidence suggests that impaired mitochondrial function plays an immense role in the underlying pathogenesis of insulin resistance and Type II diabetes and that PGC-1 alpha, being the key regulator of mitochondrial biogenesis, could play an important role in restoring mitochondrial function and oxidative capacity through its activation [Wu and Boss 2007]. As previously mentioned, mitochondrial biogenesis is PPAR alpha-PGC-1 alpha driven. A recent study conducted by Duncan et al. [2007] looked at mitochondria in the hearts of insulin resistant UCP-DTA (insulin-resistant uncoupling protein-diphtheria toxin A ) transgenic mice, a murine model of metabolic syndrome, and found that

there was a significant increase in the levels of expression of both PPAR-alpha and PGC-1 alpha as well as a significant increase in the number of mitochondria present between the myofibrils, mitochondrial volume density, mitochondrial DNA content, and the expression of nuclear and mitochondrial genes involved in energy transducing and ATP synthetic pathways. It is likely that this mitochondrial biogenic response that occurs during the initial stages of insulin resistance, before the onset of Type II Diabetes, is aimed at increasing the heart's capacity for ATP generation as a potentially adaptive response, but will eventually become maladaptive with the onset of diabetes. These findings provide important insight into the role metabolic derangements play in the pathogenesis of heart failure due to common diseases such as atherosclerosis, hypertension and diabetes. And that PPARs or, perhaps more likely, downstream metabolic pathways could act as possible targets for new therapeutics aimed at normalizing cardiac fuel metabolism in order to prevent or possibly treat cardiovascular diseases [Madrazo and Kelly 2008].

Mitochondrial biogenesis is a complex process that involves the synthesis, import, and incorporation of protein as well as lipids to the existing mitochondrial reticulum, and the replication of the mitochondrial DNA [Hock and Kralli. 2009].

## 1.10 ADAPTIVE AND MALADAPTIVE RESPONSES OF THE HEART:

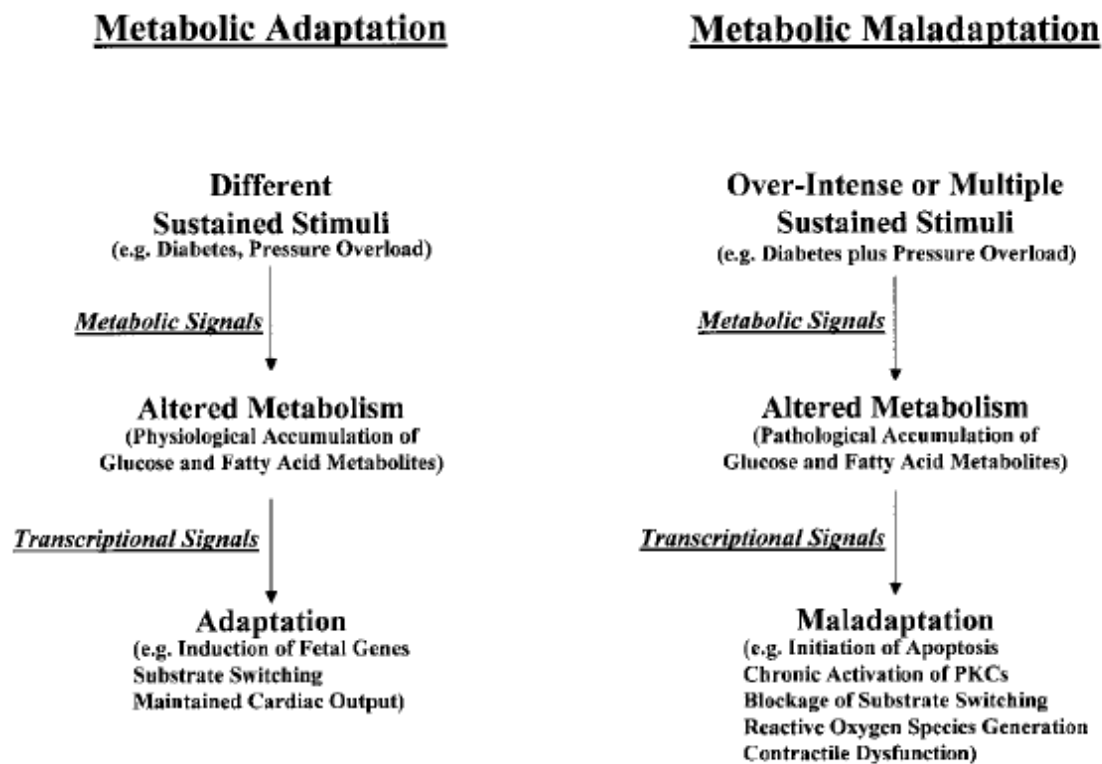


**Figure 21: Metabolic adaptation and maladaptation of the heart.** Various stimuli can result in rapid alterations in fatty acid and glucose metabolites within the cardiomyocytes. These metabolites then act as essential signalling molecules for the adaptation process. However, if the intensity of the stimulus is too great, or multiple stimuli act simultaneously (e.g. pressure overload plus diabetes), pathological accumulation of metabolites results in metabolic maladaptation [Young et al. 2001].

The heart's response to alterations in its environment is an intricate network of interconnecting signal transduction cascades [Sugden and Clerk 1998]. The concept of alterations in the metabolic flux within the cell aimed at creating essential signals for the adaptation of the heart to disorders such as diabetes that cause metabolic dysregulation has been considered in the liver and is novel for



the heart [Young et al. 2001]. These changes in metabolic flux occur rapidly and are brought about by the same signal transduction cascades allegedly involved in the adaptation of the heart to changes in its environment [Young et al. 2001]. Certain key metabolic proteins such as PI3 kinase,  $\text{Ca}^{2+}$  and PKC, which play a crucial role in cardiac adaptation, are involved in the regulation of metabolism in the heart as well [Doenst and Taegtmeyer 1999; Cohen 1979] suggesting that metabolic remodelling could possibly be involved in cardiac adaption.

### **1.10.1 Metabolic adaptation**

Metabolic adaptation appears to be fundamental for the preservation of contractile function of the heart under different stresses such as diabetes. Metabolic adaptation involves the alteration of contractile protein gene expression to the re-expression of fetal genes with concomitant adult gene repression [Young et al. 2001]. The aim of this kind of adaptation is to compensate for the reduction in cardiac output by inducing the expression of fetal genes and facilitating substrate switching in order to maintain cardiac output [Young et al. 2001].

The fetal heart primarily utilizes glucose for the production of energy however at birth the increase in dietary fatty acid intake results in an increase in the availability of fatty acids as a fuel substrate and in the activation of genes involved in fatty acid metabolism. PPAR alpha is partly responsible for the mediation of this effect [Brown et al. 1995; Makinde et al. 1998].

#### **1.10.1.1 Metabolic adaptation in the diabetic heart**

The diabetic heart relies a great deal on fatty acids for the production of energy. However fatty acids inhibit glucose oxidation through the pyruvate dehydrogenase complex. PDC is the enzyme responsible for catalyzing the committed step for glucose oxidation. In the diabetic heart, increased

mitochondrial acetyl-CoA levels as well as phosphorylation by PDK 4 inhibit the actions of the pyruvate dehydrogenase complex [Wu et al. 1999, Randle et al. 1978]. The increased citrate levels usually present in the diabetic heart as a result of increased fatty acid utilization results in the potentiation of inhibition of phosphofructokinase (PFK) by ATP which acts to further prevent the oxidation of glucose.

Having said that, we have to ask the question of whether substrate switching is essential for the adaptation of the diabetic heart. Studies using PPAR alpha knockout fasted mice show that these animals develop contractile dysfunction and die [Leone et al. 1999]. The origin of cardiac dysfunction in this particular model appears to be as a result of the accumulation of lipids within cardiomyocytes also known as lipotoxicity [Leone et al. 1999]. This phenomenon suggests that the inability of the heart to respond to increased fatty acid availability, via the activation of PPAR alpha-regulated genes, ultimately results in heart failure [Young et al. 2001].

Early hyperinsulinemia, hyperglycaemia, and hyperlipidemia are all features of type 2 diabetes mellitus/insulin resistance and the increase in plasma nonesterified fatty acid levels associated with the presence of diabetes results in the activation of PPAR alpha which induces the expression of PPAR alpha regulated genes i.e. FAT, MCPT1, MCAD, LCAD, PDK 4, MCD and UCP 3 [Gulick et al. 1994; Brandt et al. 1998; van der Lee et al. 2000; Young et al. 2001a; Young et al. 2001b; Wu et al. 1999 (b)]. The induction of these genes together with increased availability of fatty acids is associated with enhanced utilization of fatty acids by the diabetic heart [Stanley et al. 1997]. Additionally it is believed that sustained elevations in the availability of glucose can inhibit fatty acid utilization at the level of gene expression as recent work done in islet cells show that exposure to glucose decreases the expression of PPAR alpha and several PPAR alpha regulated genes such as the above mentioned proteins involved in fatty acid oxidation [Roduit et al. 2000]. This phenomenon, if present

in the heart, could explain why PPAR alpha expression is low in the fetal and diabetic heart [Young et al. 2001; Lehman et al. 2000; Barger and Kelly 2000].

### **1.10.2 Metabolic Maladaptation**

Three mechanisms of metabolic maladaptations are known in the heart, they include lipotoxicity, glucotoxicity and a combination of the two known as glucolipotoxicity [Young et al. 2001].

#### **1.10.2.1 Lipotoxicity**

As previously mentioned the diabetic heart is exposed to a hyperglycaemic and hyperlipidemic environment to which initially it adapts by increasing the expression of fatty acid oxidation proteins and increasing the heart's reliance on fatty acids as fuel. This form of compensation allows the heart to maintain cardiac output under the hyperglycaemic and hyperlipidemic conditions. However the long –term effects of such a mechanism is detrimental to the heart as the availability of excessive lipids and fatty acids will eventually surpass the use of these substrates by the heart and lead to lipid accumulation inside the cardiomyocytes [Young et al. 2001]. Previous studies have shown that in rat hearts a dramatic decrease in the expression of PPAR alpha occurs as diabetes progresses [Young et al. 2001]. Sustained exposure to high levels of fatty acids along with the limiting PPAR alpha activity present during diabetes accelerates lipid accumulation within the heart. This phenomenon is known as lipotoxicity [Zhou et al. 2000; Lee et al. 1994]. Hearts isolated from insulin-resistance ZDF rats show increased lipid deposition within the cardiomyocytes, increased ceramide levels, DNA laddering indicative of apoptosis, and contractile dysfunction [Zhou et al. 2000]. This additional evidence supports the notion that increased ceramide levels, produced from excessive lipids and fatty acids, can induce the accumulation of ROS, INOS (inducible nitric oxide synthase) and

apoptosis [Bielawska et al. 1997; Unger and Unger 2001] which may result in contractile dysfunction of the heart.

The accumulation of glucose metabolites can be just as detrimental as the accumulation of excessive lipids and can lead to the development of glucose-induced insulin resistance in skeletal muscle, liver and adipose tissue [Rossetti et al. 1987]. In addition decreased insulin sensitivity is a common trait in both glucose induced insulin resistance and the diabetic heart [Doenst et al. 2001; Tahiliani and McNeil 1986; Sakamoto et al. 2000].

### **1.10.3 Mitochondrial dysfunction and insulin resistance:**

Metabolic changes that occur in the insulin resistant state have been shown to be accompanied by reduced mitochondrial oxidative activity as well as mitochondrial ATP synthesis, which are both indicative of reduced mitochondrial function [Qatanani and Lazar 2007]. Because mitochondria are the primary cellular site for both FA oxidation and utilization it has led to a great deal of interest in the role of reduced mitochondrial function.

There are a variety of techniques that allow you to measure mitochondrial function. In our study we used 1) estimates of oxidative phosphorylation potential by measuring key enzymes involved in the TCA cycle, such as pyruvate dehydrogenase and citrate synthase, 2) active measures of mitochondrial function by isolating mitochondria and measuring oxygen consumption capacity with varying substrates e.g. glutamate, palmitoyl-L-carnitine, malate, succinate, in the presence or absence of pharmaceutical modifiers such as rotenone, succinate, oligomycin and CCCP (Carbonyl cyanide 3-chlorophenylhydrazone), quantifying ATP production during state 3 respiration (HPLC) and 3) key mitochondrial biogenesis biomarkers such as PGC-1 alpha, PPAR alpha and AMPK .

## 1.11 MOTIVATION FOR STUDY

### **The Early Effects of Diet-induced Obesity on Myocardial Function in a Rat Model**

A study aimed at assessing the early effects of diet-induced obesity (DIO) on myocardial function in a rat model showed that after only 8 weeks of diet-induced obesity these obese rats were already starting to display signs of insulin resistance. Significant elevations in the blood glucose levels (mmol/L) (control:  $3.78 \pm 0.13$  vs. Diet:  $4.66 \pm 0.20$ ;  $p=0.0034$ ), serum insulin levels (mIU/ml) (control:  $25.16 \pm 5.21$  vs. Diet:  $52.58 \pm 9.0$ ;  $p=0.04$ ) as well as an elevation in the body weight (g) (control:  $358.29 \pm 5.12$  vs. Diet:  $396.08 \pm 7.07$ ;  $p=0.0006$ ) confirmed this. In addition these obese rats also showed significantly elevated plasma triglyceride, phospholipid, and lipid peroxidation levels as well as a significant decrease in aortic output recovery after global ischaemia [Huisamen et al. 2007].

In contrast, these obese rats displayed a significant decrease in the infarct size after regional ischaemia [Huisamen et al. 2007]. This was unexpected in view of many studies done on obesity, insulin resistance and the subsequent development of a myocardial infarction with larger infarct sizes in the obese group when compared to their age-matched controls. For example one such study found that the hearts from young insulin resistant Zucker obese (ZO) rats developed significantly larger infarcts than their lean (ZL) counterparts (infarct size:  $57.3 \pm 3\%$  in ZO vs.  $39.2 \pm 3.2\%$  in ZL;  $P < 0.05$ ) [Katakam et al. 2006].

We therefore set out on a systematic investigation of signalling pathways involved in myocardial substrate utilization after a switch to a high caloric diet. We hypothesized that pathways involved in glucose utilization will be down regulated with concomitant up regulation of fatty acid utilization pathways leading to mitochondrial adaptations and eventually myocardial maladaptation.

## **1.12 AIMS**

Our specific aims were:

- 1) To determine whether the expression of key proteins involved in the regulation of glucose and fatty acid metabolism as well as mitochondrial oxidative phosphorylation has changed
- 2) To determine the oxidative phosphorylation potential of mitochondria in the hearts of control vs. DIO rats after 8 weeks (early) or 16 weeks (late) of diet

## **CHAPTER 2: METHODS**

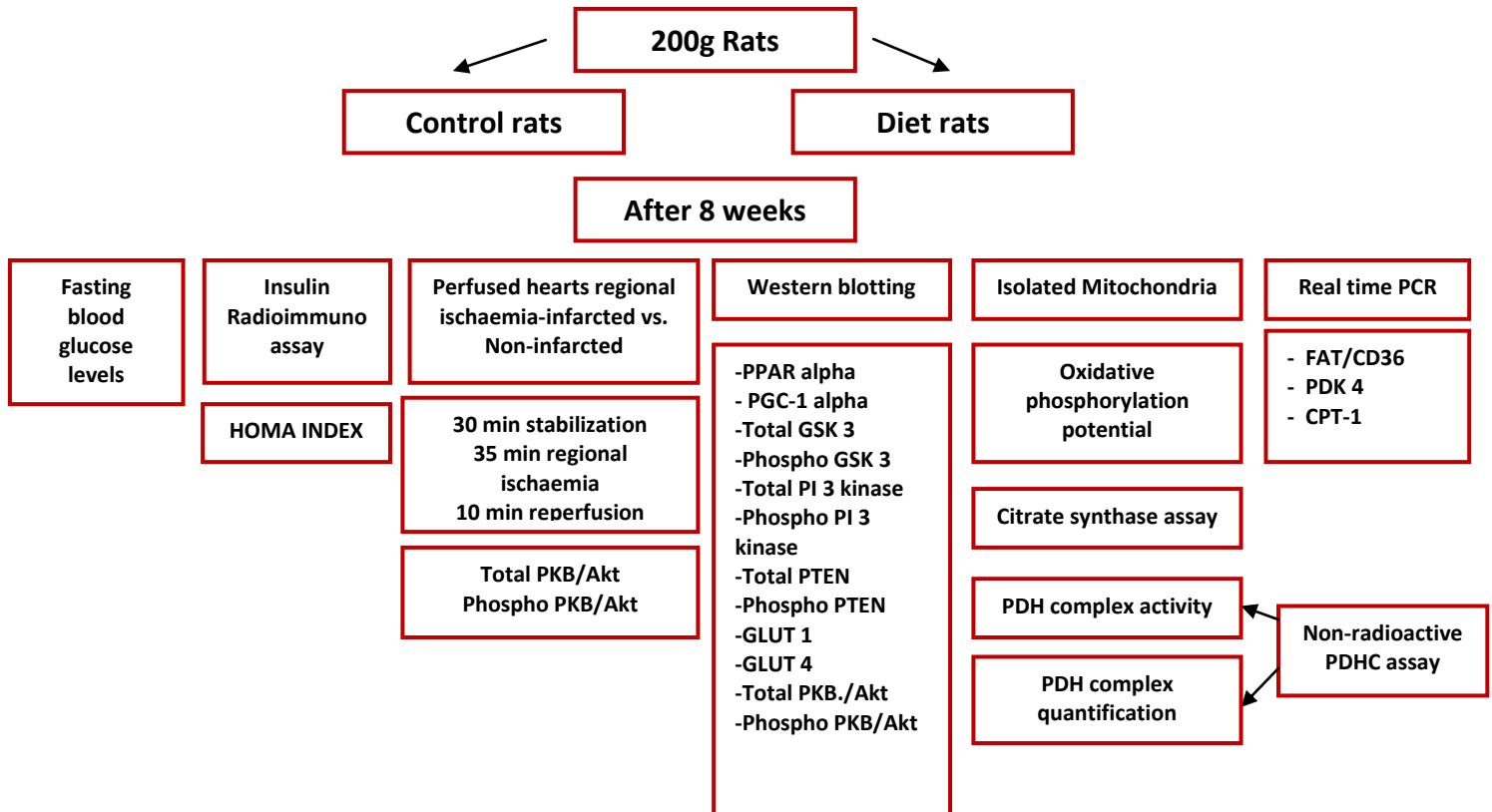
### **2.1 Animals**

Age and weight matched male Wistar rats were used for this study. Rats were weaned at 4 weeks of age and were allowed free access to food and water. Rats were housed in the University of Stellenbosch Central Research Facility, with a 12-hour artificial day-night cycle where a constant temperature of 22°C and humidity of 40% were maintained. Throughout the study, the revised South African National Standard for the care and use of laboratory animals for scientific purposes was followed [South African Bureau of Standards, SANS 10386, 2008]. Ethical clearance for all projects were obtained from the committee for ethics in animal research of the University of Stellenbosch.

#### **2.1.1 Study design**

Upon reaching ~200g, rats were randomly assigned to either a control or a diet (DIO) group. Control rats were fed a standard rat chow diet while the diet group received a special diet i.e. standard rat chow supplemented with sucrose and condensed milk. Rats were fed for a period of either 8 or 16 weeks. At the appropriate time the rats were weighed, sacrificed and their hearts removed. A group of hearts were freeze clamped immediately at baseline and another group of hearts were used to isolate mitochondria. Freeze clamped hearts were stored at -80°C and were used for biochemical analysis at a later stage. A separate series of rats were used for each protocol (Figure 22 pg 95-96).

(A)





(B)

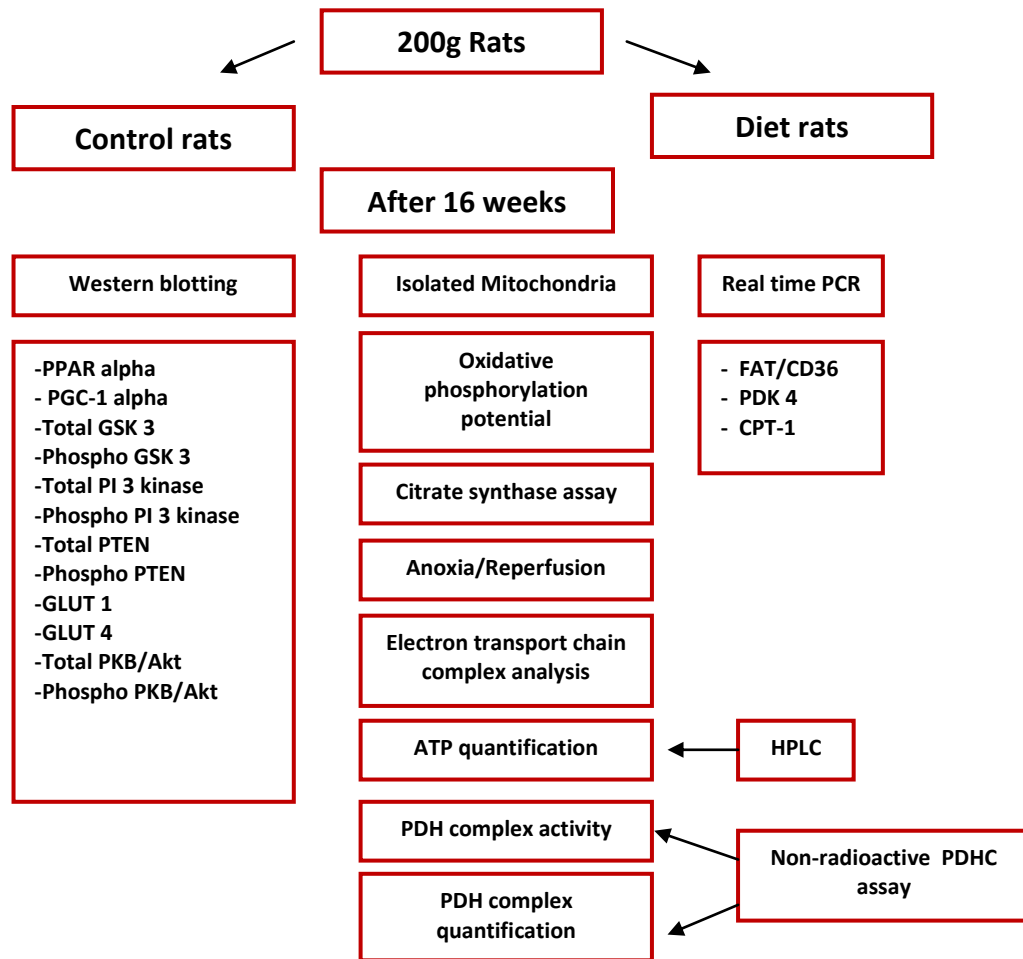


Figure 22: (A) and (B) Study design for the respective groups after 8 and 16 weeks of diet.

### 2.1.2 Diet

The special obesity inducing diet contained standard rat chow supplemented with sucrose and condensed milk. This high caloric diet consisted of 33% standard rat chow, 33% sweetened full cream condensed milk (Clover), 7% sucrose and 27% water [Pickavance et al. 1999]. Obesity in this model was induced primarily by hyperphagia. The food was replaced daily to avoid fermentation of wet food.

**Table 1: Composition of control and DIO group's diet.**

	<b>Control:</b>	<b>DIO:</b>
<b>Carbohydrates:</b>	60%	65%
<b>Protein:</b>	30%	19%
<b>Fat:</b>	10%	16%
<b>Kj/day</b>	371±8	570±23

All animals were anaesthetized by intra-peritoneal injection of Eutha-naze (sodium pentobarbital) (0.16 g/kg animal body mass) prior to being slaughtered.

### 2.2 Blood glucose determination

Rats were fasted overnight and blood samples were collected from the tail vein. A drop of the blood was placed on the absorbent film of an Accu-check advantage II slip (Roche Diagnostics, USA). The slip was subsequently inserted into an Accu-Check glucometer (Roche Diagnostics, USA) in order to determine blood glucose levels.

## **2.3 Measurement of serum insulin levels**

Non-fasting blood samples were collected from the thoracic cavity after the rats had been sacrificed and were stored at 4°C until analyzed. The Coat-A-Count® Insulin assay was used for the quantitative measurement of the serum insulin levels. This assay is a solid-phase  $^{125}\text{I}$  radioimmunoassay, in which a fixed amount of  $^{125}\text{I}$ -labeled insulin competes with the insulin, present in the blood sample, for binding sites on an insulin specific antibody. The insulin specific antibody is immobilized in the wall of the polypropylene tube and therefore, simply decanting the supernatant eliminates the competition and isolates the antibody-bound fraction of the radiolabeled insulin. Radioactivity was then measured by using a gamma scintillation counter (Cobra II Auto Gamma, A.D.P, South Africa).

### **2.3.1 Experimental procedure**

All tests were done in duplicate and all assay components were brought to room temperature according to the manufacturer's instructions. Four uncoated polypropylene tubes were labeled: total counts (1-2) and non-specific binding (3-4). Fourteen insulin antibody-coated tubes were labeled [A (maximum binding)-G]. Additionally, tubes for the controls and samples were also labeled.

200  $\mu\text{l}$  of the zero calibrator A was pipetted into the non-specific binding tube as well as the tube labeled A (maximum binding) and 200  $\mu\text{l}$  of each remaining calibrator, control and sample was pipette into their respective prepared tubes. 1.0 ml of  $^{125}\text{I}$  insulin was added to every tube and vortexed. Samples were then incubated for 18-24 hours at room temperature. After the incubation period the samples were decanted by placing each tube (except the total count tube) in a foam decanting rack and allowing the tubes to drain for approximately 3 minutes after which each tube was struck on absorbent paper to remove excess moisture.

Removal of the excess moisture ensures a more precise assay. The radioactivity of each tube was then measured in a gamma counter (Cobra II Auto Gamma, A.D.P, South Africa) for 1 minute per tube.

### **2.3.2 HOMA index**

The HOMA (homeostasis model assessment) is a noninvasive measurement technique for insulin sensitivity. The product of the fasting concentrations of glucose (mmol/L) and insulin (mIU/mL) is divided by a constant (22.5 – if glucose concentration is expressed in Système International units). The HOMA calculation, unlike other measurement techniques for insulin sensitivity, compensates for fasting hyperglycemia [Quon 2001]. Results from previous studies indicate that HOMA is highly sensitive and specific for measuring insulin resistance [Keskin et al. 2005]. Additionally it is a much simpler, non-invasive, inexpensive, less laborious and time consuming than other measures of insulin sensitivity [Keskin et al. 2005].

## 2.4 Pilot study

A pilot study was conducted to determine whether differences in the activation of PKB/Akt was responsible for smaller infarct development found in hearts of rats after 8 weeks of diet.

### 2.4.1 Perfusion protocol

Isolated rat hearts were excised and placed in ice cold Krebs-Henseleit buffer containing NaCl 119 mM, NaHCO<sub>3</sub> 24.9 mM, KCl 4.74 mM, KH<sub>2</sub>PO<sub>4</sub> 1.19 mM, MgSO<sub>4</sub> 0.6 mM, Na<sub>2</sub>SO<sub>4</sub> 0.59 mM, CaCl<sub>2</sub> 1.25 mM, glucose 11 mM. This buffer was also used as the perfusate and was kept at a pH of 7.4 and oxygenated by continuously gassing it with 95% oxygen/5% carbon dioxide. The perfusion protocol for hearts from obese animals (n=6) and hearts from control animals (n=6) was as follows: 30 minutes stabilization, 35 minutes regional ischaemia, accomplished by ligating the left anterior descending artery, and 10 minutes of reperfusion. The Langendorff perfusion system was used. At the end of reperfusion the infarcted zone was dissected out and frozen separately from the non-infarcted zone.

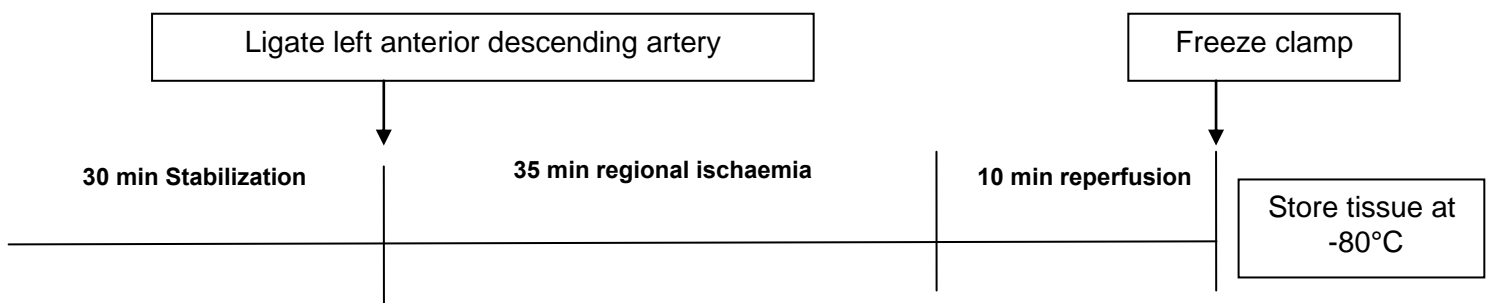


**Figure 23: Retrograde perfusion protocol**

## **2.5 Biochemical analysis**

### **2.5.1 Infarcted vs. Non-infarcted zones**

Lysates were prepared from frozen tissue as described in section 2.5.2. The standard Bradford protein determination method [Bradford 1976] and Western blotting techniques were used to determine the level of expression of total and phosphorylated PKB/Akt in the infarcted and non-infarcted zones of all the perfused hearts (control n=6; diet n=6).

A separate set of hearts were freeze clamped at baseline without perfusion (control n=6; diet n=6) and later used to determine the level of expression of the following proteins:

- PPAR  $\alpha$
- PGC-1  $\alpha$
- GLUT1
- GLUT 4
- GSK -3 (total and phosphorylated)
- PI 3 kinase (total and phosphorylated)
- PTEN (total and phosphorylated)
- PKB/Akt (total and phosphorylated)
- AMPK (total)

### **2.5.2 Preparation of lysates**

Tissue lysates were prepared using a lysis buffer (Ph 7.4), containing 20 mM Tris , 1 mM EGTA, 150 mM NaCl, 1 mM EDTA, 2.5 mM sodium pyrophosphate, 1 mM  $\beta$ -glycerophosphate, 1 mM  $\text{Na}_3\text{VO}_4$ , 1 mM PMSF,

10 µg/ml Leupeptin, 10 µg/ml Aprotinin, 1% Triton X-100. This lysis buffer was used for the analysis of GLUT 1, GLUT 4, GSK-3, PI 3 kinase, PTEN and AMPK.

PPAR alpha and PGC-1 alpha protein were extracted with a modified lysis buffer (pH 7.4), containing 20 mM Tris , 1 mM EGTA, 150 mM NaCl, 1 mM EDTA, 2.5 mM sodium pyrophosphate, 1 mM β-glycerophosphate, 1 mM Na<sub>3</sub>VO<sub>4</sub>, 1 mM PMSF, 10 µg/ml Leupeptin, 10 µg/ml Aprotinin, 1% Triton X-100, 1 mM Mg Cl<sub>2</sub>.

Frozen heart tissue was added to the lysis buffer and homogenized using a Polytron PT10 homogenizer (2 x 5 seconds setting 4). The homogenized tissue was then transferred to eppendorf tubes and centrifuged for 10 minutes at 4°C. The supernatant was transferred to clean eppendorf tubes, kept on ice and the protein concentration determined using the Bradford protein determination method.

#### **2.5.2.1 The Bradford protein determination method**

50 µl of the supernatant from each sample was diluted 10 x with dH<sub>2</sub>O to dilute all detergents that may interfere with the assay.

##### **2.5.2.1.1 Bradford procedure**

- Dilute the Bradford reagent stock solution 1:5 and filter through 2x filter paper
- Generate a standard curve using a bovine serum albumin (BSA) stock solution of known concentration
- Pipette 5 µl of each diluted sample and add 95 µl H<sub>2</sub>O
- Add 900 µl Bradford reagent to each tube, vortex and incubate samples for at least 15 minutes at room temperature
- Read the optical density at 595 nm

- Use the standard curve generated in excel (protein concentration on x-axis and OD values on the y-axis) and calculate the protein content ( $\mu\text{g}/\mu\text{l}$ ) of each sample
- Use the protein concentration to dilute the samples with lysis buffer to equalize the protein concentration/volume
- Add Laemli sample buffer (3:1) and boil for 5 minutes
- Store samples at  $-20^{\circ}\text{C}$  until further use in imMune blotting procedure



## 2.5.3 Immuno Blotting

### 2.5.3.1 Separation of proteins

**Table 2: Protocol for stack gel**

Reagent	Stock	4%
H <sub>2</sub> O (Millipore)		2.7 ml
Tris-HCl (pH 6.8)	0.5 M	1.25 ml
SDS	10%	50 µl
Acrylamide	40%	450 µl
APS (AmMonium persulfate)	10%	50 µl
TEMED (Tetramethylethylenediamine)	99%	10 µl

**Table 3: Protocol for separation gel**

Reagent	Stock	10%	12%
H <sub>2</sub> O (Millipore)		3.85 ml	3.35 ml
Tris-HCl (pH 8.8)	1.5 M	2.50 ml	2.50 ml
SDS	10%	90 µl	90 µl
Acrylamide	40%	2.25 ml	2.7 ml
APS	10%	50 µl	50 µl
TEMED (Tetramethylethylenediamine)	99%	20 µl	20 µl

After casting and polymerizing the gels, the samples were boiled for 5 minutes, microfuged for 5 minutes and equal protein concentrations loaded onto the gels. The tank (BioRad Protean III apparatus) was then filled with running buffer (composition: 50 mM Tris, 384 mM Glycine, 1.0%w/v SDS) and run according to the protocol listed below in tables 4-10.

**Table 4: Western blotting protocol for PPAR alpha and PGC-1 alpha**

Protein	PPAR $\alpha$	PGC-1 $\alpha$
Size of Protein (kDa)	52	92
% Polyacrylamide gel	12	10
Run period (min)	10 min + 70 min	10 min + 70 min
Blocking period (min)	120 min	120 min
Primary antibody ( $\mu$ l)	20 $\mu$ l in 5 ml 5% Milk (1:250)	20 $\mu$ l in 5 ml 5% Milk (1:250)
Secondary antibody ( $\mu$ l)	4 $\mu$ l in 20 ml 5% Milk (1:5000)	4 $\mu$ l in 20 ml 5% Milk (1:5000)
Exposure time (min)	5 min	5-10 min

**Table 5: Western blotting protocol for GLUT 1 and GLUT 4**

Protein	GLUT 1	GLUT 4
Size of Protein (kDa)	55	45
% Polyacrylamide gel	12	12
Run period (min)	10 min + 90 min	10 min + 90 min
Blocking period (min)	90 min in 2.5% milk	90 min in 5% milk
Primary antibody ( $\mu$ l)	20 $\mu$ l in 5 ml 1% milk (1:250)	5 $\mu$ l in 5 ml TBS tween (1:1000)
Secondary antibody ( $\mu$ l)	3 $\mu$ l in 20 ml 2.5% milk (1:6667)	5 $\mu$ l in 20 ml 2.5% milk (1:4000)
Exposure time (min)	25-30 min	25-30 min

**Table 6: Western blotting protocol for total and phospho GSK-3**

Protein	GSK-3	Phospho GSK-3
Size of Protein (kDa)	52	52
% Polyacrylamide gel	12	12
Run period (min)	10min + 70 min	10 min + 70 min
Blocking period (min)	90 min	90 min
Primary antibody ( $\mu$ l)	5 $\mu$ l in 5 ml TBS tween (1:1000)	5 $\mu$ l in 5 ml TBS tween (1:1000)
Secondary antibody ( $\mu$ l)	5 $\mu$ l in 20 ml 5% milk (1:4000)	5 $\mu$ l in 20 ml 5% milk (1:4000)
Exposure time (min)	10-15 min	10-15 min

**Table 7: Western blotting protocol for total and phospho PI 3 kinase**

Protein	PI 3 kinase	Phospho PI 3 kinase
Size of Protein (kDa)	85	85
% Polyacrylamide gel	12	12
Run period (min)	10min + 70 min	10min + 70 min
Blocking period (min)	90 min	90 min
Primary antibody (µl)	5 µl in 5 ml TBS Tween (1:1000)	5 µl in 5 ml TBS tween (1:1000)
Secondary antibody (µl)	5 µl in 20 ml 5% milk (1:4000)	5 µl in 20 ml 5% milk (1:4000)
Exposure time (min)	20-23 min	20-30 min

**Table 8: Western blotting protocol for total and phospho PTEN**

Protein	PTEN	Phospho PTEN
Size of Protein (kDa)	54	54
% Polyacrylamide gel	12	12
Run period (min)	10 min + 70 min	10min + 70 min
Blocking period (min)	120 min	120 min
Primary antibody (µl)	5 µl in 5 ml TBS tween (1:1000)	5 µl in 5 ml TBS tween (1:1000)
Secondary antibody (µl)	5 µl in 20 ml 5% Milk (1:4000)	5 µl in 20 ml 5% milk (1:4000)
Exposure time (min)	12 – 14 min	10-12 min

**Table 9: Western blotting protocol for total and phospho PKB/Akt**

Protein	PKB/Akt	Phospho PKB/Akt
Size of Protein (kDa)	60	60
% Polyacrylamide gel	12	12
Run period (min)	10 min + 60 min	10min + 60 min
Blocking period (min)	120 min	120 min
Primary antibody (µl)	5 µl in 5 ml TBS tween (1:1000)	5 µl in 5 ml TBS tween (1:1000)
Secondary antibody (µl)	5 µl in 20 ml 5% Milk (1:4000)	5 µl in 20 ml 5% milk (1:4000)
Exposure time (min)	15-20 min	15-20 min

**Table 10: Western blotting protocol for total AMPK**

Protein	Total AMPK
Size of Protein (kDa)	62
% Polyacrylamide gel	10
Run period (min)	10 min + 50 min
Blocking period (min)	120 min
Primary antibody (µl)	11 µl in 5 ml TBS tween (1:1000)
Secondary antibody (µl)	10 µl in 20 ml 5% Milk (1:4000)
Exposure time (min)	5-7 min

Proteins were separated by SDS PAGE (sodium dodecyl sulfate polyacrylamide gel electrophoresis – a control sample was loaded in the first well/lane of each gel and used as a reference point to normalize data) and were transferred to a polyvinylidene fluoride (PVDF) membrane (ImMobilon™ P, Millipore) in a transfer apparatus containing transfer buffer (composition: 25.0 mM Tris-HCl pH 8.3, 192 mM glycine, 20%v/v methanol, 0.02%w/v SDS). 5% fat free milk in Tris buffered saline (TBS) 0.1% Tween 20 (TBST) (composition: 200 mM Tris-HCl pH 7.6, 1.37 M NaCl) was used to block non-specific binding sites on membranes after which they were washed extensively with TBST (3 x 5 minutes). The membranes were incubated overnight with antibodies specific for each of the proteins of interest. TBST was used to repeatedly wash membranes (3 x 5 min). Diluted anti-rabbit HRP linked secondary antibody was allowed to conjugate with immobilized antibody on the membrane. Membranes were then again washed thoroughly with TBST. Membranes were covered with ECL™ detection reagents and exposed to autoradiography film (Hyperfilm ECL, RPN 2103 – Amersham). This was done to detect light emission through a non-radioactive method (ECL™ Western-blotting). The films that were obtained were then analyzed with laser scanning densitometry (UN-SCAN-IT, Silkscience).

## **2.6 Preparation and analysis of mitochondrial function**

### **2.6.1 Preparation of mitochondria from fresh heart tissue**

The measurement of oxygen consumption in isolated mitochondria was pioneered by Britton Chance over 50 years ago and is still being used today to assess the function of freshly isolated mitochondria [Chance et al. 1956].

Fresh isolated rat hearts were arrested in ice cold isolation medium (pH 7.4), containing 0.18 M KCl (13.42g/L), 0.01 M EDTA (3.72g/L), cut into pieces, washed repeatedly with isolation medium to remove as much blood as possible, and put on ice. The tissue was then homogenized with a Polytron PT10 homogenizer (2 x 4 seconds on setting 4) on ice and centrifuged for 10 min at 4°C at 2 500 rpm (755 x g) in a Sorvall SS34 rotor. The resultant supernatants were centrifuged at 12 500 rpm (18 800 x g) to obtain a mitochondrial pellet which was finally suspended in 0.5 ml isolation medium using a glass Teflon Potter Elvehjem homogenizer. For each of the mitochondrial experiments, a 50 µl mitochondrial aliquot was allowed to precipitate in 1.0 ml 10% TCA (trichloroacetic acid) overnight or for 30 minutes at 4°C for protein determination

#### **2.6.1.1 Lowry's protein determination method**

The Lowry protein determination method [Lowry et al.1951]. Was used to determine the protein content of the 50 µl aliquot of mitochondria that was precipitated in 10% TCA.

##### **2.6.1.1.1 Sample preparation**

The precipitated samples were centrifuged for 15 minutes at 2 500 rpm (755 x g), and the supernatant removed. 500 µl 1N NaOH was added to the pellet and vortexed. The samples were then heated in a water bath at 70°C for

approximately 10 minutes (or until the solution turned clear) in order to dissolve the proteins. To this mixture 500 µl dH<sub>2</sub>O was added and vortexed. The sample was now ready for protein determination.

#### **2.6.1.1.2 Procedure**

50 µl of the prepared protein sample was added to lacham-tubes in duplicate. Separate tubes were set aside and an albumin stock solution of known concentration was used to generate a standard curve (0.5 N NaOH was used as a blank). 1.0 ml NaK-Tartrate-CuSO<sub>4</sub> (composition: 2% NaK-Tartrate, 1% CuSO<sub>4</sub>·5H<sub>2</sub>O, 2% Na<sub>2</sub>CO<sub>3</sub>) was added to all tubes with 10-30 second time intervals, vortexing after each addition. After 10 minutes had elapsed (measured from the first addition) 100 µl Folin Ciocalteu's reagent (diluted 1:3) was added at the same time intervals, vortexing after each addition. After at least 30 minutes the optical density was read at 750 nm (visible light) against the blank (0.5 NaOH). The standard curve and OD values were then used to determine the protein concentration (mg/ml).

#### **2.6.2 Analysis of mitochondrial function**

Respiration of isolated mitochondria was measured at 25°C using a Clarke electrode (Hansatech Oxygraph), whereby the O<sub>2</sub> consumption was measured in nmolO<sub>2</sub>/ml/min.

An aliquot (volume dependent on end reaction volume) of incubation medium pH 7.4 (250 mM Sucrose, 10 mM Tris-HCl, 8.5 mM K<sub>2</sub>HPO<sub>4</sub>·2H<sub>2</sub>O, 50 mM Glutamate, 20 mM Malate) was placed into the chamber of the oxygraph. The chamber was then made anaerobic by adding sodium dithionite and the instrument calibrated to a 0 and 100% oxygen level. After calibration the chamber was rinsed repeatedly with dH<sub>2</sub>O to ensure that all traces of sodium dithionite had been removed.

A 0.65 ml aliquot of incubation medium was added to the chamber and allowed to become air saturated/equilibrate with ambient oxygen. After approximately 90 seconds equilibration, an aliquot (50  $\mu$ l) of mitochondrial suspension was added to the chamber and the recording allowed to run for 90-120 seconds. 50  $\mu$ l ADP was then added and the stopper closed, sealing the chamber. Mitochondria were allowed to utilize all ADP to produce ATP (State 3 respiration) where after state 4 respiration was allowed to progress for at least 2 min.

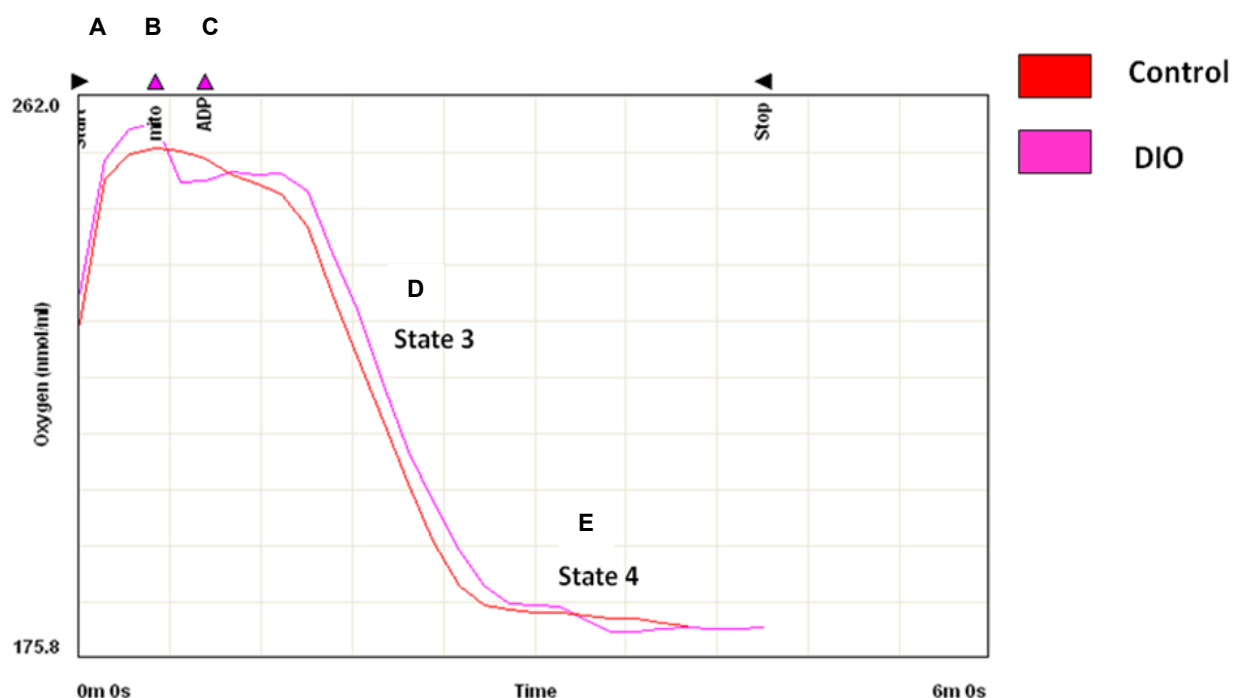


**Figure 24: Typical respiration graph generated by an oxygraph –** (A) At the start of the experiment only the incubation medium is present containing either glutamate or palmitoyl-L-carnitine, then the mitochondria (B) are added and then the ADP and the chamber closed (C), the mitochondria are then able to utilize the substrates and oxygen to rapidly produce ATP (State 3 respiration) (D), and when almost all of the ADP has been converted to ATP respire at a slower rate (State 4 respiration) (E).

In a separate set of experiments palmitoyl-L-carnitine (5 mM) was also used as a substrate instead of glutamate.

#### **2.6.2.1 Anoxia/Reperfusion of isolated cardiac mitochondria**

0.60 ml incubation medium (containing either glutamate and malate or palmitoyl-L-carnitine and malate) was added to the chamber. After approximately 90 seconds 100  $\mu$ l mitochondrial suspension was added. Subsequent to the addition of the mitochondria and after approximately 90 seconds equilibration, 50  $\mu$ l ADP was added to the reaction mixture and the stopper closed. This sealed the chamber. After state 4 had been reached, ADP was added (injected through a small capillary tube in the chamber stopper using a Hamilton syringe) at a saturating level (100  $\mu$ l of a 17.7 mM ADP solution) that maximally stimulated respiration in the presence of glutamate and malate. This lead to total oxygen depletion which made the chamber completely anoxic i.e. no oxygen was available for the mitochondria to use. After 20 minutes of sustained anoxia the mitochondria were reperfused by removing the stopper and bubbling oxygen through the reaction mixture. The mitochondria were allowed to regain state 3 respiration which was recorded over 2 min of re-oxygenation.

In a separate set of experiments palmitoyl-L-carnitine (5 mM) with malate (20 mM) was also used as substrates.

#### **2.6.3 Mitochondrial electron transport chain complex analysis**

Mitochondrial function may be determined via different methods. One of these include the measuring of oxygen consumption in isolated mitochondria [Chance et al. 1956]. This technique allows you to measure the functional capacity of mitochondria as organelles and not as single enzyme complexes [Lanza et al. 2009]. However, it is also crucial to combine measurements of maximal ATP production with measures of mitochondrial respiration, by using various substrates which will offer the opportunity to assess defects at specific levels



within the process of mitochondrial energy metabolism. In addition, different pharmacological substances may be used to determine the function of the individual enzyme complexes.

#### **2.6.3.1 Experimental Procedure**

0.68 ml of incubation medium was added to the oxygraph chamber. After approximately 90 seconds a 20  $\mu$ l aliquot of mitochondrial suspension was added. Subsequent to the addition of mitochondria and after approximately another 90 seconds had elapsed, 50  $\mu$ l ADP was added and the stopper closed. Thereafter pharmaceutical substances were added to the chamber (injected through a small capillary tube in the chamber stopper using Hamilton syringes) sequentially with  $\pm 120$  second intervals. These substances include (listed in order of addition): 45  $\mu$ l succinate (80 mM), 8  $\mu$ l rotenone (50  $\mu$ M), 5  $\mu$ l oligomycin (5mg/1ml), and 8  $\mu$ l carbonyl cyanide m-chlorophenylhydrazone (CCCP) (5 mM). In a separate set of experiments palmitoyl-L-carnitine chloride (5 mM) and malate (20 mM) was also used as substrates.

In our study we used a protocol described by Lanza et al. as an outline for the assessment of mitochondrial function of isolated mitochondria in vitro [Lanza et al 2009]. This protocol involves serial additions of various substrates, inhibitors and uncouplers which allow for the comprehensive assessment of mitochondrial function in isolated mitochondria.

##### **1) Gas phase equilibration:**

The first step in this protocol states the instrument be equilibrated with ambient oxygen.

2) Baseline mitochondrial respiration:

This is followed by measuring the baseline respiration which is achieved by adding an aliquot of the mitochondrial suspension to the chamber, closing it and measuring respiration in the absence of exogenous substrates.

3) Substrates glutamate and malate (State 2 respiration, complex I):

A combination of glutamate and malate is then added which will reflect state-2 respiration specific to complex I. The substrate combination of glutamate and malate provides carbon sources for dehydrogenase reactions in the TCA cycle. These dehydrogenase reactions generate NADH which is subsequently oxidized by complex I [Lanza et al. 2009]. Additionally high concentrations of malate will result in product inhibition of the succinate dehydrogenase reaction.

ADP is added at a saturating level in order to stimulate state 3 respiration by complex I as much as possible in the presence of glutamate and malate.

4) Addition of succinate:

Succinate provides additional electron flow through complex II. The addition of succinate will therefore stimulate respiration above glutamate-malate stimulated state 3. Complex II or succinate dehydrogenase, unlike complex I, is not a proton pump. Complex II consists of four protein subunits and is responsible for funnelling additional electrons into the quinone pool by removing electrons from succinate and transferring them via FAD to Q (Figure 20.6, pg. 367 Lanza et al. 2009).

5) Addition of rotenone:

In addition to adding succinate, rotenone is also added to assess the functioning of complex II. Rotenone selectively inhibits complex I, which induces a redox shift that effectively inhibits all of the NADH-linked dehydrogenases in the TCA cycle. Therefore in the presence of rotenone, succinate selectively stimulates the flow of electrons through complex II.

7) Addition of Oligomycin:

The addition of oligomycin serves as an indicator of the degree of uncoupled respiration or proton leak. It is used to induce state 4 respiration by inhibiting the  $F_o$  unit of the ATP synthase enzyme, blocking the proton channel and effectively eliminating ATP synthesis. In the absence of ADP phosphorylation the leakage of protons across the inner mitochondrial membrane can be attributed to residual oxygen consumption.

8) Addition of CCCP:

CCCP induces an uncoupled state by dissipating the proton gradient across the inner mitochondrial membrane.

In a separate set of experiments we substituted glutamate with palmitoyl-L-carnitine, in order to assess ATP production by fatty acid  $\beta$ -oxidation [Lanza et al. 2009].

## **2.6.4 QUANTIFICATION OF MITOCHONDRIAL ATP PRODUCTION**

### **2.6.4.1 Experimental procedure**

For each of the ATP quantification experiments, the reaction was stopped and the reaction mixture (containing: incubation medium, mitochondria and ADP) removed directly after completion of state 3 respiration. The reaction mixture was then added to 6% Perchloric acid (PCA) and placed on ice for the determination of ATP via HPLC.

In a separate set of experiments palmitoyl-L-carnitine chloride (5 mM) and 20 mM malate was also used as a substrate.

### **2.6.4.2 HIGH PERFORMANCE LIQUID CHROMATOGRAPHY**

#### **2.6.4.2.1 Principle of experiment**

The analysis of high energy phosphates (HEPs) such as adenosine triphosphate (ATP), adenosine diphosphate (ADP), adenosine monophosphate (AMP) and creatine phosphate (CrP) by the reversed phase high pressure liquid chromatography (HPLC) technique was developed by Victor et al. 1987.

We used reversed-phase HPLC which has a non-polar stationary phase and an aqueous polar mobile phase. Reverse phase chromatography operates on the principle of hydrophobic forces, which originate from the high symmetry in the dipolar water structure. RPC is allowing the measurement of these interactive forces. The binding of the analyte to the stationary phase is proportional to the contact surface area around the non-polar segment of the analyte molecule upon association with the ligand in the aqueous eluent. The structural properties of the analyte molecule play an important role in its retention characteristics i.e. in general an analyte with a larger hydrophobic surface (e.g. C-H, C-C, S-S )area

results in a longer retention time because it increases the non-polar surface area of the molecule, which is non-interacting with the water structure. This is contrary to polar groups, such as  $\text{-OH}$ ,  $\text{-NH}_2$ ,  $\text{COO}^-$  or  $\text{-NH}_3^+$  which reduce retention as they are well integrated into water.

#### Column

Packing:	LUNA C18 (2)
Length:	250 mM
ID:	4.6 mM
Particle size:	5 $\mu$
Liquid:	Methanol: $\text{H}_2\text{O}$ (66:34)
Supplier:	Phenomenex

An On-line UV detector (210 nm) was used and the mobile phase (Buffer) was composed of 257 mM  $\text{KH}_2\text{PO}_4$ , 1.18 MM tetrabutylammoniumphosphate (TBAP), 12.5 % (v/v) HPLC graded methanol, pH 4.0 with  $\text{H}_3\text{PO}_4$ , filtered and de-gassed with Helium.

High energy phosphates were quantitated with appropriate standards (STD from Sigma), with known concentrations:

ATP = 0.4535 nmol/10 µl

ADP = 0.5853 nmol/10 µl

AMP = 0.7200 nmol/10 µl

CrP = 0.7640 nmol/10 µl

A:

$$\frac{\text{Area of sample}}{\text{Area of STD}} \times \frac{\text{Concentration of STD}}{1} = \text{Conc. of sample in nmol/10 } \mu\text{l}$$

B:

$$\frac{(A)\text{nmol}}{0.01} \times \frac{[1.2 \text{ ml} + (0.78 \times \text{weight in g})] \times [1 \text{ ml} + \text{neutrl vol} + 0.005 \text{ ml indicator}]}{1} \times \frac{1}{\text{weight in g}}$$

= (nmol/g wet weight) / 1000

= (µmol/g wet weight)

#### 2.6.4.2.2 Preparation of samples for HPLC

The volume of reaction mixture taken from the oxygraph incubation chamber, ranging from 650 µl – 700 µl, was added to 1 ml of 6% PCA (Perchloric acid), and placed on ice for no longer than 30 minutes otherwise the acid will start to break down the ATP to precipitate. After the 30 minute precipitation period the mixture was centrifuged at 4000 rpm at 4°C for 10 minutes and 1 ml of the supernatant removed and added to 5 µl Universal indicator (the addition of the Universal indicator will transform the supernatant from colourless to purple). To this a neutralization mixture is gradually added (5 µl at a time) until a green colour is reached (green represents a neutral pH of 7.0-7.). This mixture is then microfuged at 4000 rpm at 4°C for 3 minutes and the supernatant filtrated through a 0.45 µm nitrocellulose filter. These samples were then ready for ATP quantification by means of HPLC and stored at -80°C.

## 2.6.5 CITRATE SYNTHASE ASSAY

### 2.6.5.1 Principle of experiment

Citrate synthase is the initial enzyme of the tricarboxylic acid (TCA) cycle. It catalyzes the reaction of 2 carbon acetyl coenzyme A (acetyl CoA) with 4 carbon oxaloacetate (OAA) to form the 6 carbon citrate.

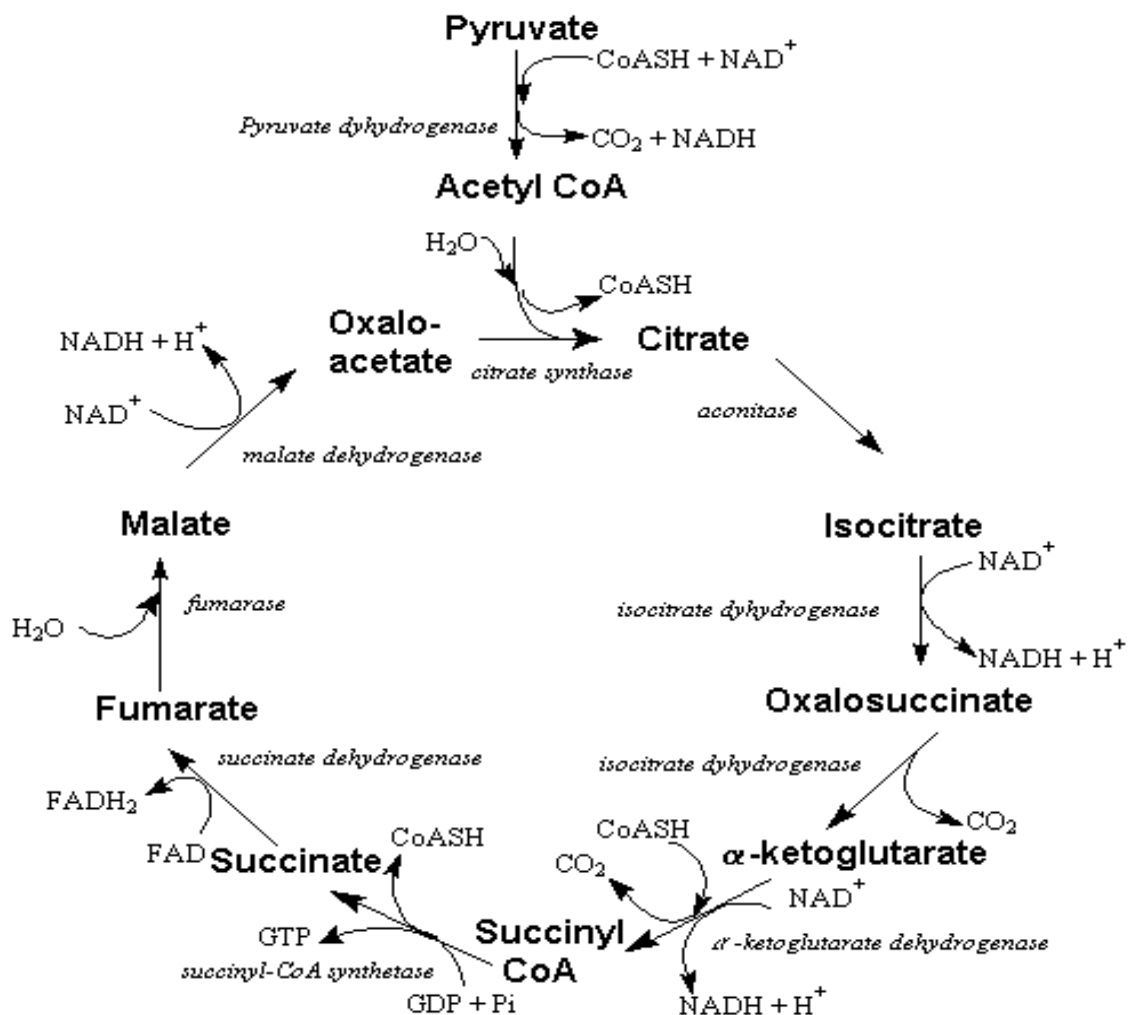
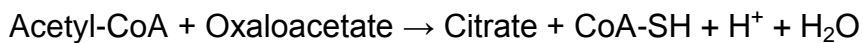


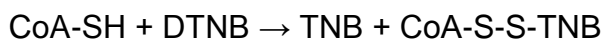
Figure 25: Citric acid cycle [<http://www.uic.edu>]

This enzyme is an exclusive marker of the mitochondrial matrix and its activity is measured by spectrophotometrically following the colour development of 5-thio-2-nitrobenzoic acid (TNB). The addition of 5,5'-Dithiobis-(2-nitrobenzoic acid) (DTNB) will allow the activity of the enzyme to be measured, as TNB (generated from DTNB) which is the overall reaction product absorbs light at 412 nm

Reaction catalyzed by citrate synthase:



Colorimetric reaction:



An aliquot (50 µl) of each preparation was stored at -80°C and used to determine the amount of mitochondria per mg of total protein by means of the citrate synthase assay. Citrate synthase assay kit (CS0720) from Sigma was used to determine the level of citrate synthase activity.

#### **2.6.5.2 Sample preparation**

For the detection of total citrate synthase activity in mitochondria, the stored mitochondria (50 µl mitochondria was stored at -80°C in KE isolation medium ) was suspended in CellLytic M Cell lysis reagent (Catalog Number C2978) using ~200 µl per g of tissue.



**Samples were prepared according to the reaction scheme in Table 11:**

Description	Sample	1xAssay Buffer	30 mM Acetyl-CoA Solution	10 mM DTNB Solution	10 mM OAA Solution Last to be added
CellLytic M Sample	(10 µl)	920 µl	10 µl	10 µl	50 µl
Citrate Synthase (positive control) Diluted solution	(10 µl)	90 µl	10 µl	10 µl	50 µl

All of the reaction components were added except for the 10 mM OAA solution.

### **2.6.5.3 Experimental procedure**

After sample preparation each assay solution was warmed to 25 °C and placed in a 1 ml cuvette. The optical density (OD) measurements were then taken at a wavelength of 412 nm every 20 seconds for 1.5 minutes to measure the baseline reaction, endogenous levels of thiol or deacetylase activity. The oxaloacetate solution (10 mM) was then added, the sample gently mixed and the OD measurements taken again every 20 seconds for 1.5 minutes to measure total activity. Positive controls (positive for containing the enzyme citrate synthase) were also tested for citrate synthase activity. These OD values were then used to calculate the level of citrate synthase activity (umol/mgprot/min).

### **2.6.6 PYRUVATE DEHYDROGENASE (PDH) COMBO (ACTIVITY + QUANTITY) MICROPLATE ASSAY**

We used the pyruvate dehydrogenase (PDH) Combo (Activity and Quantity) microplate assay kit (Catalog # MSP20) from MitoSciences. This kit contains two components: a PDH activity assay component (MSP 18), and a PDH quantity assay component (MSP 19), used for the quantitative and qualitative analysis of PDH.

### 2.6.6.1 Principle of MSP 18

This kit is used to determine the activity of the pyruvate dehydrogenase enzyme in a sample. The PDH enzyme is immunocaptured within the wells of the microplate and the PDH activity is determined by following the reduction of  $\text{NAD}^+$  to NADH. This reaction is coupled to the reduction of a reporter dye to yield a coloured (yellow) reaction product. The concentration of the product of this reaction can be determined by measuring the increase in absorbance at a wavelength of 450nm.

### 2.6.6.2 Experimental procedure

The mitochondria were isolated, homogenized and the final pellet suspended in PBS (1.4 mM  $\text{KH}_2\text{PO}_4$ , 8.0 mM  $\text{Na}_2\text{HPO}_4$ , 140 mM NaCl, 2.7 mM KCl, pH 7.3). The protein concentrations of all samples were determined using the Lowry protein determination method prior to solubilisation and diluted to the specified concentration (~2 mg/ml). The sample was then solubilized and diluted to within the linear range of measurement as described below:

Component	Purified mitochondria at ~2 mg/ml
Sample	19 volumes
Detergent	1 volume
Final protein concentration (mg/ml)	5.0

The samples were incubated on ice (10 min) and then centrifuged for 10 min at 4 °C at 5, 000 RCF (x g). The supernatant was carefully collected and the pellet discarded. 10 ml of the 20x Buffer (in kit) was added to 190 ml of deionized  $\text{H}_2\text{O}$  to make a 1X Buffer which was used to dilute the samples to the desired concentrations.

200 µl of the diluted samples (in duplicate), as well as a positive and negative control, was added to the wells of the microplate and incubated for 3 hours at room temperature.

After the 3 hour incubation period the wells were emptied and 300 µl of 1x Stabilizer (prepared by mixing 1 volume of thawed 5x stabilizer (in kit) with 4 volumes of 1x Buffer) added to each well. This step was repeated and 200 µl of the Assay solution was added to each of the wells and the absorbance measured at 450 nm at room temperature for 15 minutes with 1 minute intervals. The optical density was then plotted vs. Time (s) and the PDH activity expressed as the initial rate of reaction determined from the slopes of the curves generated.

#### **2.6.6.3 Principle of MSP 19**

This kit can be used to determine the amount of PDH protein in a sample. The PDH enzyme is purified and immobilized by an anti-PDH capture antibody pre-coated in the microplate wells. The amount of captured PDH is determined by adding a second anti-PDH antibody (detector) which binds to the captured PDH, followed by binding of an HRP conjugated goat-anti-mouse antibody that binds the detector anti-PDH antibody. The detector-bound HRP then changes the colourless HRP development solution to blue and the colour intensity (absorbance) is proportional to the amount of PDH captured.

#### **2.6.6.4 Experimental procedure**

The isolation of the mitochondria, measurement of the protein concentration, dilution and solubilisation of the samples as well the 10 minute incubation period on ice and the 10 min centrifugation step at 4°C is the same as described for MSP 18.

After collecting the supernatant all the samples were diluted to the desired concentration (as described above for MSP 18) using the Incubation solution [prepared by mixing 1 part 10x Blocking Buffer with 9 parts 1x Buffer (prepared by adding 15 ml of 20x Buffer to 285 ml deionised H<sub>2</sub>O)]. 200 µl of the diluted samples were then loaded into the microplate wells and incubated at room temperature for 3 hours. This was followed by 3 wash steps with 300 µl 1x stabiliser (prepared by mixing 1 part 5x stabiliser with 4 parts 1x Buffer). 200 µl of 1x Detector (1 part 20x Detector Antibody + 19 parts incubation solution) was added to each well and incubated for 1 hour at room temperature. Two more wash steps were performed with 1x Buffer prior to adding 200 µl 1x HRP Label (1 part 20x HRP label with 19 parts incubation solution) to each well and incubating at room temperature for 1 hour. Finally 3 washes were performed with 1x Buffer and 200 µl of HRP Development solution added to each well and the absorbance read immediately at 600 nm for 15 min with 1 min intervals. The blue colour development over time in each well is then examined and the initial absorbance reading subtracted from the final absorbance reading to determine the quantity of PDH in each well.

## **2.7 QUANTITATIVE RT- PCR (REAL TIME – POLYMERASE CHAIN REACTION) ANALYSIS**

### **2.7.1 mRNA isolation**

We used the RiboPure<sup>TM</sup> Kit by AEC- Amersham (Catalog # AM 1924) to isolate high quality total RNA. This kit is designed specifically for the purification of high quality RNA from tissue samples by combining the robust lysis/denaturant, TRI reagent, with glass filter purification to yield pure RNA, free of residual proteins and lipids.

### **2.7.1.1 Procedure**

Frozen heart tissue from both groups (following 8 and 16 weeks DIO) stored at -80°C were homogenized in TRI reagent (1ml TRI reagent / ~100mg tissue) which is a monophasic solution containing phenol and guanidine thiocyanate which rapidly lyses cells and inactivates nucleases. The samples were then incubated for 5 min at room temperature and centrifuged at 12 000 x g for 10 min at 4°C, and the supernatant transferred to a new eppendorf tube. The next step was the extraction of the RNA. 200 µl of chloroform was added to 1 ml of the homogenate/supernatant and mixed well. After incubating the homogenate for 5 min at room temperature it is centrifuged at 12 000 x g for 10 min at 4°C. The addition of chloroform results in the separation of the homogenate into aqueous and organic phases. RNA partitions to the aqueous phase while DNA and protein remain in the interphase and organic phase. 400 µl of the aqueous phase was then transferred to a new eppendorf tube for the final RNA purification step. 200 µl of 100% ethanol was added to the aqueous phase, mixed immediately and passed through a filter cartridge. The filter was then washed twice with 500 µl of the wash solution and then finally the RNA was eluted with 100 µl of the elution buffer. The purified RNA sample was then stored at -80°C.

### **2.7.2 TURBO DNA –free™**

The TURBO DNA free kit from Ambion was used to remove all traces of DNA to render a completely DNA free RNA sample.

### 2.7.2.1 Procedure overview

#### **Add Dnase Digestion reagents**

1. Add 0.1 volume 10x TURBO Dnase Buffer and 1  $\mu$ l TURBO Dnase to the purified RNA, and mix gently



#### **Incubate**

2. Incubate at 37°C for 20-30min



#### **Add Dnase inactivation reagent**

3. Add resuspended Dnase inactivation reagent (typically 0.1 volume) and mix well



#### **Incubate and mix**

4. Incubate 5 min at room temp mixing occasionally



#### **Centrifuge and transfer RNA**

5. Centrifuge at 10 000 x g for 1.5min and transfer the RNA to a fresh tube (store RNA at -80°C until further use)

### 2.7.3 Quantitation of RNA

The concentration of RNA is determined by measuring the absorbance at 260 nm (A<sub>260</sub>) in a spectrophotometer. The reading at 260 nm allows for the calculation of the concentration of RNA in the sample. Before measuring the absorbance the extracted RNA sample was diluted [1:200 5 µl RNA + 995 µl DEPC (diethylpyrocarbonate) H<sub>2</sub>O] and the absorbance then measured in a 1 ml quartz cuvette (spectrophotometer calibrated with DEPC H<sub>2</sub>O). The concentration of the RNA was then calculated according to the following formula:

$$OD_{260} \times 50 \text{ ng}/\mu\text{l} \times \text{dilution factor} = \text{RNA concentration}$$

### 2.7.4 Purity of RNA

The purity of the RNA sample was determined by measuring the absorbance at both 260 nm and 280 nm and calculating the ratio between the two (OD<sub>260</sub> / OD<sub>280</sub>). This ratio gives you an indication of the purity of the RNA. Pure preparations of RNA will have an OD<sub>260</sub> / OD<sub>280</sub> ratio of 2.0. If the ratio is significantly less than this value, the sample has most likely been contaminated with protein or phenol. However this ratio is influenced considerably by Ph and since water (DEPC H<sub>2</sub>O) is not buffered the Ph and the resulting OD<sub>260</sub> / OD<sub>280</sub> ratio can vary greatly. A lower pH results in a lower ratio and reduced sensitivity to protein contamination [Wilfinger et al. 1997].

### 2.7.5 Integrity of RNA

The integrity and size distribution of total RNA extracted with the RiboPure™ kit was checked by denaturing formaldehyde agarose gel electrophoresis and ethidium bromide staining.

### 2.7.6 Formaldehyde Agarose Gel Electrophoresis

A formaldehyde agarose gel (1.2 % agarose) was prepared by mixing 1.2 g agarose with 10 ml 10x formaldehyde agarose gel buffer (200 mM 3-[N-morpholino]propanesulfonic acid {MOPS}, 50 mM sodium acetate, 10 mM EDTA, pH =7.0 with 10 M NaOH), and 50 ml of RNase-free water (DEPC H<sub>2</sub>O). This mixture was then heated to allow the agarose to melt. To the heated agarose an additional 40 ml of RNase-free water was added (to make the solution up to 100 ml) to cool the mixture to ~65°C. 1.8 ml of 37% formaldehyde and 1 µl of a 10mg/ml ethidium bromide stock solution was added to the cooled mixture, mixed thoroughly and poured onto gel support. The gel was allowed to equilibrate in 1x formaldehyde agarose gel running buffer (100 ml 10x formaldehyde agarose gel buffer, 20 ml 37% formaldehyde and 880 ml RNase-free water).

To prepare the RNA sample for formaldehyde agarose gel electrophoresis, RNA, DEPC water and 5x RNA loading buffer (16 µl saturated aqueous bromophenol blue solution, 80 µl 500 mM EDTA, pH 8.0, 720 µl 37% formaldehyde, 2 ml 100% glycerol, 3084 µl formamide, 4 ml 10x formaldehyde agarose gel buffer and Rnase free water to 10 ml) were added in a 4:6 ratio (RNA, DEPC water: loading buffer) and mixed. It was then incubated for 3-5 min at 65°C, chilled on ice and then loaded onto the equilibrated gel. The gel was run for 2hrs (70 V, 100 mA) in 1x formaldehyde agarose gel running buffer and the bands visualized using a UV box and SynGene GeneSnap version 6.07 (serial no. 11496\*9125\*vacutec\*mpcs) software.



### **2.7.7 cDNA synthesis**

High capacity cDNA reverse transcription kit with RNase inhibitor for 200 reactions from Applied Biosystems was used (part no. 4374966) to synthesise cDNA from the RNA that we isolated.

#### **2.7.7.1 cDNA reaction preparation**

The kit contains reagents that, when combined, form a 2x Reverse transcription (RT) master mix. An equal volume of RNA sample should be added. To avoid RNase contamination, RNase-free reagents and consumables must be used.

**Table 12: Instruction by the manufacturer to prepare the 2x RT master mix (per 20 µl reaction):**

1.	Allow the kit components to thaw on ice	
2.	Referring to the table below, calculate the volume of components needed to prepare the required number of reactions. Note: Prepare the RT master mix on ice	
	<b>Component:</b>	<b>Volume (µl) / reaction kit</b>
		<b>With RNase inhibitor kit</b>
	10x RT buffer	2.0
	25x Dntp Mix (100 mM)	0.8
	10x RT random primers	2.0
	MultiScribe™ Reverse Transcriptase	1.0
	RNase Inhibitor	1.0
	Nuclease-free water	3.2
	Total per reaction	10.0
	IMPORTANT: include additional reactions in the calculations to provide excess volume for the loss that occurs during reagent transfers.	
3.	Place the 2x RT master mix on ice and mix gently.	

**Table 13: Instructions from the manufacturer to prepare the cDNA  
Reverse Transcription reactions**

1.	Pipette 10 µl of 2x RT master mix into each well of a 96-well reaction plate or individual tube
2.	Pipette 10 µl of RNA sample into each well, pipetting up and down two times to mix
3.	Seal the plates or tubes
4.	Briefly centrifuge the plate or tubes to spin down the contents and to eliminate any air bubbles
5.	Place the plate or tubes on ice until you are ready to load the thermal cycler

**Table 14: Instructions to program the thermal cycling conditions**

1.	Program the thermal cycler using the conditions below.				
	<b>IMPORTANT:</b> These conditions are optimized for use with the high-capacity Cdna reverse transcription kits				
		<b>Step 1</b>	<b>Step 2</b>	<b>Step 3</b>	<b>Step 4</b>
	<b>Temperature</b>	25°C	37°C	85°C	4°C
	<b>Time</b>	10 min	120 min	5 min	∞

The newly synthesised cDNA was then stored at -80°C for use in the real-time PCR reactions.

### 2.7.8 Taqman gene expression assays

We used the PRE-DEVELOPED TAQMAN® ASSAY REAGENTS kit from Applied biosystems together with the Taqman gene expression assays for our three target genes PDK 4, FAT/CD 36 and CPT-1.

Applied Biosystems developed the Pre-Developed TaqMan® Assay reagents products as a research tool for real time, in vitro relative quantitative evaluation of gene expression. The Pre-Developed TaqMan® Assay reagents detect the expression of target sequences in complementary DNA (cDNA) samples.

- Primer sequences:
  - “Downstream” IL-1α primer for reverse transcription and amplification of Paw109 RNA sequence:  
  
5' –CATGTCAAATTTCACTGCTTCATTCATCC- 3'
  - “Upstream” IL-1α primer for amplification of Paw109 sequence:  
  
5'-GTCTCTGAATCAGAAATCCTTCTATC-3'

### **2.7.8.1 About the kit**

This kit is used to amplify purified DNA and contains primers and probes which is used to detect known sequences of, in our case, cDNA. The TaqMan ® MGB probes contain:

- A reporter dye linked to the 5' end of the probe
- A minor groove binder (MGB) at the 3' end of the probe and
- A nonfluorescent quencher (NFQ) at the 3' end of the probe (because the quencher does not fluoresce, the Applied Biosystems real-time PCR systems can measure reporter dye contribution more accurately).

The 5' nuclease assay process takes place during PCR amplification and occurs in every cycle and does not interfere with the exponential accumulation of product. During PCR, the TaqMan MGB probe anneals specifically to a complementary sequence between the forward and reverse primer sites (Figure 24, pg. 133). When the probe is intact (Figures 25 and 26, pg. 133), the proximity of the reporter dye to the quencher dye results in the suppression of the reporter fluorescence, primarily by Förster-type energy transfer [Förster 1984; Lakowicz, 1983].

The DNA polymerase cleaves only probes that are hybridized to the target (Figure 26, pg. 133). Cleavage separates the reporter dye from the quencher dye which results in increased fluorescence by the reporter. The increase in fluorescence occurs only if the target sequence is complementary to the probe and is amplified during PCR. Nonspecific amplification is not detected because of these requirements. Polymerization of the strand continues, but because the 3' end of the probe is blocked, no extension of the probe occurs during PCR (Figure 27, pg 133).

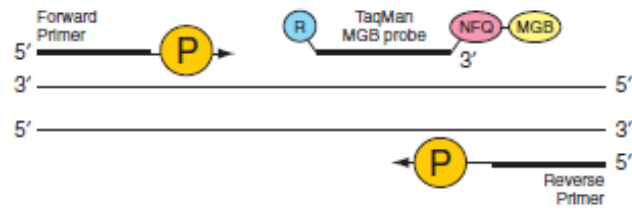


**Figure 26: Polymerization reaction**

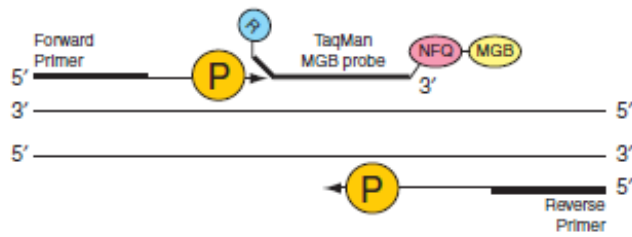


**Figure 27: Strand displacement**

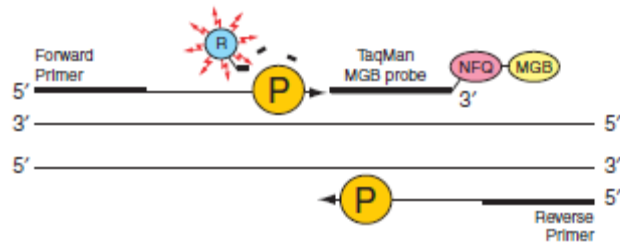


**Figure 28: Cleavage**

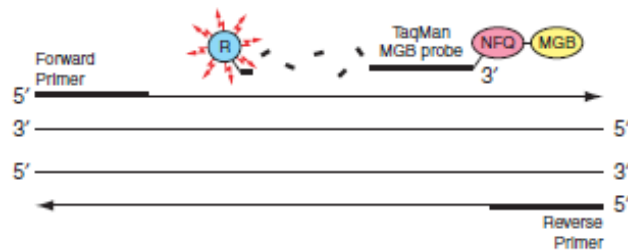


**Figure 29: Completion of polymerization**

This product contains sufficient control primers and probe to detect the control sequence. The control reagent is optimized for use with TaqMan® Universal PCR master mix to perform 1000 PCR reactions (50 µl each) but does not contain TaqMan® Universal PCR master mix.

#### **2.7.8.2      Preparing the PCR reaction mix**

The preparation of the reaction mix used in the following tables is crucial for the accurate calculation of relative quantification values.

Prepare the PCR reaction mixture for each sample in a separate microcentrifuge tube before aliquoting the samples to the reaction plate for thermal cycling and fluorescence analysis. The volume of PCR reaction mix per well must be 50 µl minus the volume of the cDNA sample. Load 10 ng to 1 µg of cDNA (converted from total RNA) per well, depending on your target of interest. The contents of the PCR reaction mix are as follows:

**Table 15: Components (Multiplex: Target + Control reactions)**

<b>Concentration</b>	<b>Volume/tube (µl)</b>	<b>Final</b>
RNase-free water	20 µl – y	-
2x TaqMan® Universal PCR master mix	25 µl	1x
20x Target primers and probe	2.5 µl	1x
20x Control primers and probe	2.5 µl	1x
cDNA sample	y (µl)	-
Total volume	50 µl	1x

Note: This reaction is optimized for TaqMan ® Universal PCR master mix. Mix the PCR reaction mixture and cDNA samples prior to addition to the MicroAmp® optical 96 well reaction plate to ensure optimal performance of your PCR reactions.



**Table 16:                    Setting thermal cycler conditions:**

Times and Temperatures				
Initial Steps			Each of 40 cycles	
			Melt	Anneal/extend
Stage	Hold	Hold	Cycle	
Temperature	50.0°C	95.0°C	95.0°C	60.0°C
Time	2 min	10 min	15 sec	1 hour

#### **2.7.8.2.1      Analysis of results**

Our results generated from the 7900 HT thermal cycler was analyzed using REST 2009 software from Qiagen.

## **2.8      Statistical analysis**

All data is expressed as mean  $\pm$  S.E.M. Statistical significance between groups was assessed by two way analysis of variance (ANOVA) followed by a Bonferroni post-hoc test for multiple comparisons. Alternatively an unpaired Student t test was used to compare statistical differences between control and DIO groups. A p-value of less than 0.05 ( $p < 0.05$ ) is considered as statistically significant. Statistical analysis of data was performed using GraphPad Prism 5. REST 2009 software was used for statistical analysis of relative expression of the genes of interest in our PCR experiments, and represented as whisker-box plots. A hypothesis test is used by REST 2009 software to determine whether a

significant difference exists between diet and controls, while taking reaction efficiency and reference gene normalization into account.

The box area in a whisker-box plot provides additional information about the skew of the data distributions that would not be available simply by plotting the sample mean. The whisker-box plot encompasses 50% of all observations, the dotted line represents the sample median and the whiskers represent the outer 50% of observations (Figure 30) [Rest 2009 Software Guide].

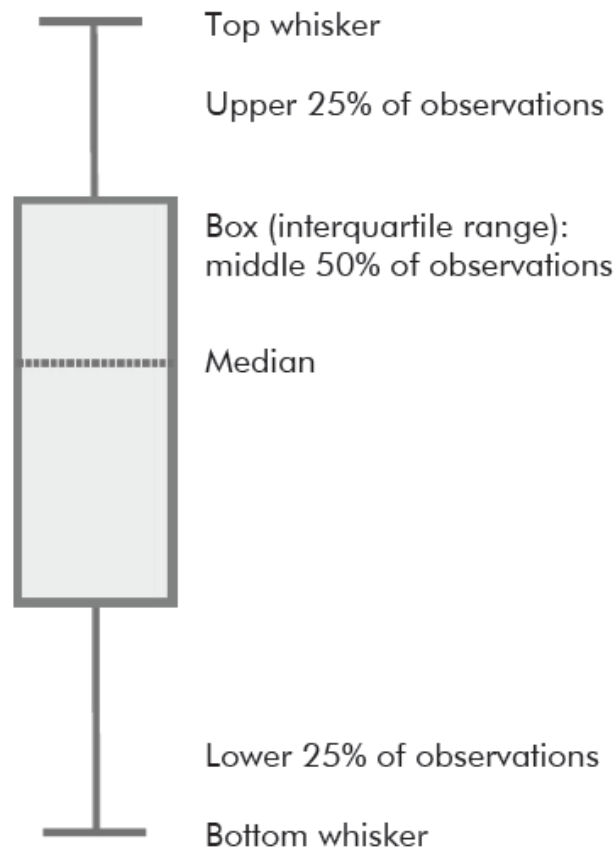


**Figure 30: Whisker-box plot**

## CHAPTER 3: RESULTS

### 3.1 CHARACTERISTICS OF THE DIET-INDUCED OBESITY MODEL

#### 3.1.1 Body weight

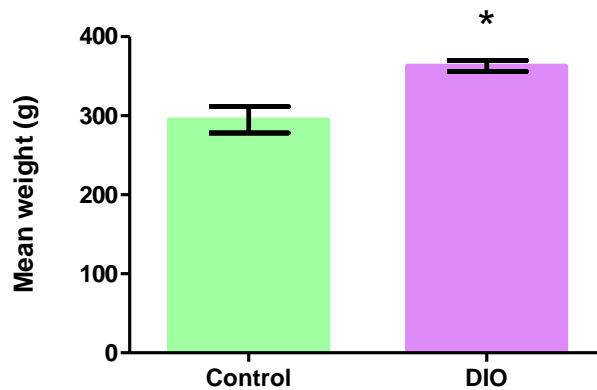


**Figure 31: Mean weight (g) after 8 weeks of DIO (n=6 per group)**

A significant increase was found in the mean body weight (g) in the diet group when comparing control and DIO groups ( $294.8 \pm 16.7$  vs.  $362.8 \pm 6.9$ ;  $p=0.0037$ ) 23.08% weight gained in DIO group.

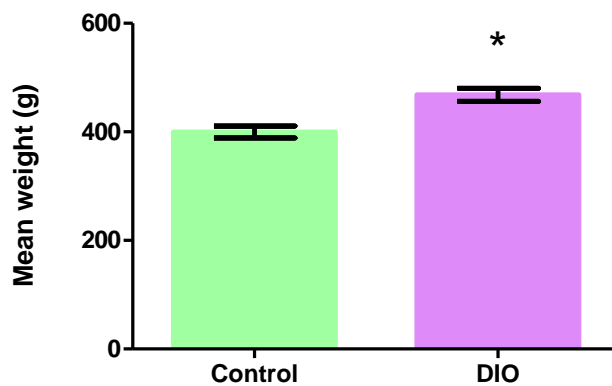


**Figure 32: Mean weight (g) after 16 weeks of DIO (n=8 Control n=9 DIO)**

A significant increase was found in the mean body weight (g) in the diet group when comparing control and DIO groups ( $399.7 \pm 11.1$  vs.  $468.2 \pm 12.0$ ;  $p=0.0008$ ) 31.8% weight gained in DIO group.

### 3.1.2 Intra-peritoneal fat weight

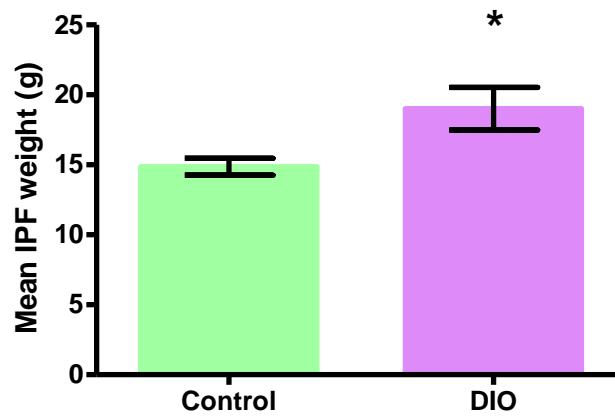


**Figure 33: Mean intra-peritoneal fat weight (g) after 8 weeks of DIO (n=15 control n=19 DIO).** A significant increase was found in the mean intra-peritoneal fat weight (g) in the diet group when comparing control and DIO groups ( $14.9 \pm 0.60$  vs.  $19.0 \pm 1.58$ ;  $p=0.0276$ ) 61.9% IPF weight gained in DIO.

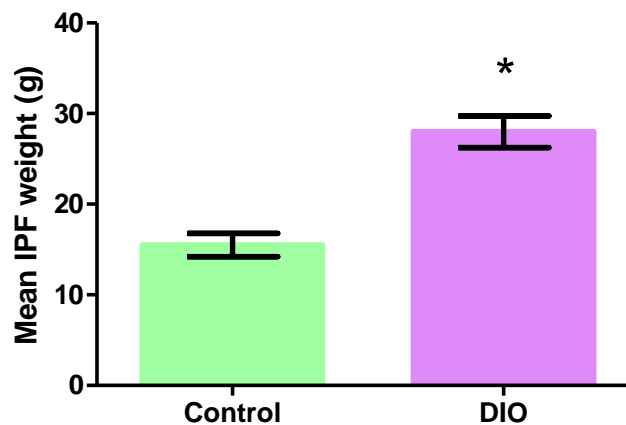


**Figure 34: Mean intra-peritoneal fat weight (g) after 16 weeks of DIO (n=8 control n=9 DIO).** A significant increase was found in the mean intra-peritoneal fat weight (g) in the diet group when comparing control and DIO groups ( $15.5 \pm 1.28$  vs.  $28.0 \pm 1.74$ ;  $p<0.0001$ ) 103.2% IPF weight gained in DIO group.

### 3.1.3 Fasting blood glucose and insulin levels

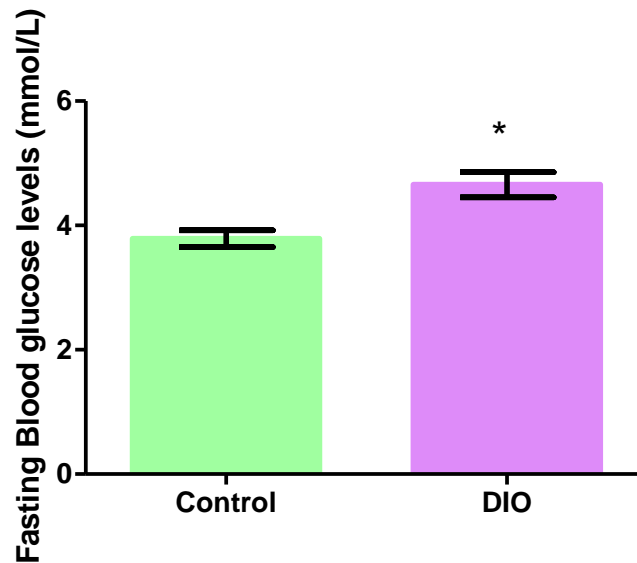


**Figure 35: Fasting blood glucose levels (mmol/L) measured after 8 weeks of DIO.** A significant increase was found in the blood glucose levels in the diet group when comparing control and DIO groups (n=8 Control; n=9 DIO) ( $3.78 \pm 0.13$  vs.  $4.65 \pm 0.13$ ; \*p=0.0034)

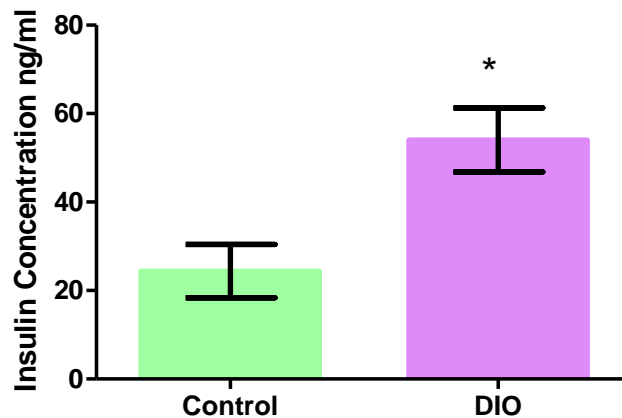


**Figure 36: Insulin levels measured after 8 weeks of DIO.** A significant increase was found in the insulin levels in the diet group when comparing control and DIO groups (n=6 Control; n=6 DIO) ( $24.4 \pm 4.74$  vs.  $54.1 \pm 8.36$ ; \*p=0.0102)

### 3.1.4 HOMA index

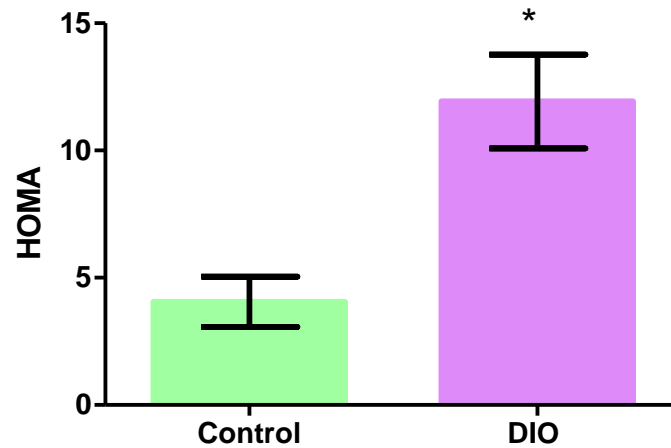


**Figure 37: HOMA index calculated from insulin levels after 8 weeks of DIO.** A significantly higher HOMA index was found in the diet group when comparing control and DIO groups (n=6 Control; n=6 DIO) ( $4.06 \pm 0.98$  vs.  $11.9 \pm 1.82$ ; \*p=0.0037)

### 3.2 PKB/AKT EXPRESSION AND ACTIVATION BETWEEN NON-INFARCTED AND INFARCTED ZONES COMPARED BETWEEN DIO AND CONTROL GROUPS

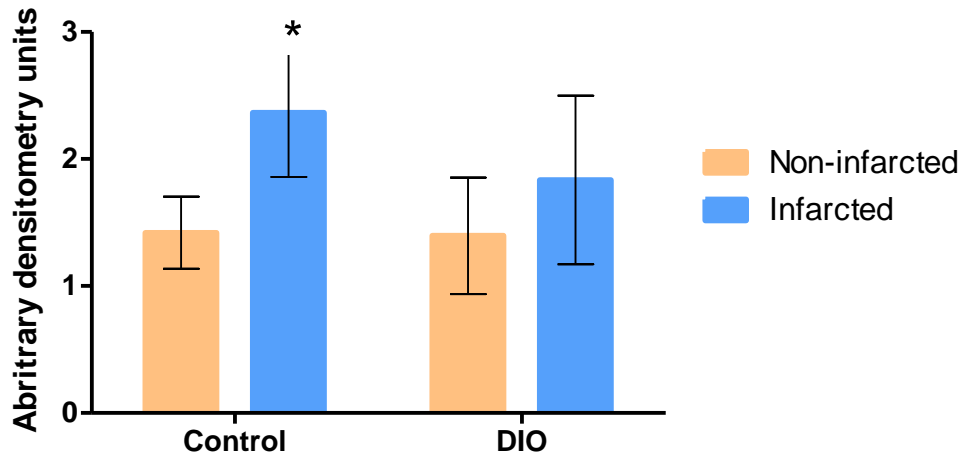


**Figure 38: Phosphorylated PKB/Akt levels in the infarcted and non-infarcted zones in both the diet and control group after 8 weeks of DIO (after 35 min regional ischaemia followed by 10 min reperfusion).**

A significant difference in the level of phosphorylated PKB/Akt was found between the infarcted and non-infarcted zones in the control group ( $2.36 \pm 0.50$  vs.  $1.42 \pm 0.28$ ;  $p < 0.05$ ). No significant difference was found between the infarcted and non-infarcted zones in the diet group ( $1.83 \pm 0.66$  vs.  $1.40 \pm 0.46$ ;  $p > 0.05$ ).

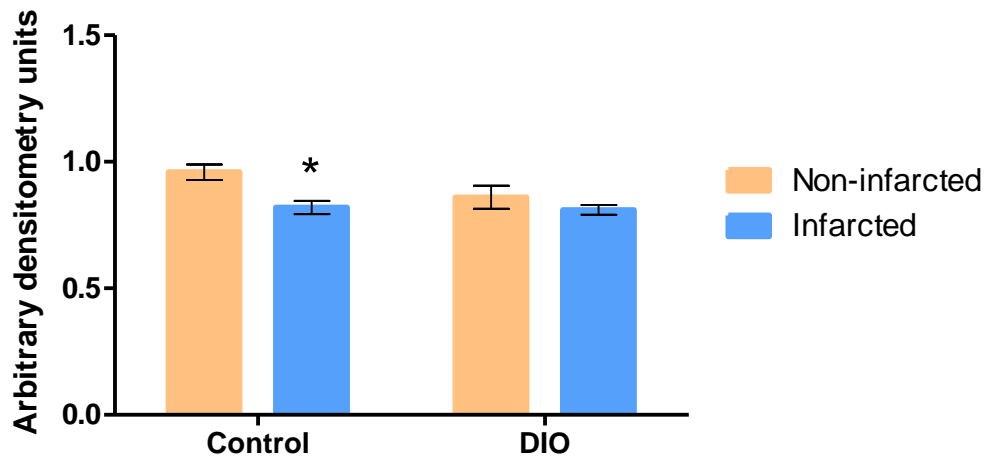


**Figure 39: Total PKB/Akt expression in the infarcted and non-infarcted zones in both the diet and control group after 8 weeks of DIO (after 35 min regional ischaemia followed by 10 min reperfusion).** A significant difference in the total PKB/Akt levels was found between the infarcted and non-infarcted zones in the control group ( $0.82 \pm 0.02$  vs.  $0.96 \pm 0.03$ ;  $p < 0.05$ ). No significant difference was found between the infarcted and non-infarcted zones in the diet group ( $0.81 \pm 0.02$  vs.  $0.86 \pm 0.05$ ;  $p > 0.05$ ).



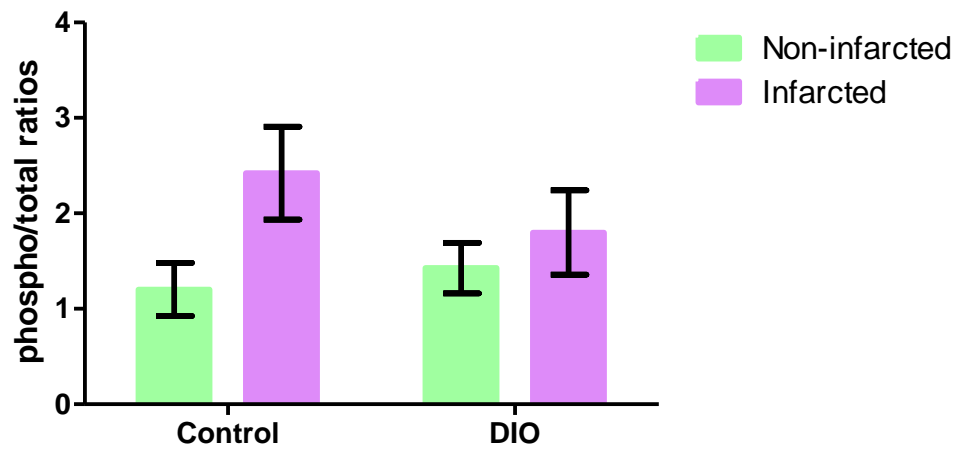


**Figure 40: Phosphorylated/Total ratios in infarcted and non-infarcted zones between control and DIO groups (n=5 Control; n=6 Diet).**

No significant differences were found.

### 3.3 THE EXPRESSION OF THE REGULATORS OF METABOLIC GENES

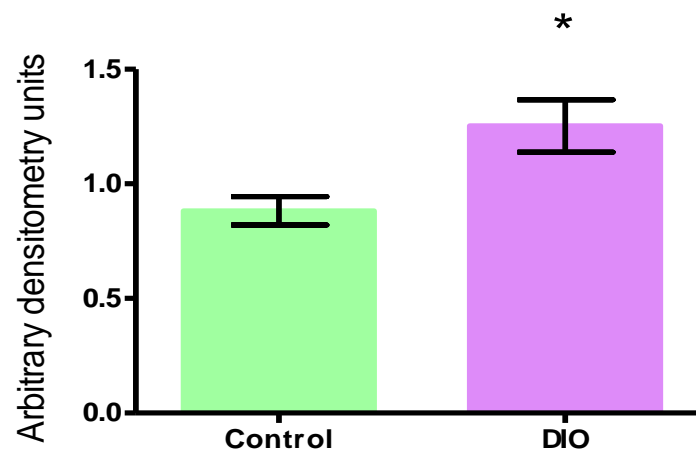


**Figure 41: PPAR-alpha expression in control and diet group after 8 weeks of DIO (n=4 per group).** A significant difference was found in the level of PPAR alpha expression between the control and diet group ( $0.88 \pm 0.06$  vs.  $1.25 \pm 0.11$ ;  $p=0.03$ ).

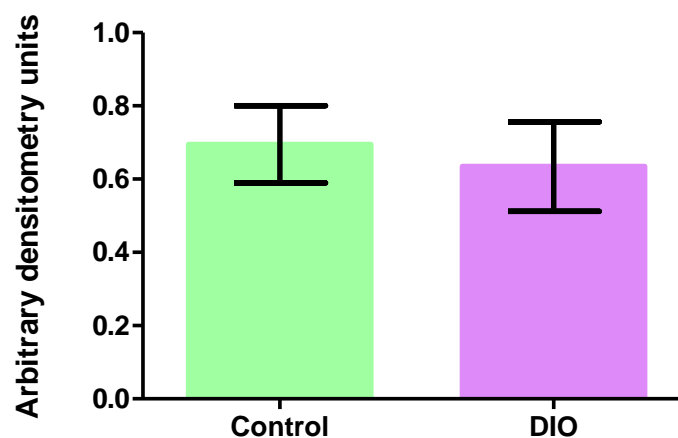


**Figure 42: PPAR-alpha expression in control and diet group after 16 weeks of DIO (n=4 per group).** No significant differences were found when comparing the level of PPAR-alpha expression between control and DIO groups ( $0.69 \pm 0.11$  vs.  $0.63 \pm 0.122$ ).

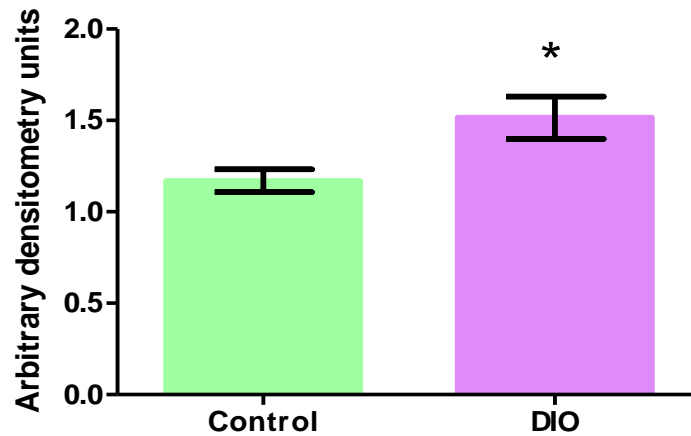


**Figure 43: PGC-1 alpha expression in control and diet group after 8 weeks of DIO (n=4 per group).** A significant difference was found in the level of PGC-1 alpha expression between the control and diet group ( $1.16 \pm 0.06$  vs.  $1.42 \pm 0.12$ ;  $p=0.03$ ).

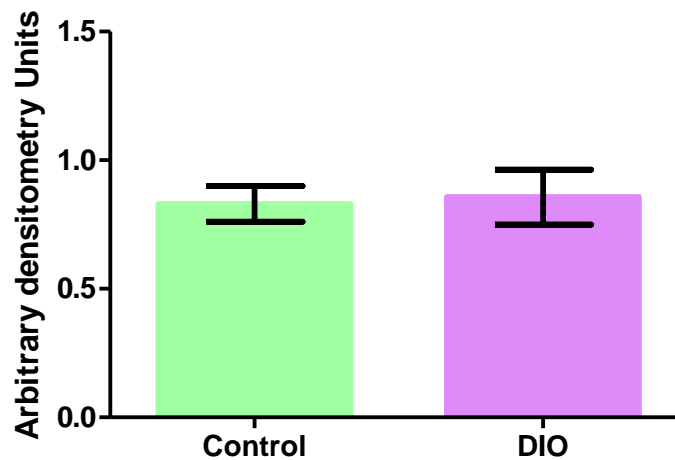


**Figure 44: PGC-1 alpha expression in control and diet group after 16 weeks of DIO (n= 4 per group).** No significant differences were found when comparing the level of PGC-1 alpha expression between control and DIO groups ( $0.83 \pm 0.07$  vs.  $0.86 \pm 0.11$ ).

### 3.4 THE EXPRESSION OF METABOLIC PROTEINS

#### 3.4.1 GLUT 4

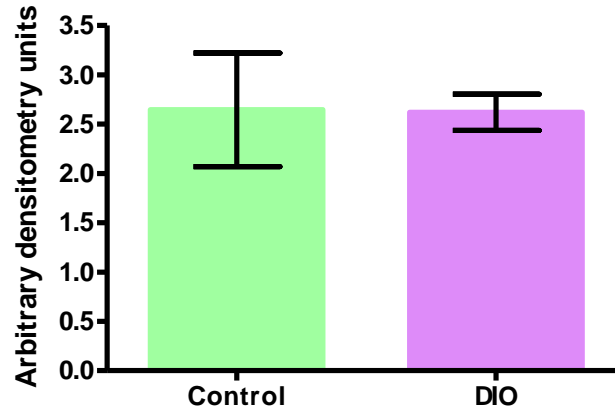


**Figure 45: GLUT 4 expression in control and diet group after 8 weeks of DIO (n=4 per group).** No significant differences were found when comparing the level of GLUT 4 expression between control and DIO groups ( $2.65 \pm 0.57$  vs.  $2.62 \pm 0.18$ ;  $p=0.97$ ).

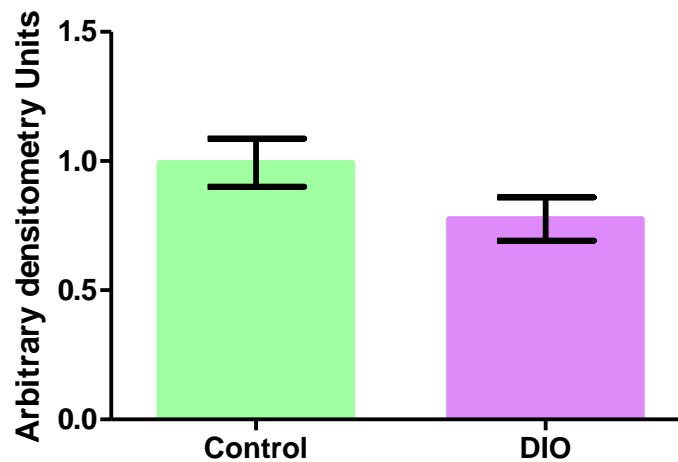


**Figure 46: GLUT 4 expression in control and diet group after 16 weeks of DIO (n=4 per group).** No significant differences were found when comparing the level of GLUT 4 expression between control and DIO groups ( $0.99 \pm 0.09$  vs.  $0.77 \pm 0.08$ ,  $p=0.1130$ ).

### 3.4.2 GLUT 1

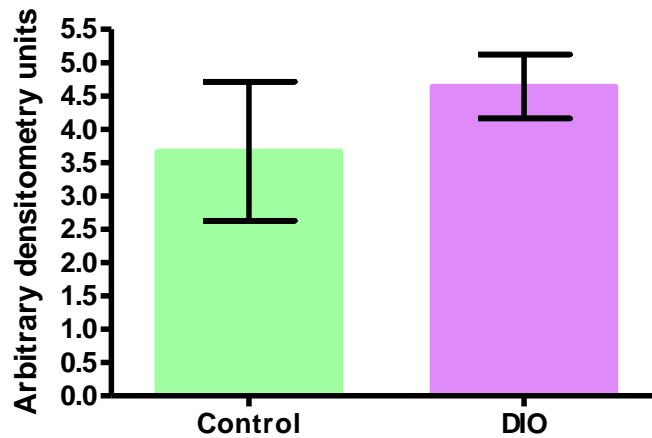


**Figure 47: GLUT 1 expression in control and diet group after 8 weeks of DIO (n=4 per group).** No significant differences were found when comparing the level of GLUT 1 expression between control and DIO groups ( $3.67 \pm 1.04$  vs.  $4.64 \pm 0.48$ ;  $p=0.43$ ).

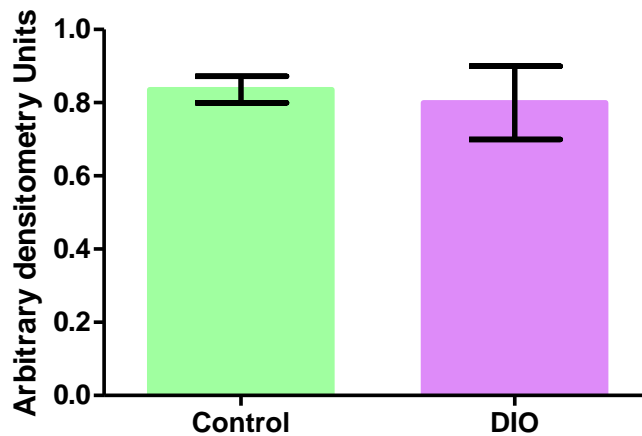


**Figure 48: GLUT 1 expression in control and diet group after 16 weeks of DIO (n= 4 per group).** No significant differences were found when comparing the level of GLUT 1 expression between control and DIO groups ( $0.84 \pm 0.04$  vs.  $0.80 \pm 0.10$ ).

### 3.4.3 Glycogen synthase kinase expression

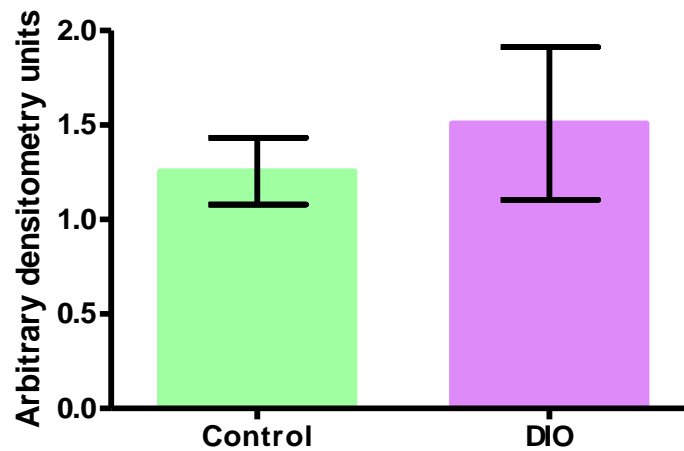


**Figure 49: Phosphorylated GSK-3 in control and diet group after 8 weeks of DIO (n=4 per group)** No significant differences were found when comparing the level of phosphorylated GSK-3 between control and DIO groups ( $1.26 \pm 0.18$  vs.  $1.51 \pm 0.40$ ;  $p=0.589$ ).

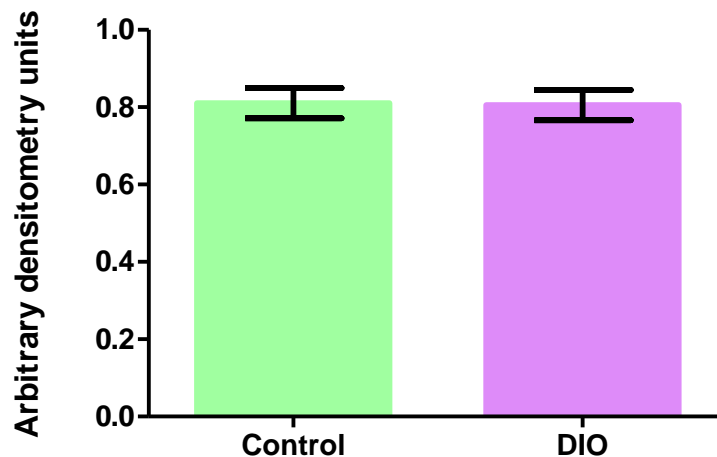


**Figure 50: Phosphorylated GSK-3 in control and diet group after 16 weeks of DIO (n=4 per group).** No significant differences were found when comparing the level of phosphorylated GSK-3 between control and DIO groups ( $0.81 \pm 0.04$  vs.  $0.81 \pm 0.04$ ;  $p=0.9293$ ).

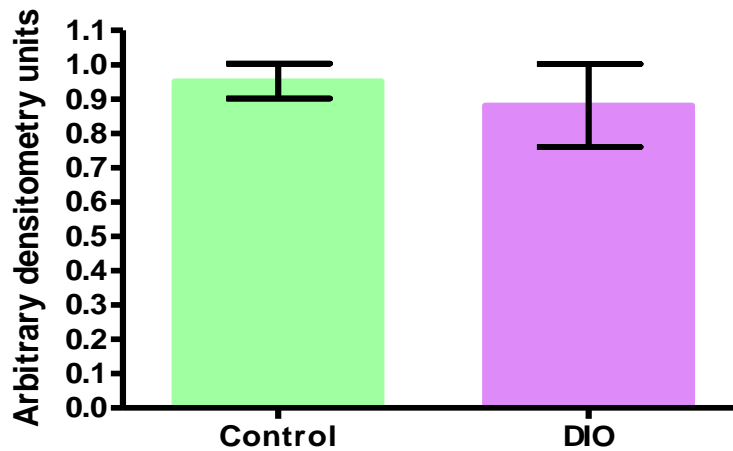


**Figure 51: Total GSK-3 expression in control and diet group after 8 weeks of DIO (n=4 per group).** No significant differences were found when comparing the level of total GSK-3 expression between control and DIO groups ( $0.95 \pm 0.05$  vs.  $0.88 \pm 0.12$ ;  $p=0.611$ ).

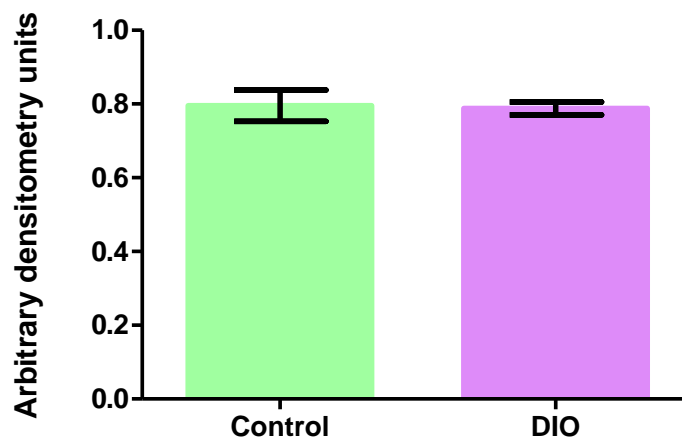


**Figure 52: Total GSK-3 expression in control and diet group after 16 weeks of DIO (n=4 per group).** No significant differences were found when comparing the level of total GSK-3 expression between control and DIO groups ( $0.80 \pm 0.04$  vs.  $0.79 \pm 0.02$ ;  $p=0.8680$ ).

#### 3.4.4 PI-3 kinase expression

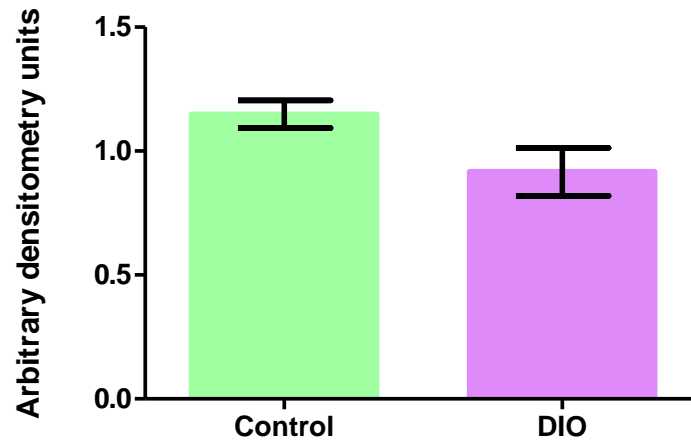


**Figure 53: Phosphorylated PI 3- kinase in control and diet group after 8 weeks of DIO (n=5 per group).** No significant differences were found when comparing the level of phospho PI 3-kinase between the control and DIO groups ( $1.15 \pm 0.06$  vs.  $0.92 \pm 0.09$ ;  $p=0.0716$ ).

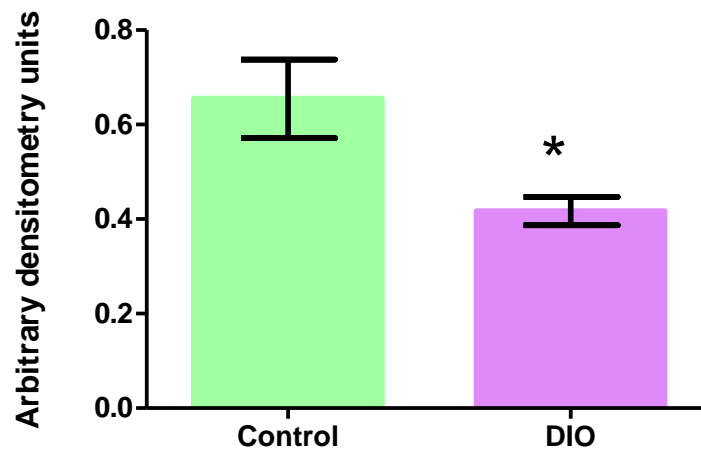


**Figure 54: Phosphorylated PI 3-kinase in control and diet group after 16 weeks of DIO (n=6 per group).** A significant decrease was found in the level of phosphorylated PI 3 kinase in the diet group when comparing control and DIO groups ( $0.65 \pm 0.08$  vs.  $0.42 \pm 0.03$ ;  $p=0.03$ )



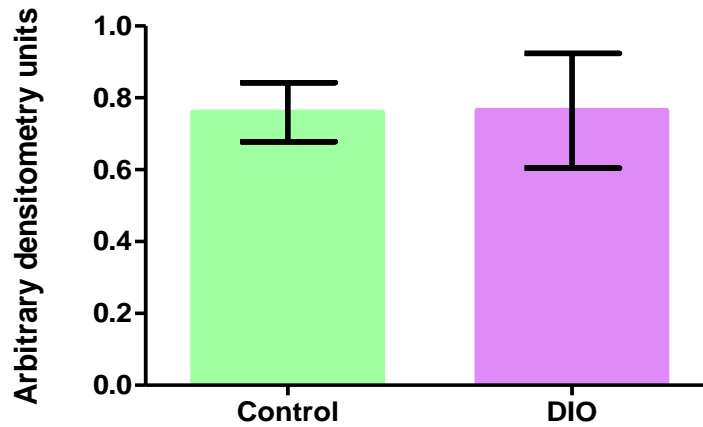


**Figure 55: Total PI 3-kinase expression in control and diet group after 8 weeks of DIO (n=5 per group).** No significant differences were found when comparing the level of total PI-3 kinase expression between control and DIO groups ( $0.96 \pm 0.05$  vs.  $1.01 \pm 0.08$ ;  $p=0.9814$ ).

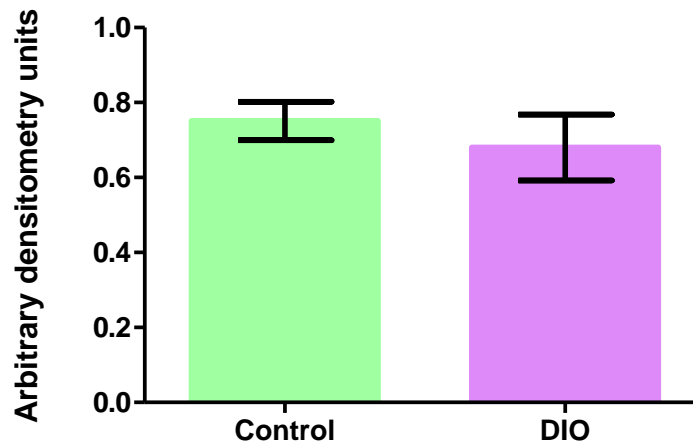


**Figure 56: Total PI 3-kinase expression in control and diet group after 16 weeks of DIO (n=4 per group).** No significant differences were found when comparing the level of total PI 3-kinase expression between control and DIO groups ( $0.75 \pm 0.05$  vs.  $0.68 \pm 0.08$ )  $p=0.5023$ .

### 3.4.5 PTEN expression

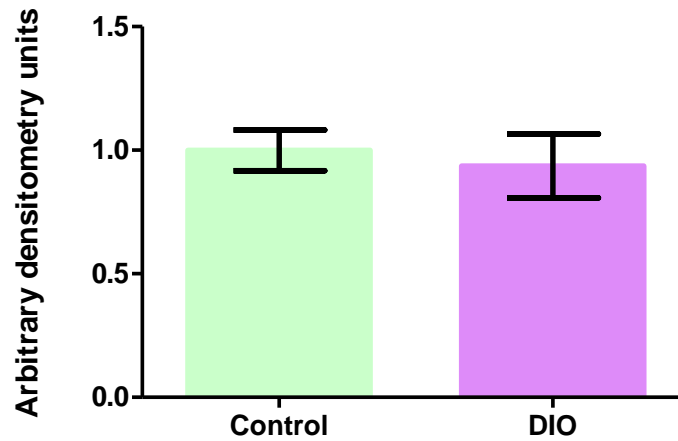


**Figure 57: Phosphorylated PTEN in control and diet group after 8 weeks of DIO (n=6 per group).** No significant differences were found when comparing the level of phosphorylated PTEN between control and DIO groups ( $0.99 \pm 0.08$  vs.  $0.94 \pm 0.13$ ;  $p=0.6889$ ).

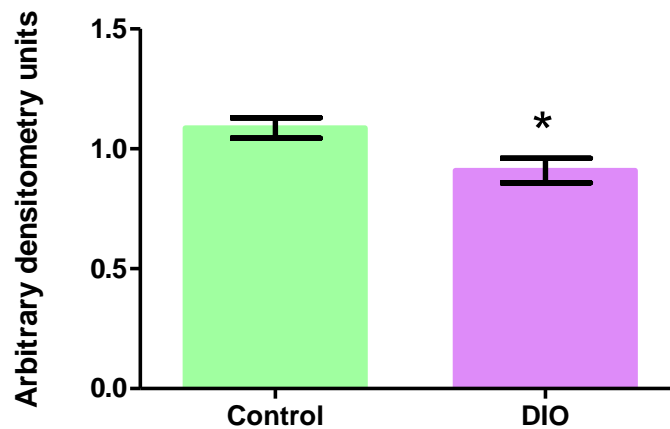


**Figure 58: Phosphorylated PTEN in control and diet group after 16 weeks of DIO (n=6 per group).** A significant decrease was found in the diet group when comparing the level of phosphorylated PTEN between control and DIO groups ( $1.09 \pm 0.04$  vs.  $0.91 \pm 0.05$ ;  $p=0.0233$ ).

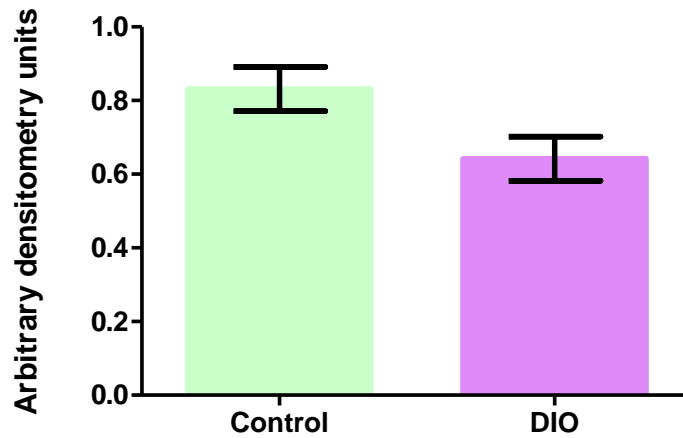


**Figure 59: Total PTEN expression in control and diet group after 8 weeks of DIO (n=6 per group).** No significant differences were found when comparing the level of total PTEN expression between control and DIO groups ( $0.86 \pm 0.03$  vs.  $0.86 \pm 0.04$ ;  $p=0.0506$ ).

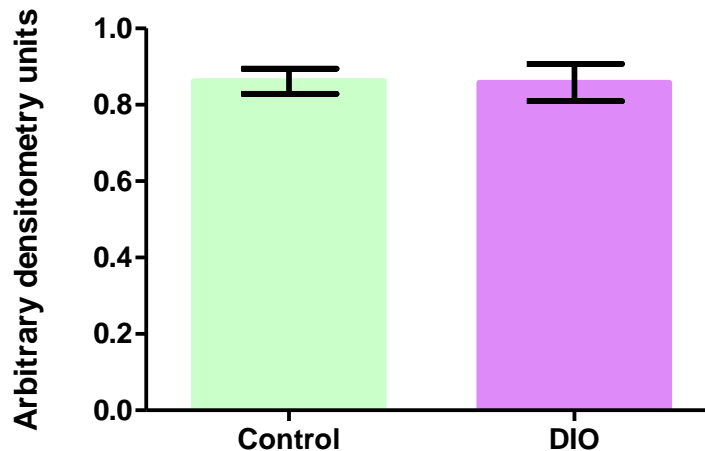


**Figure 60: Total PTEN expression in control and diet group after 16 weeks of DIO (n=6 per group).** No significant differences were found when comparing the level of total PTEN expression between control and DIO groups ( $0.83 \pm 0.06$  vs.  $0.64 \pm 0.06$ ;  $p=0.953$ ).

### 3.4.6 AMPK expression

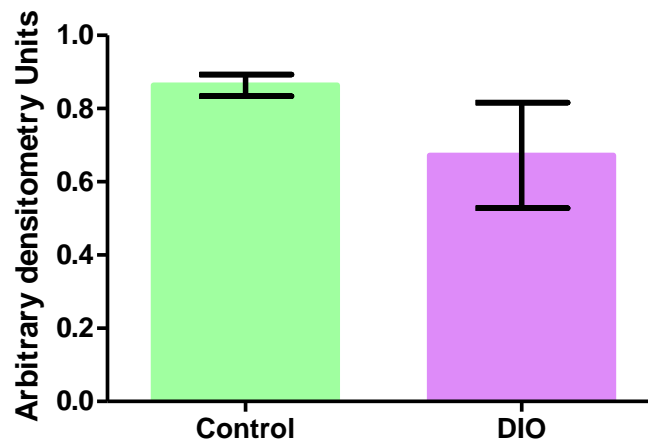


**Figure 61: Total AMPK expression in control and diet group after 8 weeks of DIO (n=4 per group).** No significant differences were found when comparing the level of total AMPK expression between control and DIO groups ( $0.95 \pm 0.05$  vs.  $0.88 \pm 0.12$ ;  $p=0.611$ ).

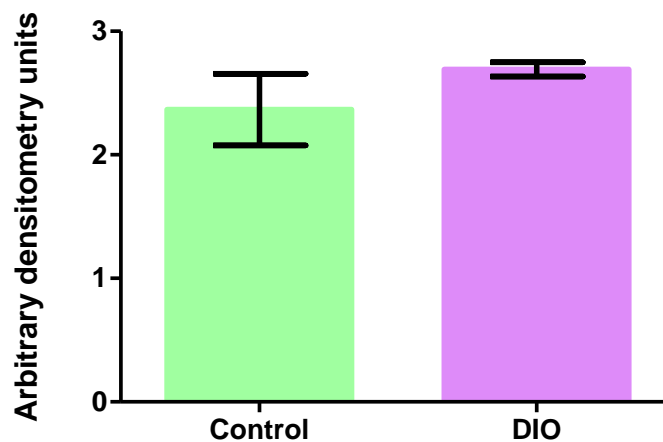


**Figure 62: Total AMPK expression in control and diet group after 16 weeks of DIO (n=6 per group).** No significant differences were found when comparing the level of total AMPK expression between control and DIO groups ( $2.37 \pm 0.29$  vs.  $2.69 \pm 0.05$ ;  $p=0.2954$ ).

### 3.5

## MITOCHONDRIAL FUNCTION

### 3.5.1

## Oxidative phosphorylation potential

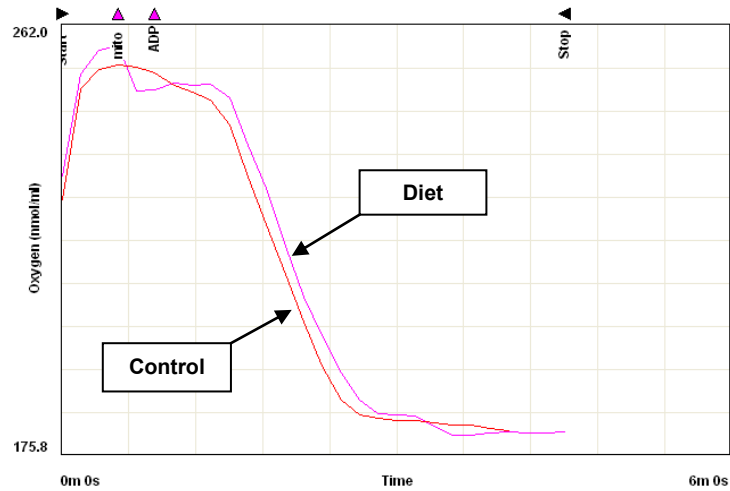


**Figure 63:** Oxygen consumption (nmol/ml) vs. time (seconds) for control and DIO groups, after 8 weeks of DIO, using glutamate as a substrate.

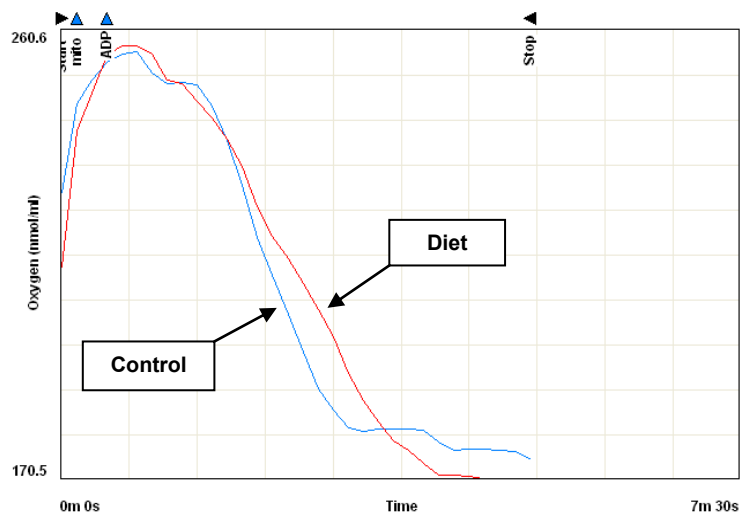


**Figure 64:** Oxygen consumption (nmol/min) vs. time (seconds) for control and DIO groups, after 8 weeks of DIO, using palmitoyl-L-carnitine as a substrate.

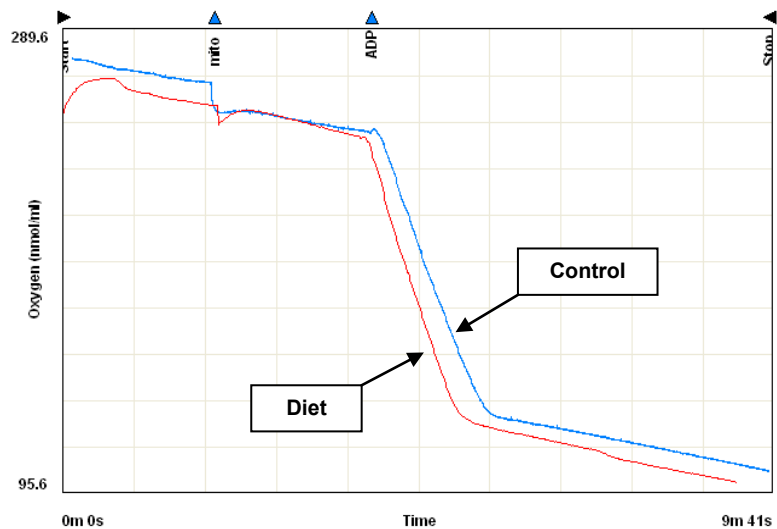


**Figure 65:** Oxygen consumption (nmol/min) vs. time (seconds) for control and DIO groups after 16 weeks of DIO using glutamate as a substrate.

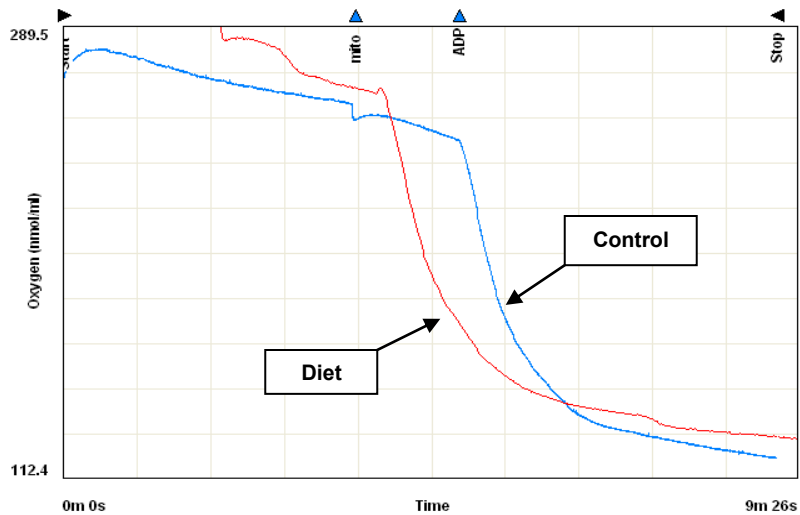


**Figure 66:** Oxygen consumption (nmol/min) vs. time (seconds) for control and DIO groups, after 16 weeks of DIO, using palmitoyl-L-carnitine as a substrate.

**Table 17: ADP/O ratio, State 3, State 4, RCI and oxidative phosphorylation rates of control and diet groups using glutamate as a substrate after 8 weeks of DIO**

	<b>ADP/O ratio:</b>	<b>State 3:</b>	<b>State 4:</b>	<b>RCI:</b>	<b>Oxphos rate:</b>
		<b>natoms O<sub>2</sub>/mg prot/min</b>			
<b>Control:</b>	2.89±0.10	104.17±15.56	11.62±3.68	18.40±5.48	299.17±46.23
<b>DIO:</b>	3.10±0.16	107.18±16.19	13.9±4.90	24.46±10.69	338.60± 59.11
<b>p-value:</b>	0.2931	0.8950	0.8950	0.6035	0.0875

**Table 18: ADP/O ratio, State 3, State 4, RCI and oxidative phosphorylation rates of control and diet groups using palmitoyl-L-carnitine as a substrate after 8 weeks of DIO**

	<b>ADP/O ratio:</b>	<b>State 3:</b>	<b>State 4:</b>	<b>RCI:</b>	<b>Oxphos rate:</b>
		<b>natoms O<sub>2</sub>/mg prot/min</b>			
<b>Control:</b>	9.44±4.57	95.92±25.4	13.92±5.41	15.59±5.56	538.05±144.7
<b>DIO:</b>	14.87±5.45	59.83±10.17	16.45±4.48	5.07±1.34	653.77± 201.2
<b>p-value:</b>	0.4626	0.2168	0.6652	0.0955	0.6506

**Table 19: ADP/O ratio, State 3, State 4, RCI and oxidative phosphorylation rates of control and diet groups using glutamate as a substrate after 16 weeks of DIO**

	<b>ADP/O ratio:</b>	<b>State 3:</b>	<b>State 4:</b>	<b>RCI:</b>	<b>Oxphos rate:</b>
		<b>natoms O<sub>2</sub>/mg prot/min</b>			
<b>Control:</b>	2.67±0.12	134.98±7.08	9.92±0.36	13.62±0.58	361.31±24.42
<b>DIO:</b>	2.48±0.08	125.46±8.96	8.88±0.95	14.77±1.11	309.21± 22.59
<b>p-value:</b>	0.2016	0.4203	0.3244	0.3773	0.1433

**Table 20: ADP/O ratio, State 3, State 4, RCI and oxidative phosphorylation rates of control and diet groups using palmitoyl-L-carnitine as a substrate after 16 weeks of DIO**

	<b>ADP/O ratio:</b>	<b>State 3:</b>	<b>State 4:</b>	<b>RCI:</b>	<b>Oxphos rate:</b>
		<b>natoms O<sub>2</sub>/mg prot/min</b>			
<b>Control:</b>	5.84±1.57	75.76±22.31	6.39±0.89	10.27±2.49	251.11±42.84
<b>DIO:</b>	5.32±1.08	66.59±18.42	4.91±0.44	13.73±4.06	248.64± 36.48
<b>p-value:</b>	0.7899	0.7568	0.1585	0.4808	0.9657



### 3.5.2 Anoxia/reperfusion of isolated cardiac mitochondria

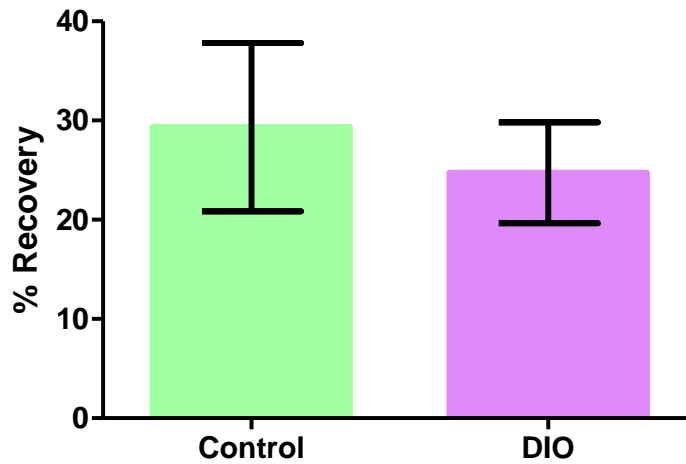


**Figure 67:** The percentage recovery after 20 minutes of anoxia in control and diet groups using glutamate as a substrate. No significant differences were found when comparing the % recovery after 20 minutes of anoxia between control and diet groups ( $29.33 \pm 8.47$  vs.  $24.74 \pm 5.08$ ;  $p=0.6505$ ).

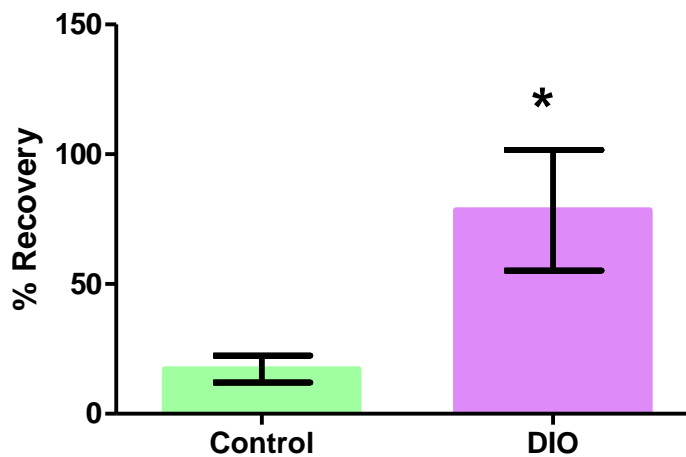


**Figure 68:** The percentage recovery after 20 minutes of anoxia in control and diet groups using palmitoyl-L-carnitine as a substrate. A significant increase was found in the diet group when comparing the % recovery after 20 minutes of anoxia between control and diet groups ( $17.22 \pm 5.1$  vs.  $78.46 \pm 23.22$ ;  $p=0.0362$ ).

### 3.5.3 Quantification of ATP production

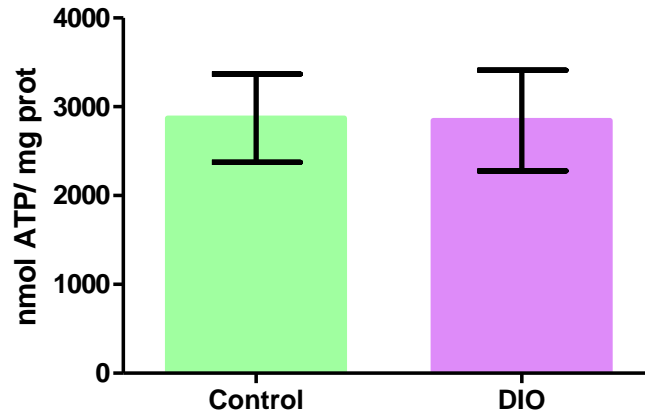


**Figure 69: Amount of ATP produced during state 3 respiration.** No significant difference was found when comparing the amount of ATP produced between control and DIO groups (2872.41 ± 497.2 vs. 2844.98 ± 566.7;  $p=0.9717$ )

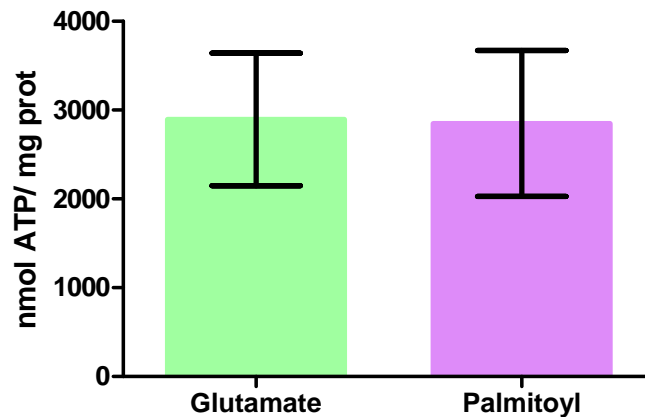


**Figure 70: Amount of ATP produced during state 3 respiration by the control group when using either glutamate or palmitoyl-L-carnitine as substrates.** No significant difference was found when comparing the amount of ATP produced by the control group when using either glutamate or palmitoyl-L-carnitine as substrates (2895.28 ± 747.53 vs. 2849.55 ± 822.63;  $p=0.969$ )

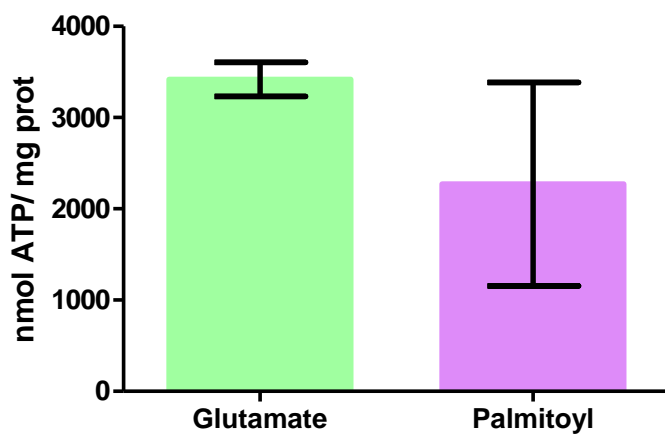


**Figure 71: Amount of ATP produced during state 3 respiration by the diet group when using either glutamate or palmitoyl-L-carnitine as substrates.** No significant difference was found when comparing the amount of ATP produced by the diet group when using either glutamate or palmitoyl-L-carnitine as substrates (3419.69 ± 186.40 vs. 2270.27 ± 1113.85; p=0.3663)

### 3.6 ELECTRON TRANSPORT CHAIN COMPLEX ANALYSIS

**Table 21: State 3 respiration (natoms O<sub>2</sub>/mg prot/min): succinate, rotenone, oligomycin and CCCP when using glutamate as a substrate**

	<b>Succinate</b>	<b>Rotenone</b>	<b>Oligomycin</b>	<b>CCCP</b>
<b>Control</b>	297.45 ± 42.70	72.43 ± 8.25	58.46 ± 6.09	10.47 ± 2.68
<b>DIO</b>	288.85 ± 33.14	94.78 ± 11.18	76.39 ± 9.56	17.63 ± 1.14
<b>p-value</b>	0.8797	0.1296	0.1310	0.0413 *

\* P<0.05 significant difference

**Table 22: State 3 respiration (natoms O<sub>2</sub>/mg prot/min): succinate, rotenone, oligomycin, and CCP when using palmitoyl-L-carnitine as a substrate**

	<b>Succinate</b>	<b>Rotenone</b>	<b>Oligomycin</b>	<b>CCCP</b>
<b>Control</b>	288.85 ± 33.14	94.78 ± 11.18	76.39 ± 9.56	17.63 ± 1.14
<b>DIO</b>	152.16 ± 59.17	73.21 ± 14.64	55.19 ± 12.17	16.87 ± 5.20
<b>p-value</b>	0.3841	0.5933	0.3262	0.1699

### 3.7 CITRATE SYNTHASE ACTIVITY

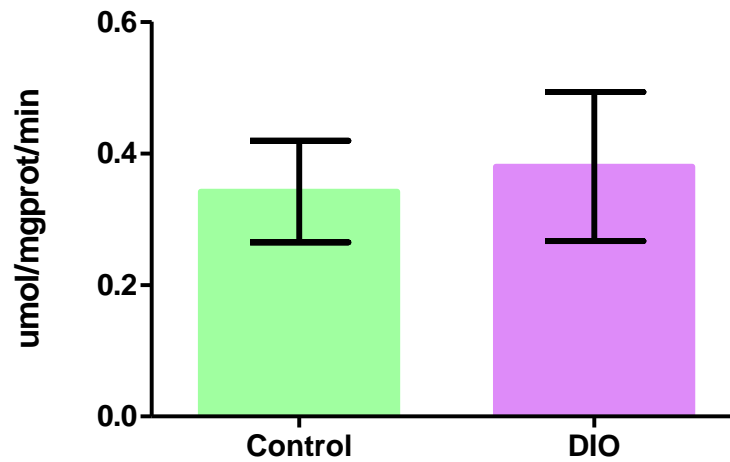


**Figure 72:** The level of citrate synthase activity ( $\mu\text{mol/mgprot/min}$ ) in both the control and diet groups after 8 weeks of DIO. No significant difference in the level of citrate synthase activity was found between the control and diet group ( $0.53 \pm 0.01$  vs.  $0.76 \pm 0.11$ ;  $p=0.166$ ).

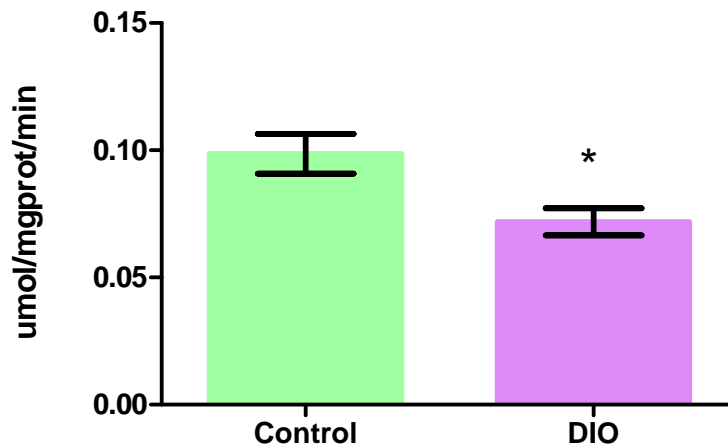


**Figure 73:** The level of citrate synthase activity ( $\mu\text{mol/mgprot/min}$ ) in control and diet groups after 16 weeks of DIO. A significant decrease was found in the level of citrate synthase activity in the diet group when comparing control and diet groups ( $0.099 \pm 0.007$  vs.  $0.072 \pm 0.005$ ;  $p= 0.0085$ )

### 3.8 PYRUVATE DEHYDROGENASE ENZYME QUANTITY AND ACTIVITY

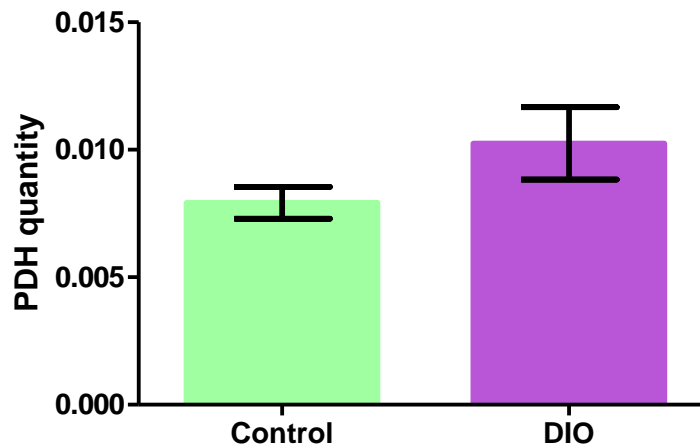


**Figure 74:** The level of pyruvate dehydrogenase enzyme quantity after 8 weeks of DIO. No significant difference was found between the quantity of PDH enzyme when comparing control and diet groups ( $0.007 \pm 0.0006$  vs.  $0.01 \pm 0.0014$ ;  $p = 0.165$ )

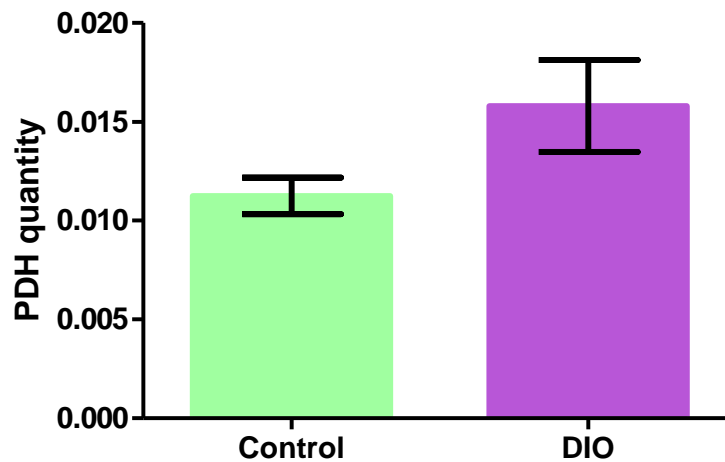


**Figure 75:** The level of pyruvate dehydrogenase enzyme quantity after 16 weeks of DIO. No significant difference was found between the quantity of PDH enzyme when comparing control and diet groups ( $0.011 \pm 0.0009$  vs.  $0.02 \pm 0.0021$ ;  $p = 0.0835$ )

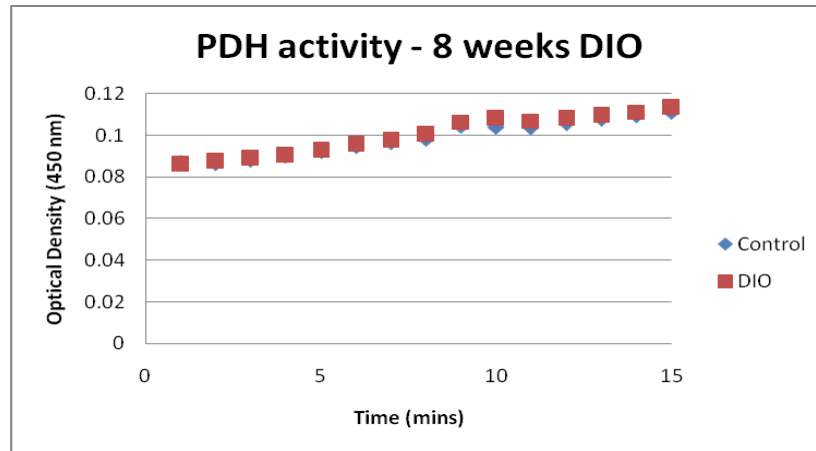


**Figure 76:** The level of PDH activity measured after 8 weeks of DIO. No differences were found in PDH activity when comparing the control and DIO groups ( $0.09 \pm 0.0022$  vs.  $0.10 \pm 0.0024$ ;  $p=0.6569$ )

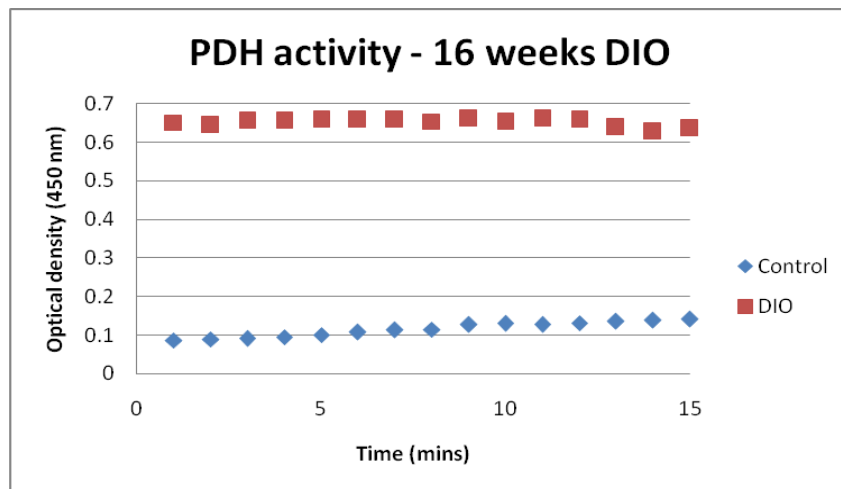


**Figure 77:** The level of PDH activity measured after 16 weeks of DIO. A significant increase in PDH activity was found in the diet group when comparing the control and DIO groups ( $0.11 \pm 0.005$  vs.  $0.65 \pm 0.0026$ ;  $p<0.0001$ )

### 3.9 RELATIVE TRANSCRIPT LEVELS MEASURED BY RT-PCR

#### 3.9.1 PDK 4 expression

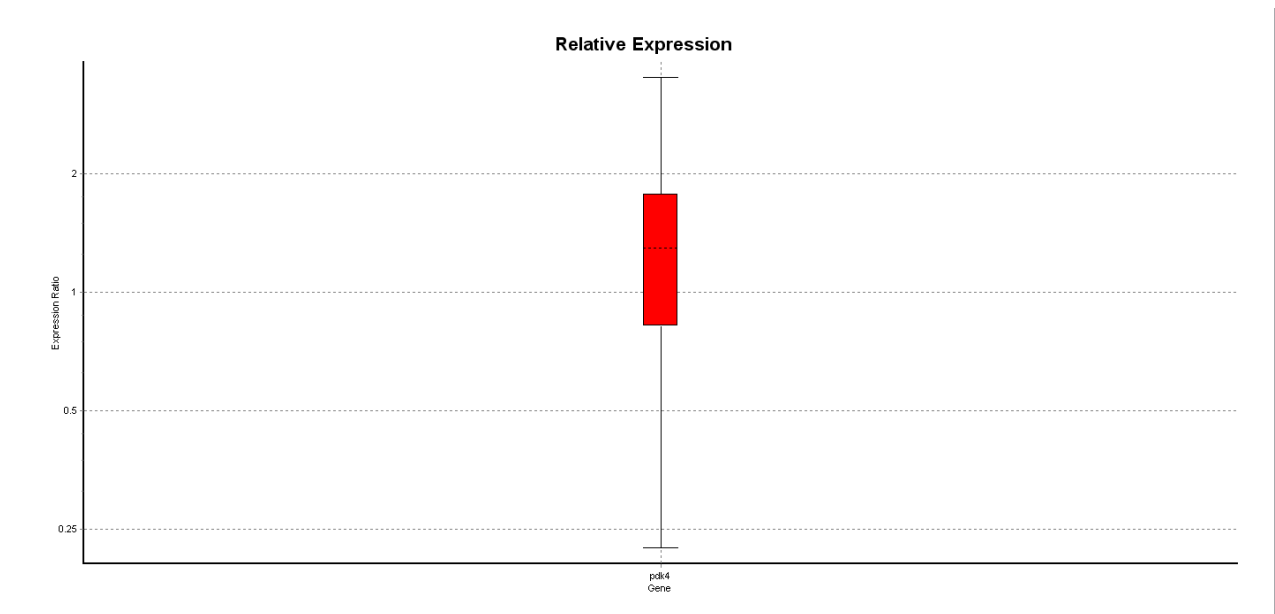


**Figure 78:** The level of PDK 4 expression after 8 weeks of DIO. The PDK 4 expression was significantly up-regulated in the diet group ( $p=0.004 \pm 0.573$ -2.081)



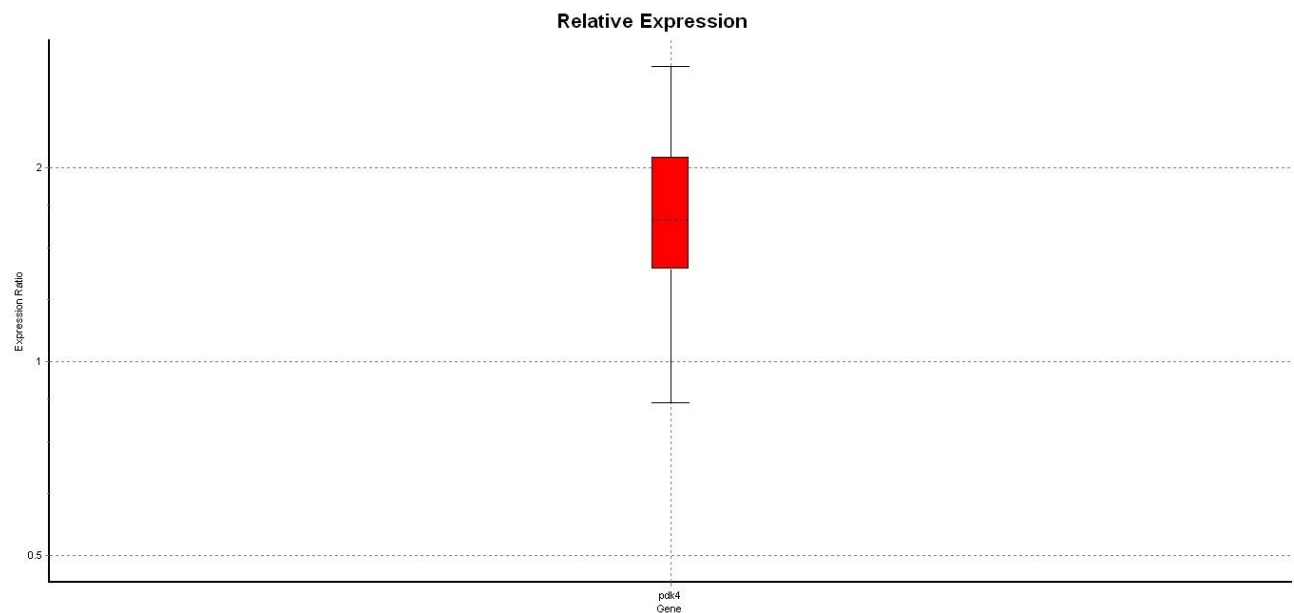


**Figure 79:** The level of PDK 4 expression after 16 weeks of DIO. No difference was found in the level of expression of PDK 4 when comparing control and DIO groups ( $p=0.608 \pm 1.262-2.295$ )

### 3.9.2 FAT/CD36 expression

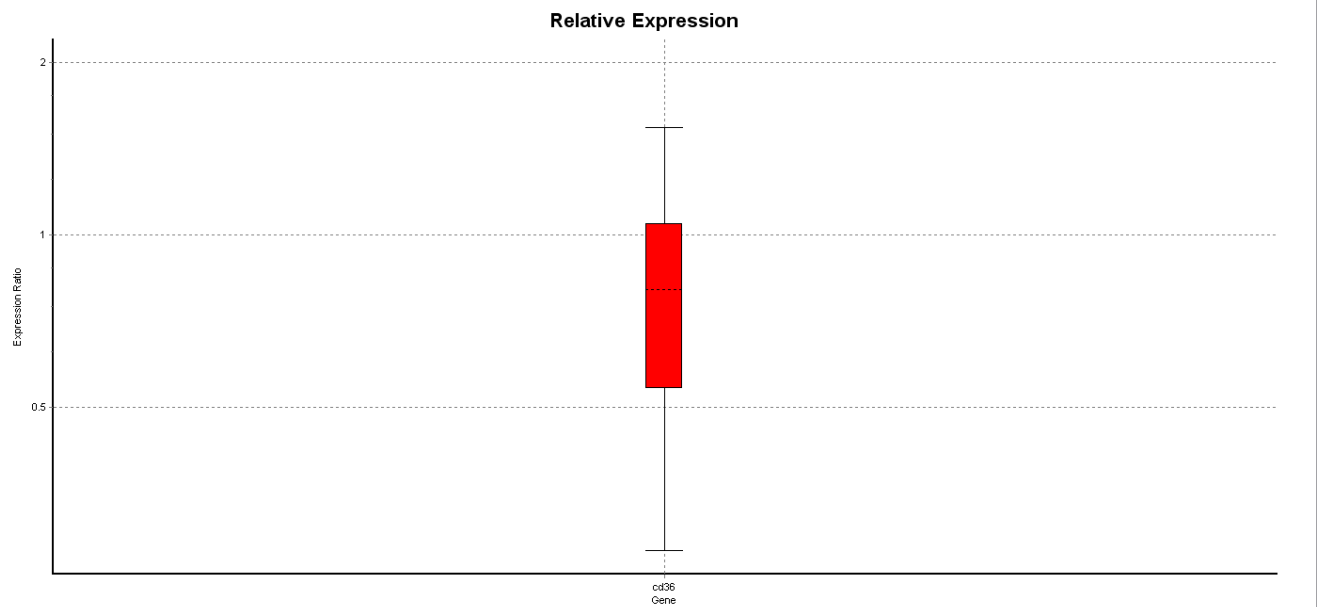


**Figure 80:** The level of FAT/CD36 expression after 8 weeks of DIO. No difference was found in the expression of FAT/CD36 when comparing control and DIO groups ( $p=0.159 \pm 0.449-1.168$ )

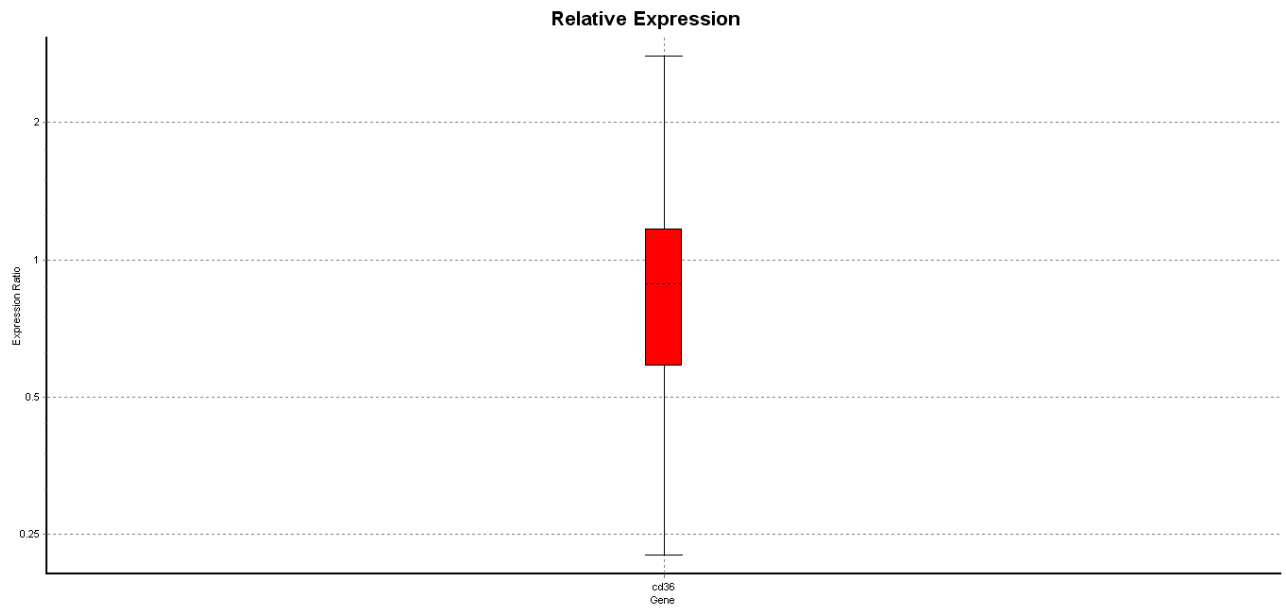


**Figure 81:** The level of FAT/CD36 expression after 16 weeks of DIO. NO differences were found in the level of expression of FAT/CD36 when comparing the control and DIO groups ( $p=0.520 \pm 0.445-1.306$ )

## CHAPTER 4: DISCUSSION

Cardiovascular disease is globally the primary cause of death in patients suffering from obesity and type-2 diabetes mellitus. The development of cardiac dysfunction and insulin resistance in these conditions are thought to be due to alterations in substrate metabolism [Coort et al. 2007]. We hypothesized that, in a rat model of diet-induced obesity, pathways involved in myocardial glucose utilization would be down regulated with simultaneous up regulation of FA utilization pathways and that this will lead to certain metabolic adaptations which will eventually become maladaptive. We therefore aimed to elucidate mitochondrial oxidative capacity and biogenesis, as well as signalling pathways involved in substrate utilization and energy production in rats on the obesity inducing diet for a period of 8 or 16 weeks.

In our study we were able to establish that our model of diet-induced obesity displayed visceral obesity and insulin resistance with significantly elevated blood glucose and serum insulin levels.

The intra-peritoneal fat weight was measured and used as a measure of abdominal obesity in all of our animals. Measuring the IP fat weight was important because it is well documented that there is a close relationship between abdominal obesity and a range of metabolic risk factors for heart disease [Kissebah et al. 1982; Folsom et al. 2000; Chan et al. 1994; Poulliot et al. 1992]. These risk factors include insulin resistance and diabetes. French physician Jean Vague was first to report an association between the obesity phenotype and diabetes [Vague 1956], which has sparked a multitude of epidemiological and physiological studies which have all confirmed the relationship between abdominal obesity and insulin resistance. It is important to note that environmental, biological or inherited factors that induce insulin resistance can also cause abdominal fat accumulation, and that the association between abdominal fat and insulin resistance does not prove causality

[Frayn 2000]. A link between abdominal fat, fatty acid metabolism and insulin resistance has been suggested and is supported by observations that basal whole body FFA flux rates are increased in upper body obese subjects when compared to lower-body obese and lean subjects [Horowitz et al. 1999; Jensen et al. 1989], and the fact that diet-induced weight loss can decrease whole-body FFA flux and improve insulin sensitivity [Klein et al. 1996]. The fact that we found a significant increase in the IPF weight in the obese animals is a good indication that the diet was adequate in producing visceral obesity and that our diet-induced obese model may also be insulin resistant.

#### **4.1 Early and progressed metabolic remodelling in response to obesity**

In the presence of metabolic dysregulation as can be seen in the case of obesity and insulin resistance the heart responds to the changes in its environment by making specific metabolic alterations to favour the production of energy in order to maintain normal cardiac function. This phenomenon is often referred to in literature as metabolic adaptation. Metabolic adaptation in the case of obesity and insulin resistance aims to maintain cardiac function mainly by increasing the utilization of FAs, which in this scenario becomes the preferred substrate for energy production as glucose uptake and signalling pathways appear to be suppressed, by the increase in the availability of circulating FFAs [Young et al. 2001]. As the regulators of the expression of metabolic genes in cardiomyocytes, PPAR alpha and PGC-1 alpha play a pivotal role in initiating this form of myocardial metabolic adaptation to obesity [Brown et al. 1995; Makinde et al. 1998]. Literature suggests that this early metabolic adaptive response could possibly become maladaptive as the pathological accumulation of both glucose and FA metabolites will lead to the initiation of apoptosis, chronic activation of PKCs, ROS generation and contractile dysfunction [Young et al. 2001]. We were therefore particularly interested to investigate the effects of a prolonged high caloric diet (16 weeks DIO) on cardiac metabolism and more specifically how

efficient this so-called metabolic adaptive response will remain. In addition, we studied how mitochondrial function would be influenced.

Results from our study indicate an early adaptive metabolic response. After 8 weeks of DIO we observed significant elevations in the expression of PPAR alpha and PGC-1 alpha in the diet group. This confirms that an increase in the availability of circulating FFAs, based on the increase in visceral obesity, sparked an early metabolic adaptive response by increasing the expression of these two regulators of the expression of metabolic genes in the heart. Consequently we wanted to investigate how the expression of key metabolic proteins involved in both FA metabolism as well as glucose metabolism had been affected by this increase in the expression of PPAR alpha and PGC-1 alpha as well as the increase in FAs and the presence of insulin resistance, which of course will compromise glucose metabolism both at the level of glucose uptake i.e. defective insulin signalling, as well as at the level of the pyruvate dehydrogenase complex, which catalyzes the committed step for glucose oxidation [Young et al. 2002]. It appears however that after 16 weeks of diet, the hearts had apparently adapted metabolically to the increased levels of FAs and were able to maintain cardiac function. The early changes in the expression of PPAR alpha and PGC-1 alpha were now not noticeable which corroborates the findings of Young et al. 2001.

We were able to observe some interesting metabolic changes that once again indicate an early adaptive metabolic response i.e. an increase in the expression of PDK 4 in the diet group after 8 weeks of DIO, as well as slightly compromised insulin signalling pathway at a later stage in the diet i.e. a decrease in the phosphorylation of PTEN and PI 3 kinase as well as an unexpected increase in the activity of PDH in the diet group after 16 weeks of DIO.

Studies show that in states associated with decreased cardiac glucose utilization and increased rates of lipid oxidation, the activity and expression of PDK 4 in the adult rat heart is enhanced [Wu et al. 1998] and the up-regulation of cardiac PDK

4 protein expression is closely linked to an increased FA supply and/or oxidation [Sugden et al. 2000], which could be due to either the mobilization of endogenous triacylglycerol, as experienced during diabetes, or through an increased dietary lipid supply [Sugden et al. 2001].

Long-chain FAs affect signalling pathways as well as gene expression. PPAR alpha plays an important role in the up-regulation of the expression of PDK 4, as the activation of PPAR alpha plays a role in the mediation of the effects of long-chain FAs and/or their metabolites on the metabolism [Sugden et al. 2001]. Our findings substantiate this concept as the increase in the expression of PPAR alpha and PGC-1 alpha was accompanied by an increase in the level of PDK 4 after 8 weeks of DIO. PDK 4 is also known to inhibit the pyruvate dehydrogenase enzyme complex, which is the enzyme responsible for catalyzing the committed step for carbohydrate oxidation, which will lead to a reduction in glucose oxidation [Young et al. 2002]. We however did not measure PDK 4 activity i.e. the amount of phosphorylated PDK 4, therefore we are unable to elucidate the role of PDK 4 in the activity of the PDH complex, especially after 16 weeks of DIO where we observed an increase in the activity of the PDH complex.

An increase in the PDH activity in the diet group suggests that glucose oxidation is still functional and that after 16 weeks of DIO the PDH complex might not be negatively regulated by PDK 4 or the by-products of FA oxidation.

PI 3 kinase is a key regulator of cell survival and growth and is responsible for the activation of PKB/Akt which in turn activates prosurvival substrates. PI 3 kinase is also negatively regulated by PTEN which will affect the possible cardioprotective effects of PKB/Akt [Oudit and Penninger 2009]. The activity of PTEN is down regulated by phosphorylation, therefore a decrease in the phosphorylation of PTEN in the diet group implies that there is significantly more activation of apoptotic pathways in the diet group than in the control group after

16 weeks of DIO. Similarly decreased phosphorylation of PI 3 kinase indicates a reduction in the level of protection via the activation of survival pathways.

In a pilot study we determined infarct size in hearts exposed to ischaemia/reperfusion after 8 weeks of DIO and found smaller infarcts than in control-fed animals. We therefore measured PKB/Akt expression and activity but could find no difference in the expression or activity of PKB/Akt in the infarcted or non-infarcted zones of the control and diet groups. PKB/Akt, as previously mentioned, has been implicated as a key role player in cardioprotection however these results indicate that PKB/Akt may not have been involved in the activation of survival pathways resulting in smaller infarct development. There was no change in the expression or activity of the up-stream activator of PKB/Akt, PI 3 kinase, as well as the regulator of these two proteins, PTEN after 8 weeks of diet.

We observed no other changes in the expression of the metabolic proteins that we investigated at the early, 8 week stage. Because changes may occur at a later stage, we investigated the protein expression profiles after 16 weeks on diet. Even after 16 weeks we observed no other changes other than the changes in PTEN, PI 3 kinase and PDH activity. There was also no other differences with regard to the expression of proteins involved in glucose and FA metabolism. We speculate that this could be because the metabolism has adapted and is now able to cope under the stresses of increased FAs and potential compromised glucose oxidation to maintain cardiac function.

We did not measure the translocation of key proteins involved in glucose and FA uptake i.e. GLUT 4 and FAT/CD36. It is therefore possible that although we did not observe a difference in the total expression of GLUT 4 and FAT/CD36 that these two transporters may be facilitators in the transition of the utilization of FAs as preferred substrate since GLUT 4 might be sequestered in vesicles in the cytoplasm, which will ultimately lead to a reduction in glucose uptake, and



FAT/CD36 transporters might be inserted in the plasma membrane where they can facilitate the transport of FAs into the cell.

The uptake of Long-chain FAs has been shown to be up-regulated in cardiac myocytes from obese, pre-diabetic Zucker rats, and this increase in the uptake of FAs is associated with an increase in FAT/CD36 on the cell surface and not an increase in the total expression of FAT/CD36 [Luiken et al. 2001]. Whereas in this obese and pre-diabetic state GLUT 4 is retained in intracellular storage compartments [Goodyear and Kahn 1998, Luiken et al. 2001]. Furthermore the translocation of FAT/CD36 from the intracellular storage compartment to the membrane has been shown to rapidly up-regulate the uptake of FAs into heart muscle [Glatz et al. 2010].

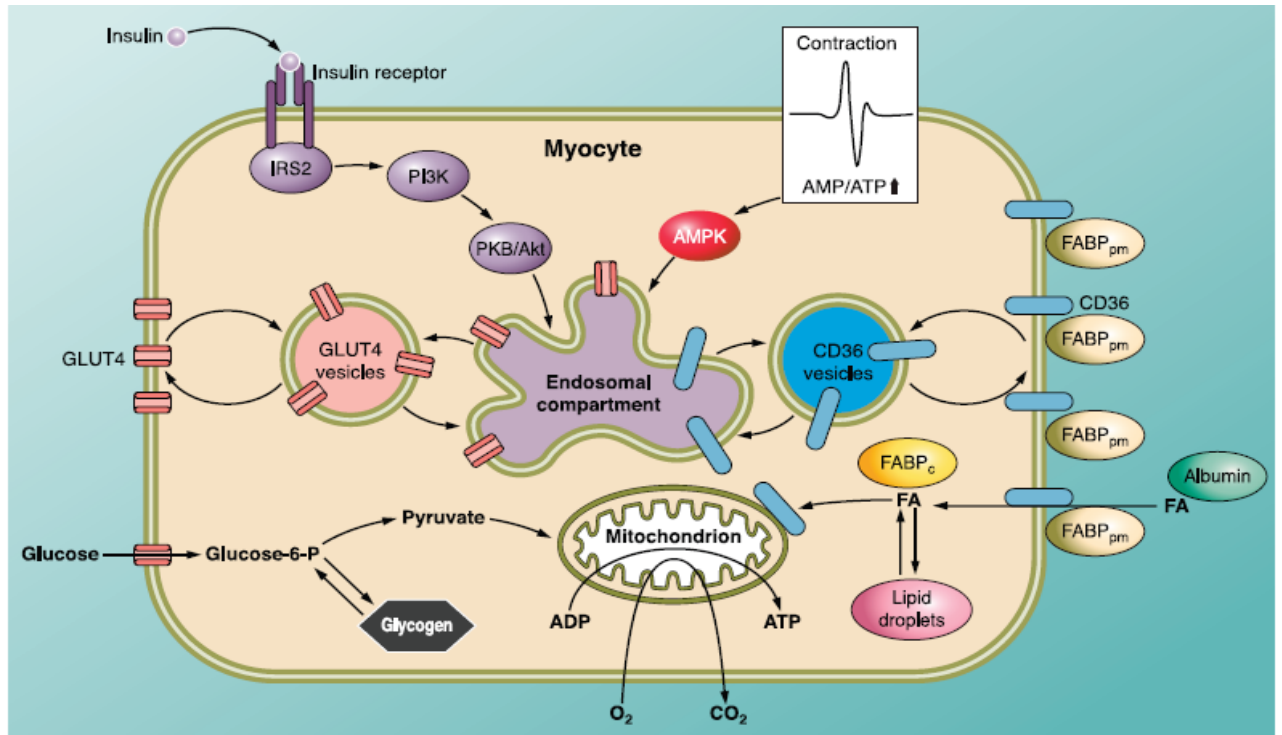


**Figure 82:** The uptake of fatty acids and glucose by cardiac muscle is increased through the translocation of specific transport proteins i.e. GLUT 4 and FAT/CD36 respectively in response to insulin stimulation or increased contractile activity [Glatz et al. 2010]

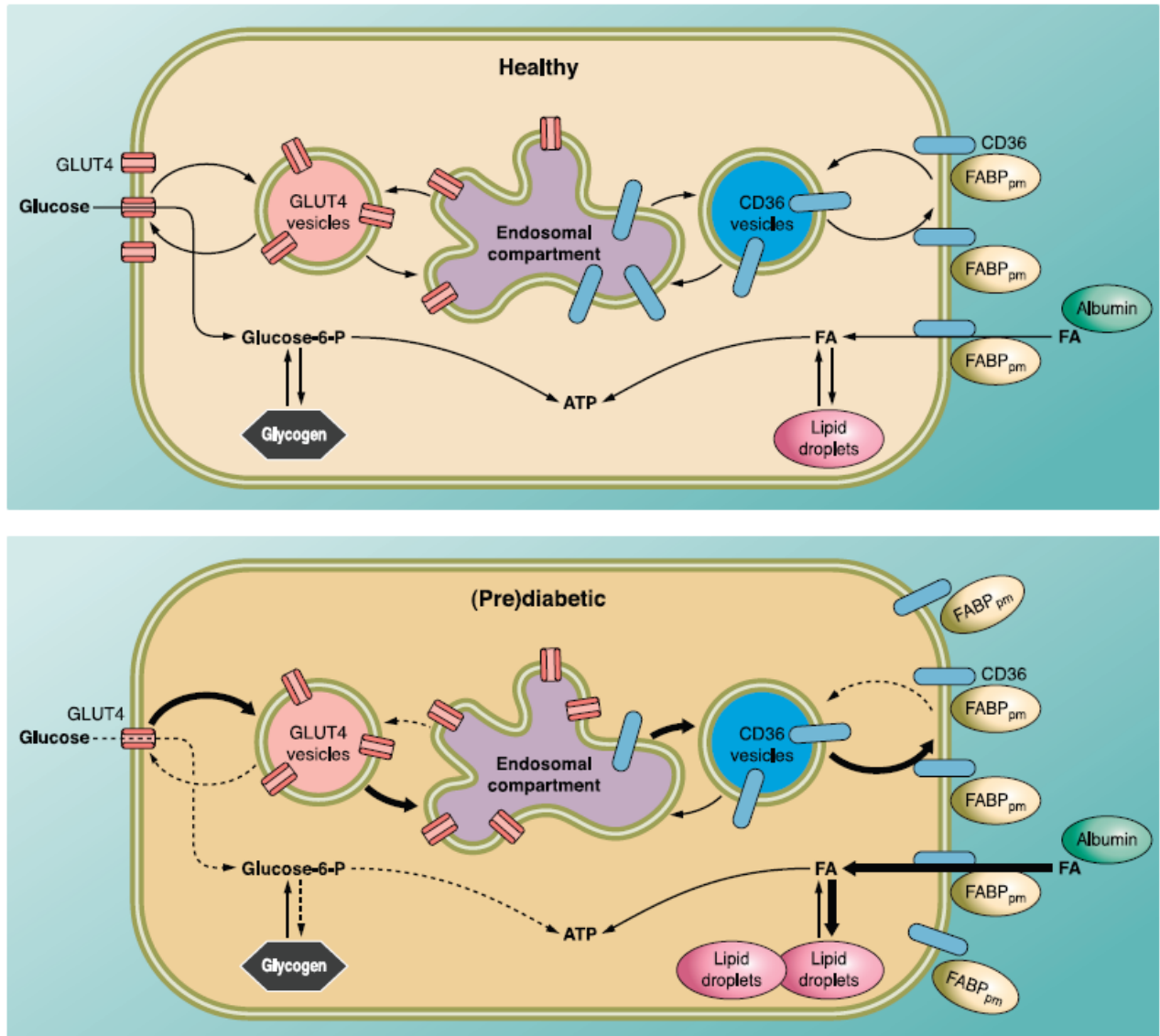


**Figure 83:** Schematic representation of FAT/CD36 and GLUT 4 translocation in healthy (top) and insulin resistant (bottom) cardiac muscle [Glatz et al. 2010]

It has been shown that in healthy heart tissue, GLUT 4 and FAT/CD36 are distributed equally between the intracellular storage compartments and the sarcolemma. This distribution of glucose and FA transporters is disturbed in the insulin-resistant state so that there is an increase in the translocation of FAT/CD36 to the membrane which results in an increase in FA uptake and the production of FA metabolites, which will interfere with and inhibit insulin signalling

and in doing so reduce the translocation of GLUT 4 to the sarcolemma resulting in reduced glucose uptake [Glatz et al. 2010]

Although we did not measure AMPK activity, it has been suggested the AMPK acts as a fuel gauge and plays a major role in the maintenance of intracellular energy balance [Cantó and Auwerx 2009]. AMPK is known to be activated in response to alterations in the AMP/ATP ratio and then acts to restore energy balance by up-regulating catabolic pathways which produce ATP and down-regulating anabolic pathways that utilizes ATP [Cantó and Auwerx 2009]. PGC-1 alpha has also been implicated as a possible mediator of AMPK-induced gene expression. The latter requires PGC-1 alpha activity in order to modulate the expression of key proteins involved in mitochondrial and glucose metabolism [Jager et al. 2007]. It has been shown that AMPK activation leads to an increase in the expression of PGC-1 alpha [Suwa et al. 2003; Terada et al. 2002] and can directly interact and phosphorylate PGC-1 alpha, which appears to increase the transcriptional activity of PGC-1 alpha [Jager et al. 2007]. Together with the elevated uptake of FAs into the heart, enhanced activity of AMPK may also be responsible for the early upregulation of PGC-1 alpha.

To summarize the expression of the metabolic proteins involved in both glucose and FA oxidation:

**Table 23: Summary of results**

	8 weeks DIO		16 weeks DIO	
	Total	Phospho	Total	Phospho
<b>PPAR alpha</b>	UP	-	x	-
<b>PGC-1 alpha</b>	UP	-	x	-
<b>GLUT 1</b>	x	x	x	x
<b>GLUT 4</b>	x	x	x	x
<b>GSK-3</b>	x	x	x	x
<b>PKB/Akt</b>	x	x	NM	NM
<b>PTEN</b>	x	x	x	DOWN
<b>PI 3 kinase</b>	x	x	x	DOWN
<b>PDK 4</b>	UP	NM	x	NM
<b>AMPK</b>	x	NM	x	NM
<b>FAT/CD36</b>	x	NM	x	NM

UP (Up regulated in the diet group)

DOWN (Down regulated in the diet group)

x (No difference in expression between the two groups)

- (Not able to measure)

NM (Not measured)

## **4.2 The role of mitochondria in the myocardial adaptive response**

Mitochondria play a putative role in the energetics of the heart. Oxidative phosphorylation is one of the main role players in the aerobic production of energy and relies on the availability of NADH, FADH<sub>2</sub> and succinate, produced by the citric acid cycle, which uses acetyl-CoA from glucose and FA oxidation [Shiojima and Walsh 2006]. Therefore we suspected that if glucose or FA oxidation is altered in any way it should affect the oxidative phosphorylation potential of the mitochondria. Furthermore, as previously stated, mitochondrial biogenesis has been implicated as a key role player in cardioprotection in the insulin resistant heart. Therefore it was crucial that we investigated mitochondrial function and biogenesis in these obese and insulin resistant animals.

In our study, on isolated mitochondria, we found no irregularities with regards to mitochondrial function after 8 weeks of DIO. We could find no differences in the oxidative phosphorylation rate and associated measures such as state 3 and state 4 respiration, the ADP/O ratio and the respiratory control index (RCI) as well as the respiration curves generated by an oxygraph between the control and diet groups using either glutamate or palmitoyl-L-carnitine as a substrate. The same was found after 16 weeks of DIO. An interesting observation was that the ADP/O ratios were higher in both the control and DIO groups when palmitoyl-L-carnitine was used as a substrate. Since the ADP/O ratio indicates the phosphorylation of ADP for every atom of oxygen used, it appears as though more ADP molecules are phosphorylated per atom of oxygen i.e. more ATP is being produced per atom of oxygen when given the FA as a substrate. Based on these results it appears as though these mitochondria are functioning well under the circumstances as there are no apparent signs of reduced mitochondrial oxidative capacity.

We were unable to find any variation in the oxidative capacity of isolated mitochondria from these obese animals. It would be ideal to measure the

respiratory rates in the two specialized mitochondrial populations i.e. subsarcolemmal and intermyofibrillar mitochondria present in cardiac muscle [Palmer et al. 1977] The study by lossa et al. 2002 showed that there is in fact a difference in the respiratory rates, regardless of the substrate used, between the two populations with the intermyofibrillar mitochondria showing higher state 3 and 4 rates. The method that we used to isolate mitochondria selects for only the subsarcolemmal mitochondria.

We then investigated the so-called mitochondrial biogenetic response i.e. PPAR alpha-PGC-1 alpha stimulated mitochondrial biogenesis. The expression of PGC-1 alpha and PPAR alpha was significantly elevated in the diet group after 8 weeks of DIO. PPAR alpha and PGC-1 alpha are known to integrate physiological signals and to enhance mitochondrial biogenesis and oxidative function [Puigserver et al. 1998, Wu et al. 2006]. We therefore expected to observe a mitochondrial biogenetic response i.e. an increase in citrate synthase activity, which is a measure of the number of mitochondria per mg of protein. Citrate synthase activity has been shown to be a sign of the expression of nuclear mitochondrial proteins, and is therefore used as a marker of mitochondrial content [Wang et al. 1999]. However, we could find no difference in the level of citrate synthase activity between the two groups. This could once again be because it is simply too early in the diet for us to see a significant change in the level of citrate synthase activity, since mitochondrial biogenesis is a complicated process that entails the synthesis, import, and incorporation of proteins and lipids to the existing mitochondrial reticulum and the replication of the mitochondrial genome i.e. the coordinated transcription of all of the mitochondrial genes in the nucleus and in the mitochondria [Hock and Kralli 2009]. After 16 weeks of DIO however we observed a significant reduction in the citrate synthase activity in the diet group. Despite the decreased level of citrate synthase the mitochondria from these obese hearts had a significantly higher % recovery after anoxia reperfusion experiments, when given palmitoyl-L-carnitine as a substrate, and showed no signs of malfunctioning of the electron transport

chain. Additionally there was no difference in the amount of ATP produced by the mitochondria during state 3 respiration when compared to mitochondria from age matched control-fed animals.

Contrary to our findings a study using skeletal muscle mitochondria showed that when young Wistar rats were fed a high-fat diet, an adaptive increase in whole body lipid utilization takes place as well as a significant increase in state 3 and state 4 lipid-supported respiration, and a selective increase in the activity of enzymes of the FA oxidation pathway which we did not measure in our study [Iossa et al. 2002]. However similar to our findings they also found no variation in mitochondrial protein mass or citrate synthase activity [Iossa et al. 2002].

Based on these results it appears as though the mitochondria from the obese hearts were able to utilize the FA as a substrate more effectively during anoxia. Under normal conditions the heart preferentially utilizes FAs as a substrate for energy metabolism as it produces more ATP per molecule than glucose [Wallhaus et al. 2001]. However theoretical calculations of ATP yield per oxygen molecule consumed show that FAs are less efficient fuel than glucose. It is also calculated that shifting from 100% palmitate to 100% glucose as a substrate would increase the production of ATP by between 12-14% [Morrow and Givertz 2005].

Thus in an insulin resistant or diabetic heart where FAs are the preferred source of fuel more oxygen is required to generate the same amount of ATP compared with a healthy heart. And as cardiac work load does not change, the higher oxygen cost for ATP generation would eventually lead to an impairment of cardiac efficiency [Bugger and Abel 2008].

Our results indicate that the mitochondria were able to utilize the FAs more efficiently than the glutamate, however this was under ideal in vitro conditions with ample oxygen supply. This could possibly mean that the metabolic



adaptation, which favours FA oxidation, could be beneficial for the heart at this stage of obesity instead of being detrimental.

Mitochondrial biogenesis does not appear to play a significant role in the adaptive response of the heart as we could find no increase in mitochondrial number, however according to Duncan et al. (2007) early mitochondrial biogenesis occurs in the interfibrillar mitochondria, which we did not isolate. Our study may therefore have missed this.

## CHAPTER 5: CONCLUSION

We were able to establish that our model of diet-induced obesity displayed visceral obesity as well as insulin resistance with concomitant increased blood glucose and serum insulin levels and HOMA index.

Early changes in the diet were depicted by a significant increase in the expression of PPAR alpha, PGC-1 alpha and PDK 4 after 8 weeks of DIO. There was no difference in the expression of any of the other metabolic proteins, involved in glucose and FA oxidation, that we investigated, which could possibly be attributed to the fact that it is too early in the diet to observe significant alterations in the metabolic profile. Similarly we observed no differences in the oxidative capacity of the mitochondria between the two groups, with no change in the level of citrate synthase activity.

After 16 weeks of DIO we found a significant decrease in the phosphorylation of PI 3 kinase and PTEN which suggests compromised glucose oxidation. However mitochondria from the diet group displayed a significantly higher % recovery after anoxia/reperfusion experiments when using palmitoyl-L-carnitine, showed no malfunctioning of the electron transport chain and had a significantly higher level of PDH complex activity despite the fact that these obese animals had significantly less mitochondria.

We therefore conclude that the hearts from these obese and insulin resistant rats are coping well and have adapted metabolically to compensate for any reduction in glucose oxidation. It is plausible that this beneficial initial adaptive response will eventually result in the occurrence of specific maladaptations as obesity, insulin resistance and diabetes progresses or if additional stresses such as hypertension is placed on the heart [Norton et al. 2009, Majane et al. 2009].

## REFERENCES

1. Abu-Elheiga L, Almarza-Ortega DB, Baldini A, Wakil SJ. Human acetyl-CoA carboxylase 2. Molecular cloning, characterization, chromosomal mapping, and evidence for two isoforms. *Journal of Biological Chemistry* 1997; 272: 10669-10677.
2. Abu-Elheiga L, Brinkley WR, Zhong L, Chirala SS, Woldegiorgis G, Wakil SJ. The subcellular localization of acetyl-CoA carboxylase 2. *Proceedings of the National Academy of Science U.S.A* 2000; 97: 1444-1449.
3. Adams SH, Esser V, Brown NF, Ing NH, Johnson L, Foster DW, McGarry JD. Expression and possible role of muscle-type carnitine palmitoyltransferase I during sperm development in rat. *Biology of Reproduction* 1998; 59: 1399-1405.
4. Alessi DR, Andjelkovic M, Caudwell B, Cron P, Morrice N, Cohen P, Hemmings BA. Mechanism of activation of protein kinase B by insulin and IGF-1. *EMBO Journal* 1996; 15: 6541-6551.
5. Alessi DR, James SR, Downes CP, Holmes AB, Gaffney PR, Reese CB, Cohen P. Characterization of a 3-phosphoinositide-dependent protein kinase which phosphorylates and activates protein kinase B $\alpha$ . *Current Biology* 1997; 7: 261-269.
6. Alloatti G, Montrucchio G, Lembo G, Hirsch E. Phosphoinositide 3-kinase gamma: kinase-dependent and -independent activities in cardiovascular function and disease. *Biochemical Society Transactions* 2004; 32: 383-386.
7. An D, Rodrigues B. Role of changes in cardiac metabolism in development of diabetic Cardiomyopathy. *American Journal of Physiology Heart Circulatory Physiology* 2006; 291: H1489-H1506.
8. Anderson S, Bankier AT, Barrell BG, de Bruijn MH, Coulson AR, Drouin J, Eperon IC, Nierlich DP, Roe BA, Sanger F, Schreier PH, Smith AJ, Staden

- R, Young IG. Sequence and organization of the human mitochondrial genome. *Nature* 1981; 290: 457-465.
9. Andersson U, Scarpulla RC. PGC-1-related coactivator, a novel, serum-inducible coactivator of nuclear respiratory factor-1-dependent transcription in mammalian cells. *Molecular and Cellular Biology* 2001; 21: 3738-3749.
  10. Antos CL, McKinsey TA, Frey N, Kutschke W, McAnally J, Shelton JM, et al. Activated glycogen synthase-3 beta suppresses cardiac hypertrophy in vivo. *Proceedings of the National Academy of Sciences* 2002; 99: 907-912.
  11. Askrafian H. Cardiac energetics in congestive heart failure. *Circulation* 2002 ; 105: 44-45.
  12. Asmann YW, Stump CS, Short KR, Coenen-Schimke JM, Guo Z, Bigelow ML, Nair KS. Skeletal muscle mitochondrial functions, mitochondrial DNA copy numbers, and gene transcript profiles in type 2 diabetic and nondiabetic subjects at equal levels of low or high insulin and euglycemia. *Diabetes* 2006; 55: 3309-3319,
  13. Baar K et al. Adaptations of skeletal muscle to exercise: rapid increase in the transcriptional coactivator PGC-1 $\alpha$ . *Federation of American Societies for Experimental Biology* 2002; 16: 1879-1886.
  14. Baldwin SA, Lienhard GE. Purification and reconstitution of glucose transporter from human erythrocytes. *Methods Enzymol* 1989; 174: 39-50.
  15. Barger PM, Brandt JM, Leone TC, Weinheimer CJ, Kelly DP. Deactivation of peroxisome proliferator-activated receptor- $\alpha$  during cardiac hypertrophic growth. *Journal of Clinical Investigation* 2000; 105: 1723-1730.
  16. Barger PM, Kelly DP. PPAR signaling in the control of cardiac energy metabolism. *Trends in Cardiovascular Medicine* 2000; 10: 238-245.
  17. Basu S, Totty NF, Irwin MS, Sudol M, Downward J. Akt phosphorylates the Yes-associated protein, YAP, to induce interaction with 14-3-3 and attenuation of p73-mediated apoptosis. *Molecular Cell* 2003; 11: 11-23
  18. Beauloye C, Marsin AS, Bertrand L, Krause U, Hardie DG, Vancouvershelde JL, Hue L. Insulin antagonizes AMP-activated protein

- kinase activation by ischemia or anoxia in rat hearts, without affecting total adenine nucleotides. *FEBS Letters* 2001; 505: 348-352.
19. Belke DD, Larsen TS, Gibbs EM, Severson DL. Altered metabolism causes cardiac dysfunction in perfused hearts from diabetic (db/db) mice. *American Journal of Physiology* 2000; 279: E1104-E1113.
  20. Berger J, Moller DE. The mechanisms of action of PPARs. *Annual Review of Medicine* 2002; 53: 409-435.
  21. Berger JP. Role of PPAR $\gamma$ , transcriptional cofactors, and adiponectin in the regulation of nutrient metabolism, adipogenesis and insulin action: view from the chair. *International Journal of Obesity* 2005; 29: S3-S4.
  22. Bianchi A, Evans JL, Iverson AJ, Nordlund AC, Watts TD, Witters LA. Identification of an isozymic form of acetyl-CoA carboxylase. *Journal of Biological Chemistry* 1990; 265: 1502-1509.
  23. Bieber LL. Carnitine. *Annual Review of Biochemistry* 1988; 57: 261-283.
  24. Bielawska AE, Shapiro JP, Jiang L, Melkonyan HS, Piot C, Wolfe CL, Tomei LD, Hannun YA, Umansky SR. Ceramide is involved in triggering of cardiomyocytes apoptosis induced by ischemia and reperfusion. *American Journal of Pathology*. 1997; 151: 1257-1263.
  25. Biggs III WH, Meisenhelder J, Hunter T, Cavenee WK, Arden KC. Protein kinase B/Akt-mediated phosphorylation promotes nuclear exclusion of the winged helix transcription factor FKHR. *Proceedings of the National Academy of Sciences. U.S.A* 1999; 96: 7421-7426.
  26. Bindoff L. Mitochondria and the heart. *European Heart Journal* 2003; 24: 221-224
  27. Boden G & Shulman GI. Free fatty acids in obesity and type 2 diabetes: defining their role in the development of insulin resistance and beta-cell dysfunction. *The European Journal of Clinical Investigation* 2002; 32: 14-23.
  28. Bonen A, Luiken JJ, Glatz JF. Regulation of fatty acid transport and membrane transporters in health and disease. *Molecular and Cellular Biochemistry* 2002; 239: 181-192.

29. Bowker-Kinley MM, Davis WI, Vu P, Harris RA, Popov KM. Evidence for existence of tissue-specific regulation of the mammalian pyruvate dehydrogenase complex. *Biochemistry Journal* 1998; 329: 191-196.
30. Brandt JM, Djouadi F, Kelly DP. Fatty acids activate transcription of the muscle carnitine palmitoyltransferase I gene in cardiac myocytes via the peroxisome proliferator activated receptor  $\alpha$ . *Journal of Biological Chemistry* 1998; 273: 23786-23792.
31. Brandt JM, Djouadi F, Kelly DP. Fatty acids activate transcription of the muscle carnitine palmitoyltransferase I gene in cardiac myocytes via the peroxisome proliferator-activated receptor alpha. *Journal of Biological Chemistry* 1998; 273: 23786-23792.
32. Brinkmann JF, Abumrad NA, Ibrahimi A, van der Vusse GJ, Glatz JF. New insights into long-chain fatty acid uptake by heart muscle: a crucial role for fatty acid translocase/CD36. *Biochemical Journal* 2002; 367: 561-570.
33. Brown N, Weis BC, Husti JE, Foster DW, McGarry JD. Mitochondrial carnitine palmitoyl-transferase isoform switching in the developing rat heart. *Journal of Biological Chemistry* 1995; 270: 8952-8957.
34. Brunet A, Bonni A, Zigmond MJ, Lin mZ, Juo P, Hu LS, Anderson MJ, Arden KC, Blenis J, Greenberg ME . Akt promotes cell survival by phosphorylating and inhibiting a Forkhead transcription factor. *Cell* 1999; 96: 857-868.
35. Bugger H, Abel ED. Cardiac efficiency in health and disease. *Heart and Metabolism* 2008; 39.
36. Buja LM, Entman ML. Modes of myocardial cell injury and cell death in ischemic heart disease. *Circulation* 1998; 98: 1355-1357.
37. Burgering B, Coffey PJ. Protein kinase B (c-Akt) in phosphatidylinositol -3-OH kinase signal transduction. *Nature* 1995; 376: 599-602.
38. Burgering BM, Medema RH. Decisions on life and death: FOXO Forkhead transcription factors are in command when PKB/Akt is off duty. *Journal of Leukocyte Biology* 2003; 73: 689-701.

39. Butler M, McKay RA, Popoff IJ, et al. Specific inhibition of PTEN expression reverses hyperglycemia in diabetic mice. *Diabetes* 2002; 51(4): 1028-1034.
40. Cai Z, Semenza GL. PTEN activity is modulated during ischaemia and reperfusion: involvement in the induction and decay of preconditioning. *Circulation Research* 2005; 97(12): 1351-1359.
41. Campbell FM, Kozak R, Wagner A, Altarejos JY, Dyck JR, Belke DD, Severson DL, Kelly DP, Lopaschuk GD. A role for PPAR $\alpha$  in the control of cardiac malonyl-CoA levels: reduced fatty acid oxidation rates and increased glucose oxidation rates in the hearts of mice lacking PPAR $\alpha$  are associated with higher concentrations of malonyl-CoA and reduced expression of malonyl-CoA decarboxylase. *Journal of Biological Chemistry* 2002; 277: 4098-4103.
42. Cantó C, Auwerx J. PGC-1 $\alpha$ , SIRT 1 and AMPK, an energy sensing network that controls energy expenditure. *Current Opinion in Lipidology* 2009; 20: 98-10.
43. Carley AN, Severson DL. Fatty acid metabolism is enhanced in type 2 diabetic hearts. *Biochimica et Biophysica Acta* 2005; 1734: 112-126.
44. Chan JM, Rimm EB, Colditz GA, Stampfer MJ, Willet WC. Obesity, fat distribution, and weight gain as risk factors for clinical diabetes in men. *Diabetes Care* 1994; 17: 961-969.
45. Chan TO, Rittenhouse SE, Tsichlis PN. Akt/PKB and other D3 phosphoinositide-regulated kinases: kinase activation by phosphoinositide-dependent phosphorylation. *Annual Review of Biochemistry* 1999; 68: 965-1014.
46. Chan TO, Rittenhouse SE, Tsichlis PN. Phosphoinositide 3-kinase signaling – which way to target? *Trends Pharmacological Sciences* 2003; 24: 366-376.
47. Chance B, Williams G. Respiratory enzymes in oxidative phosphorylation. VI. The effects of adenosine diphosphate on azide-treated mitochondria. *Journal of Biological Chemistry* 1956; 221: 477-489.

48. Chen Q, Camara AK, Stowe DF, Hoppel CL, Lesnefsky EJ. Modulation of electron transport protects cardiac mitochondria and decreases myocardial injury during ischemia and reperfusion. *American Journal of Physiology Cell Physiology* 2007; 292: 137-147.
49. Chopra M, Galbraith S, Darnton-Hill I. A global response to a global problem: the epidemic of overnutrition. *Bulletin of the World Health Organization* 2002;80:952-958
50. Cohen P. The hormonal control of glycogen metabolism in mammalian muscle by multisite phosphorylation. *Biochemical Society Transactions* 1979; 7: 459-480.
51. Coort SL, Bonen A, van der Vusse GJ, Glatz JF, Luiken JJ. Cardiac substrate uptake and metabolism in obesity and type-2 diabetes: role of sarcolemmal substrate transporters. *Molecular and Cellular Biochemistry* 2007; 299: 5-18.
52. Coort SL, Willems J, Coumans WA, van der Vusse GJ, Bonen A, Glatz JF, Luiken JJ. Sulfo-N-succinimidyl esters of Long-chain fatty acids specifically inhibit fatty acid translocase (FAT/CD36)-mediated cellular fatty acid uptake. *Molecular and Cellular Biochemistry* 2002; 239: 213-219.
53. Coqueret O. new roles for p21 and p27 cell-cycle inhibitors: a function for each cell compartment? *Trends Cellular Biology* 2003; 13: 65-70.
54. Crackower MA, Oudit GY, Kozieradzki I, Sarao R, Sun H, Sasaki T, Hirsch E, Suzuki A, Shioi T, Irie-Sasaki J, Sah R, Cheng HY, Rybin VO, Lembo G, Fratta L, Oliveira-dos-Santos AJ, Benovic JL, Kahn CR, Izumo S, Steinberg SF, Wymann MP, Backx PH, Penninger JM. Regulation of myocardial contractility and cell size by distinct PI3K-PTEN signaling pathways. *Cell* 2002; 110: 737-749.
55. Crompton M. The mitochondrial permeability transition pore and its role in cell death. *Biochemistry Journal* 1999; 341: 233-249.
56. Cross DA, Alessi DR, Cohen P, Andjelkovich M, Hemmings BA. Inhibition of glycogen synthase kinase-3 insulin mediated by protein kinase B. *Nature* 1995; 378: 785-78.



57. Czech MP, Corvera S. Signaling mechanisms that regulate glucose transport. *Journal of Biology and Chemistry* 1999; 274: 1865-1868.
58. Datta SR, Dudek H, Tao X, Masters S, Fu H, Gotoh Y, Greenberg ME. Akt phosphorylation of BAD couples survival signals to the cell-intrinsic death machinery. *Cell* 1997; 91: 231-241.
59. Del Peso L, Gonzalez-Garcia M, Page C, Herrera R, Nunez G. Interleukin-3-induced phosphorylation of BAD through the protein kinase Akt. *Science* 1997; 278: 687-689
60. Delcommenne M, Tan C, Gray V, Ruel L, Woodgett J, Dedhar S. Phosphoinositide-3-OH kinase-dependent regulation of glycogen synthase kinase 3 and protein kinase B/Akt by the integrin-linked kinase. *Proceedings of the National Academy of Sciences. U.S.A* 1998; 95: 11211-11216.
61. Dennis SC, Gever W, Opie LH. Evidence for rapid consumption of millimolar concentrations of cytoplasmic ATP during rigor-contraction of metabolically compromised single cardiomyocytes. *Molecular and Cellular Cardiology* 1991; 23: 1077-1086.
62. Depre C, Young ME, Ying J, Ahuja HS, Han Q, Garza N, Davies PJ, Taegtmeyer H. Streptozotocin-induced changes in cardiac gene expression in the absence of severe contractile dysfunction. *Journal of Molecular and Cellular Cardiology* 2000; 32: 985-996
63. Desvergne B, Wahli W. Peroxisome proliferator-activated receptors: nuclear control of metabolism. *Endocrinology Review* 1999; 20: 649-688.
64. Di Lisa F, Menabo R, Canton M, Barile M, Bernadi P. Opening of the mitochondrial permeability transition pore causes depletion of mitochondrial and cytosolic NAD<sup>+</sup> and is a causative event in the death of myocytes in postischemic reperfusion of the heart. *J. Biol. Chem.* (2001) 276: 2571-2575.
65. Djouadi F, Brandt JM, Weinheimer CJ, Leone TC, Gonzalez FJ, Kelly DP. The role of the peroxisome proliferator-activated receptor  $\alpha$  (PPAR  $\alpha$ ) in the

- control of cardiac lipid metabolism. Prostaglandins Leukotriens and Essential Fatty Acids 1999; 60: 339-343
66. Doble BW, Woodgett JR. GSK-3: tricks of the trade for a multi-tasking kinase. Journal of Cell Science 2003; 116: 1175-1186.
  67. Doenst T, Goodwin GW, Cedars AM, Wang M, Stepkowski S, Taegtmeyer H. Load-induced changes in vivo alter substrate fluxes and insulin responsiveness of rat heart in vitro. Metabolism 2001; 50: 1083-1090.
  68. Doenst T, Taegtmeyer H. Alpha-adrenergic stimulation mediates glucose uptake through phosphatidylinositol 3-kinase in rat heart. Circulation Research 1999; 84: 467-474.
  69. Donepudi M, Grutter MG. Structure and zymogen activation of caspases. Biophysical Chemistry 2002; 101-102: 145-153.
  70. Downward J. How BAD phosphorylation is good for survival. Nature Cell Biology 1999; 1: E33-E35.
  71. Dressel U et al. The peroxisome proliferator-activated receptor  $\beta/\delta$  agonist, GW501516, regulates the expression of genes involved in lipid catabolism and energy uncoupling in skeletal muscle cells. Molecular Endocrinology 2003; 17: 2477-2493.
  72. Dummler B, Hemmings B. Physiological roles of PKB/Akt isoforms in development and disease. Biochemical Society Transactions 2007; 35: 231-235.
  73. Duncan JG, Fong JL, Medeiros DM, Finck BN, Kelly DP. Insulin-resistant heart exhibits a mitochondrial biogenic response driven by the peroxisome proliferator-activated receptor- $\alpha$ /PGC-1  $\alpha$  gene regulatory pathway. Circulation 2007; 115: 909-917.
  74. Dyck JR, Barr AJ, Barr RL, Kolattukudy PE, Lopaschuk GD. Characterization of cardiac malonyl-CoA decarboxylase and its putative role in regulating fatty acid oxidation. American Journal of Physiology 1998; 275: H2122-H2129.
  75. Dyck JRB, Berthiaume L, Thomas PD, Kantor PF, Barr AJ, Barr R, Singh D, Hopkins TA, Voilley N, Prentki M, Lopaschuk GD. Characterization of rat

- liver malonyl-CoA decarboxylase and the study of its role in regulating fatty acid metabolism. *Biochemistry Journal* 2000; 350: 599-608.
76. Dzeja PP, Redfield MM, Burnett JC, Terzic A. Failing energetics in failing hearts. *Current Cardiology Reports* 2000; 2: 212-217.
  77. Ebeling P, Koistinen HA, Koivisto VA. Insulin-independent glucose transport regulates insulin sensitivity. *Federation of European Biochemical Societies* 1998; 436: 301-303.
  78. Eckel RH. Obesity and heart disease. *Circulation* 1997;96:3248-3250.
  79. Fayard E, Tintiganac LA, Baudry A, Hemmings BA. Protein kinase B/Akt at a glance. *Journal of Cell Science* 2005; 118: 5675-5678.
  80. Finck B, Han X, Courtois M, Aimond F, Nerbonne JM, Kovacs A, Gross RW, Kelly DP. A critical role for PPAR $\alpha$ -mediated lipotoxicity in the pathogenesis of diabetic Cardiomyopathy: modulation of phenotype of dietary fat content. *Proceedings of the National Academy of Sciences. U.S.A* 2003; 100: 1226-1231.
  81. Finck B, Lehman JJ, Leone TC, Welch MJ, Bennett MJ, Kovacs A, Han X, Gross RW, Kozak R, Lopaschuk GD, Kelly DP. The cardiac phenotype induced by PPAR $\alpha$  overexpression mimics that caused by diabetes mellitus. *Journal of Clinical Investigation* 2002; 109: 121-130.
  82. Finck BN. The role of the peroxisome proliferator-activated receptor alpha pathway in pathological remodeling of the diabetic heart. *Current Opinion in Clinical Nutrition and Metabolic Care* 2004; 7: 391-396.
  83. Fisher RP, Lisowsky T, Parisi MA, Clayton DA. DNA wrapping and bending by a mitochondrial high mobility group-like transcriptional activator protein. *Journal of Biological Chemistry* 1992; 267: 3358-3367.
  84. Folake S, Tola A. Obesity and cardiovascular diseases: the risk factor in African diets. *Forum on Public Policy* 2008: 1-15.
  85. Folsom AR, Kushi LH, Anderson KE, Mink PJ, Olson JE, Hong CP, Sellers TA, Lazovich D, Prineas RJ. Associations of general and abdominal obesity with multiple health outcomes in older women. *Archives of Internal Medicine* 2000; 160: 2117-2128.

86. Francis GA, Annicotte JS, Auwerx J. PPAR- $\alpha$  effects on the heart and other vascular tissues. *American Journal of Physiology: Heart and Circulatory Physiology* 2003; 285: H1-H9. (a)
87. Francis GA, Fayard E, Picard F, Auwerx J. Nuclear receptors and the control of metabolism. *Annual Review of Physiology* 2003; 65: 261-311. (b)
88. Franke TF, Yang SI, Chan TO, Datta K, Kazlauskas A, Morrison DK, Kaplan DR, Tsichlis PN. The protein kinase encoded by the Akt proto-oncogene is a target of the PDGF-activated phosphatidylinositol 3-kinase. *Cell* 1995; 81: 727-736.
89. Frayn KN. Visceral fat and insulin resistance: causative or correlative? *British Journal of Nutrition* 2000; 83: S71-S77.
90. Freude B, Master TN, Robiesek F et al. Apoptosis is initiated by myocardial ischemia and executed during reperfusion. *Journal of the American College of Cardiology* 2000; 32: 197-208.
91. Gardner A, Boles RG. Is a mitochondrial psychiatry in the future? A review. *Current Psychiatry Review* 1 2005; 3: 255-271.
92. Garesse R, Vallejo CG. Animal mitochondrial biogenesis and function: a regulatory cross-talk between two genomes. *Gene* 2001; 263: 1-16.
93. Garnier A, Fortin D, Delomenie C, Momken I, Veksler V, Ventura-Clapier R. Depressed mitochondrial transcription factors and oxidative capacity in rat failing cardiac and skeletal muscles. *Journal of Physiology* 2003; 551: 491-501.
94. Gilde AJ, Van Der Lee KA, Willemsen PH, Chinetti G, Van Der Leij FR, van der Vusse GJ, Staels B, van Bilsen M. Peroxisome proliferator-activated receptor (PPAR)  $\alpha$  and PPAR $\beta/\delta$  but not PPAR  $\gamma$ , modulate the expression of genes involved in cardiac lipid metabolism. *Circulatory Research* 2003; 92: 518-524.
95. Gill C, Mestral R, Samali A. Losing heart: the role of apoptosis in heart disease – a novel therapeutic target? *The Federation of American Societies for Experimental Biology Journal* 2002; 16: 135-146.

96. Ginsberg HN. Insulin resistance and cardiovascular disease. *The Journal of Clinical Investigation* 2000; 106(4): 453-458
97. Glatz JF, Luiken JJ, Bonen A. Involvement of membrane-associated proteins in the acute regulation of cellular fatty acid uptake. *Journal of Molecular Neuroscience* 2001; 16: 123-132.
98. Glatz JFC, Luiken JJFP, Bonen A. Membrane fatty acid transporters as regulators of lipid metabolism: implications for metabolic disease. *Physiology Review* 2010; 90: 376-417.
99. Gold MR. Akt is TCL-ish: implications for B-cell lymphoma. *Trends Immunology* 2003; 24: 104-108.
100. Goodyear LJ, Kahn BB. Exercise, glucose transport, and insulin sensitivity. *Annual Review of Medicine* 1998; 49: 235-261.
101. Goto M et al. cDNA cloning and mRNA analysis of PGC-1 in epittrchlearis muscle in swimming-exercised rats. *Biochemical and Biophysical Research Communications* 2002; 269: 349-352.
102. Gottlieb RA, Burleson KO, Kloner RA et al. Reperfusion injury induces apoptosis in rabbit cardiomyocytes. *Journal of Clinical Investigation* 1994; 94: 1621-1628.
103. Greenlund LJS, Dechwerth TL, Johnson EM Jr. Superoxide dismutase delays neuronal apoptosis: A role for reactive oxygen species in programmed neuronal death. *Neuron* 1995; 14: 303-315.
104. Gross ER, Hsu AK, Gross GJ. Opioid-induced cardioprotection occurs via glycogen synthase kinase {beta} inhibition during reperfusion in intact rat hearts. *Circulatory Research* 2004; 94: 960-966.
105. Gu D, Wildman RP, Wu X, Reynolds K, Huang J, Chen CS, He J. Incidence and predictors of hypertension over 8 years among Chinese men and women. *Journal of Hypertension* 2007; 25(3): 517-523.
106. Gulick T, Cresci S, Caira T, Moore DD, Kelly DP. The peroxisome proliferator-activated receptor regulates mitochondrial fatty acid oxidative enzyme gene expression. *Proceedings of the National Academy of Sciences Online USA* 1994; 91: 11012-11016.

107. Gupta B. Mechanism of insulin action. *Current Science* 1997; 73: 993.
108. Halliwell B, Gutteridge JMC. *Free radicals in Biology and Medicine* (3<sup>rd</sup> Edition), Oxford: Oxford University 1999.
109. Hanada M, Feng J, Hemmings BA. Structure, regulation and function of PKB/Akt – a major therapeutic target. *Biochimica et Biophysica Acta* 2004; 1679: 3-16.
110. Haq S, Choukroun G, Kang ZB, Ranu H, Matsui T, Rosezweig A, et al. Glycogen synthase kinase-3beta is a negative regulator of cardiomyocyte hypertrophy. *Journal of Cell Biology* 2000; 151: 117-130.
111. Hardie DG, Carling D. The AMP-activated protein kinase-fuel gauge of the mammalian cell? *European Journal of Biochemistry* 1997; 246: 259-273.
112. Hardie DG, Hawley SA. AMP-activated protein kinase: the energy charge hypothesis revisited. *BioEssays* 2001; 23: 1112-1119.
113. Hardie DG. AMPK: a key regulator of energy balance in the single cell and the whole organism. *International Journal of Obesity* 2008; 32: S7-S12.
114. Harris RA, Huang B, Wu P. Control of pyruvate dehydrogenase kinase gene expression. *Advances in Enzyme Regulation* 2001; 41: 269-288.
115. Haslam DW, James WP. Obesity. *Lancet* 2005; 366:1197-209.
116. Hausenloy DJ, Yellon DM. New directions for protecting the heart against ischaemia-reperfusion injury: targeting the Reperfusion Injury Salvage Kinase (RISK)-pathway. *Cardiovascular Research* 2004; 61(3): 448-460.
117. He J, Gu D, Wu X, Reynolds K, Duan X, Yao C, Wang J, Chen C, Chen J, Wildman RP, Klag MJ, Whelton PK. Major causes of death among men and women in China. *New England Journal of Medicine* 2005; 353: 1124-1134.
118. He YW. Orphan nuclear receptors in T lymphocyte development. *Journal of Leukocyte Biology* 2002; 98: 3690-3694.
119. Heiskanen KM, Bhat MB, Wang HW, Ma J, Nieminen AL. Mitochondrial depolarization accompanies cytochrome c release during apoptosis in PC6 cells. *Journal of Biological Chemistry* 1999; 274: 5654-5657.

120. Hennekens CH. Increasing global burden of cardiovascular disease in general populations and patients with schizophrenia. *Journal of Clinical Psychiatry* 2007; 68: 4-7.
121. Henze K, Martin W. Evolutionary biology: essence of mitochondria. *Nature* 2003; 426: 127-128.
122. Hlobilkova A, Knillova J, Bartek J, Lukas J, Kolar Z. The mechanism of action of the tumour suppressor gene PTEN. *Biomed Pap Med Fac Univ Palacky Olomouc Czech Repub* 2003; 147(1): 19-25.
123. Hochachka PW, Mommsen TP. Protons and anaerobiosis. *Science* 1983; 219: 1391-1397.
124. Hock BM, Kralli A. Transcriptional control of mitochondrial biogenesis and function. *Annual Review of Physiology* 2009; 71: 21.1-24.27.
125. Hopkins TA et al. Control of cardiac pyruvate dehydrogenase activity in peroxisome proliferator-activated receptor- $\alpha$  transgenic mice. *American Journal of Physiology and Heart Circulatory Physiology* 2003; 285: H270-H276 (a)
126. Hopkins TA, Dyck JRB, Lopaschuk GD. AMP-activated protein kinase regulation of fatty acid oxidation in the ischaemic heart. *Biochemical Society Transactions* 2003; 31: 207-212 (b)
127. Horowitz JF, Coppack SC, Paramore D, Cryer PE, Klein S. Effect of short-term fasting on lipid kinetics in lean and obese women. *American Journal of Physiology* 1999; 276: E278-E284.
128. Hossain P, Kavar B, Nahas ME. Obesity and diabetes in the developing world-a growing challenge. *New England Journal of Medicine* 2007; 356 (3): 213-215.
129. Huisamen B, Dietrich D, Blackhurst S, Genade S, Lochner A. Early effects of obesity on cardiovascular function. Unpublished data; 2007.
130. Huss JM, Kelly DP. Mitochondrial energy metabolism in heart failure: a question of balance. *Journal of Clinical Investigation* 2005; 115: 547-555.
131. Huss JM, Kelly DP. Nuclear receptor signaling and cardiac energetics. *Circulatory Research* 2004; 95: 568-578.

132. Huss JM, Kopp RP, Kelly DP. PGC-1 $\alpha$  coactivates the cardiac-enriched nuclear receptors estrogen-related receptor- $\alpha$  and - $\gamma$ . *Journal of Biological Chemistry* 2002; 277: 40265-40274.
133. Iossa S, Mollica MP, Lionetti L, Crescenzo R, Botta M, Liverini G. Skeletal muscle oxidative capacity in rats fed high-fat diet. *International Journal of Obesity* 2002; 26: 65-75.
134. Jager S, Handschin C, St-Pierre J, Spiegelman BM. AMP-activated protein kinase (AMPK) action in skeletal muscle via direct phosphorylation of PGC-1  $\alpha$ . *Proceedings of the National Academy of sciences of the United States of America* 2007; 104: 12017-12022.
135. Jennings RB, Sommers HM, Kaltenbach JP, West JJ. Electrolyte alterations in acute myocardial ischemic injury. *Circulation Research* 1964; 14: 260-269.
136. Kahn B, Flier J. Obesity and insulin resistance. *The Journal of Clinical Investigation* 2000; 106: 473-481.
137. Kamei Y et al. PPAR $\gamma$  coactivator 1 $\beta$ /ERR ligand 1 is an ERR protein ligand, whose expression induces a high-energy expenditure and antagonizes obesity. *Proceedings of the National Academy of Sciences. U.S.A* 2003; 100: 12378-12383.
138. Karmazyn M, Moffat MP. Role of Na<sup>+</sup>/H<sup>+</sup> exchange in cardiac physiology and pathophysiology: mediation of myocardial reperfusion injury by the pH paradox. *Cardiovascular Research* 1993; 27: 915-924.
139. Karwatowska-Prokopczuk E, Nordberg JA, Li HL, Engler RL, Gottlieb RA. Effect of vacuolar proton ATPase on pHi, Ca<sup>2+</sup>, and apoptosis in neonatal cardiomyocytes during metabolic inhibition/recovery. *Circulation Research* 1998; 82: 1139-1144.
140. Katakam P, Jordan J, Snipes J, Tulbert C, Miller A, Busija D. Myocardial preconditioning against ischemia-reperfusion injury is abolished in Zucker obese rats with insulin resistance. *American Journal of Physiology – Regulatory, Integrative and Comparative Physiology* 2006; 292: 920-926.
141. Katz AM. Metabolism of the failing heart. *Cardioscience* 1993; 4: 199-203.



142. Katz DA. Risk stratification in unstable angina: the role of clinical prediction models. *Journal of American College of Cardiology* 2000; 36: 1803-1808.
143. Kearney PM, Whelton M, Reynolds K, Muntner P, Whelton PK, He J. Global burden of hypertension: analysis of worldwide data. *Lancet* 2005; 365: 217-223.
144. Kelly DP, Scarpulla RC. Transcriptional regulatory circuits controlling mitochondrial biogenesis and function. *Genes and Development* 2004; 18: 357-368.
145. Kersten S, Seydoux J, Peters JM, Gonzalez FJ, Desvergne B, Wahli W. Peroxisome proliferator-activated receptor  $\alpha$  mediates the adaptive response to fasting. *Journal of Clinical Investigation* 1999; 103: 1489-1498.
146. Keskin M, Kurtoglu S, Kendirci M, Atabek E, Yazici C. Homeostasis model assessment is more reliable than the fasting glucose/insulin ratio and quantitative insulin sensitivity check index for assessing insulin resistance among obese children and adolescents. *Pediatrics* 2005; 115: 1-6.
147. Khan A, Pessin J. Insulin regulation of glucose uptake: a complex interplay of intracellular signaling pathways. *Diabetologia* 2002; 45: 1475-1483.
148. Kissebah AH, Vydellingum N, Murray R, Evans DJ, Hartz AJ, Kalkhoff RK, Adams PW. Relation of body fat distribution to metabolic complications of obesity. *Journal of Clinical Endocrinology and Metabolism* 1982; 54: 254-260.
149. Klein S, Luu K, Gasic S, Green A. Effect of weight loss on whole-body and cellular lipid metabolism in severely obese humans. *American Journal of Physiology* 1996; 270: E739-E745.
150. Kodde IF, van der Stok J, Smolenski RT, de Jong JW. Metabolic and genetic regulation of cardiac energy substrate preference 2007; 146: 26-39.
151. Kohn AD, Kovacina KS, Roth RA. Insulin stimulates the kinase activity of RAC-PK, a pleckstrin homology domain containing ser/thr kinase, *EMBO Journal* 1995; 14: 4288-4295.
152. Kondo T, Kahn CR. Altered insulin signaling in retinal tissues in diabetic states. *Journal of Biological Chemistry* 2004; 279 (36): 37997-38006.

153. Kops GJ, de Ruiter ND, De Vries-Smits AM, Powell DR, Bos JL, Burgering BM. Direct control of the Forkhead transcription factor AFX by protein kinase B. *Nature* 1999; 398: 630-634.
154. Kowaltowski AJ. Alternative mitochondrial functions in cell physiopathology: beyond ATP production. *Brazilian Journal of Medical and Biological Research* 2000; 33: 241-250.
155. Kressler D, Schreiber SN, Knutti D, Kralli A. The PGC-1-related protein PERC is a selective coactivator of estrogen receptor alpha. *Journal of Biological Chemistry* 2002; 277: 13918-13925.
156. Kudo N, Barr AJ, Barr RL, Desai S, Lopaschuk GD. High rates of fatty acid oxidation during reperfusion of ischemic hearts are associated with a decrease in malonyl-CoA levels due to an increase in 5'-AMP-activated protein kinase inhibition of acetyl-CoA carboxylase. *Journal of Biological Chemistry* 1995; 270: 17513-17520.
157. Kudo N, Gillespie JG, Kung L, Witters LA, Schulz R, Clanachan AS, et al. Characterization of 5'AMP-activated protein kinase activity in the heart and its role in inhibiting acetyl-CoA carboxylase during reperfusion following ischemia. *Biochimica et Biophysica Acta* 1996; 1301: 67-75.
158. Lakowicz JR, Keating S. Binding of an indole derivative to micelles as quantified by phase-sensitive detection of fluorescence. *Journal of Biological Chemistry* 1983; 258: 5519-5524.
159. Lanza IR, Nair S. Functional assessment of isolated mitochondria in vitro. *Methods in Enzymology* 2009; 457: 349-372.
160. Larsson NG, Wang J, Wilhelmsson H, Oldfors A, Rustin P, Lewandoski M, Barsh GS, Clayton DA. Mitochondrial transcription factor A is necessary for mtDNA maintenance and embryogenesis in mice. *Nature Genetics* 1998; 18: 231-236.
161. Le Roith D, Zick Y. Recent advances in our understanding of insulin action and insulin resistance. *Diabetes Care* 2001; 24: 588-593.
162. Lee Y, Hirose H, Ohneda M, Johnson JH, McGarry JD, Unger RH. Beta-cell lipotoxicity in the pathogenesis of non-insulin-dependent diabetes mellitus

- of obese rats: impairment in adipocyte-beta-cell relationship. Proceedings of the National Academy of Sciences Online USA 1994; 91: 10878-10882.
163. Lehman JJ, Barger PM, Kovacs A, Saffitz JE, Medeiros DM, Kelly DP. Peroxisome proliferator-activated receptor  $\gamma$  coactivator-1 promotes cardiac mitochondrial biogenesis. *Journal of Clinical Investigation* 2000; 106:847-856.
  164. Lehman JJ, Kelly DP. Gene regulatory mechanisms governing energy metabolism during cardiac hypertrophic growth. *Heart Failure Review* 2002; 7: 175-185.
  165. Leone TC, Weinheimer CJ, Kelly DP. A critical role for the peroxisome proliferator-activated receptor alpha (PPAR $\alpha$ ) in the cellular fasting response: the PPAR $\alpha$ -null mouse as a model of fatty acid oxidation disorders. *Proceedings of the National Academy of Sciences. U.S.A* 1999; 96: 7473-7478.
  166. Lerch R, Tamm C, Papageorgiou I, Benzi RH. Myocardial fatty acid oxidation during ischemia and reperfusion. *Molecular and Cellular Biochemistry* 1992; 116: 103-109
  167. Lesnefsky EJ, Gudiz TI, Migita CT, Ikeda-Saito M, Hassan MO, Turkaly PJ, Hoppel CL. Ischemic injury to mitochondrial electron transport in the aging heart: damage to the iron-sulfur protein subunit of electron transport complex III. *Archives of Biochemistry and Biophysics* 2001; 385: 117-128.  
(a)
  168. Lesnefsky EJ, Moghaddas S, Tandler B, Kerner J, Hoppel CL. Mitochondrial dysfunction in cardiac disease: ischemia-reperfusion, aging, and heart failure. *Journal of Molecular and Cell Cardiology* 2001; 33: 1065-1089. (b)
  169. Lesnefsky EJ, Tandler B, Ye J, Slabe TJ, Turkaly J, Hoppel CL. Myocardial ischemia decreases oxidative phosphorylation through cytochrome oxidase in subsarcolemmal mitochondria. *American Journal of Physiology Heart and Circulatory Physiology* 1997; 273: 1544-1554.

170. Li Q, Verma IM. NF- $\kappa$ B regulation in the immune system. *Nature Review Immunology* 2000; 2: 725-734.
171. Lin HK, Yeh S, Kang HY, Chang C. Akt suppresses androgen-induced apoptosis by phosphorylating and inhibiting androgen receptor. *Proceedings of the National Academy of Sciences. U.S.A* 2001; 97: 7200-7205.
172. Lin J, Puigserver P, Donovan J, Tarr P, Spiegelman BM. Peroxisome proliferator-activated receptor  $\gamma$  coactivator 1 $\beta$  (PGC-1 $\beta$ ), a novel PGC-1-related transcription coactivator associated with host cell factor. *Journal of Biological Chemistry* 2002; 277: 1645-1648.
173. Liu B, Clanachan AS, Schulz R, Lopaschuk GD. Cardiac efficiency is improved after ischemia by altering both the source and fat of protons. *Circulatory Research* 1996; 79: 940-948.
174. Liu Q, Docherty JC, Rendell JC, Clanachan AS, Lopaschuk GD. High levels of fatty acids delay the recovery of intracellular pH and cardiac efficiency in post-ischemic hearts by inhibiting glucose oxidation. *Journal of the American College of Cardiology* 2002; 39: 718-725.
175. Long X, Crow MT, Sollott SJ, O'Neill L, Menees DS, de Lourdes Hipolito M, Boluyt MO, Asai T, Lakatta EG. Enhanced expression of p53 and apoptosis induced by blockade of the vacuolar proton ATPase in cardiomyocytes. *Journal of Clinical Investigation* 1998; 101: 1453-1461.
176. Lopaschuk GD, Collins-Nakai R, Olley PM, Montague TJ, McNeil G, Gayle M, Penkoske P, Finegan BA. Plasma fatty acid levels in infants and adults after myocardial ischemia. *American Heart Journal* 1994; 128: 61-67.
177. Lopaschuk GD, Stanley WC. Glucose metabolism in the ischemic heart. *Circulation* 1997; 95: 313-315.
178. Lowry OH, Rosebrough NJ, Farr AL, Randall RJ. Protein measurement with the Folin phenol reagent. *Journal of Biological Chemistry* 1951; 193: 265-275.
179. Luiken JJ, Arumugam Y, Dyck DJ, Bell RC, Pelsers MM, Turcotte LP, Tandon NN, Glatz JF, Bonen A. Increased rates of fatty acid uptake and

- plasmalemmal fatty acid transporters in obese Zucker rats. *Journal of Biological Chemistry* 2001; 276: 40567-40573.
180. Luiken JJ, Schaap FG, van Nieuwenhoven FA, van der Vusse GJ, Bonen A, Glatz JF. Cellular fatty acid transport in heart and skeletal muscle as facilitated by proteins. *Lipids* 1999; 34: S169-S175.
  181. Luiken JJ, van Nieuwenhoven FA, America G, van der Vusse GJ, Glatz JF. Uptake and metabolism of palmitate by isolated cardiac myocytes from adult rats: involvement of sarcolemmal proteins. *Journal of Lipid Research* 1997; 38:745-758.
  182. Madrazo JA, Kelly DP. The PPAR trio: Regulators of myocardial energy metabolism in health and disease. *Journal of Molecular and Cellular Cardiology* 2008; 6: 968-975.
  183. Maher F, Vannucci SJ, Simpson IA. Glucose transporter proteins in brain. *Federation of American Societies for Experimental Biology Journal* 1994; 8: 1003-1011.
  184. Majane OH, Vengethasamy L, du Toit EF, Makaula S, Woodiwiss AJ, Norton GR. Dietary-induced obesity hastens the progression from concentric cardiac hypertrophy to pump dysfunction in spontaneously hypertensive rats. *Hypertension* 2009; 54: 1376-1383.
  185. Makinde A, Kantor P, Lopaschuk G. Maturation of fatty acid and carbohydrate metabolism in the newborn heart. *Molecular and Cellular Biochemistry* 1998; 188: 49-56.
  186. Makinde AO, Gamble J, Lopaschuk GD. Upregulation of 5'-AMP-activated protein kinase is responsible for the increase in myocardial fatty acid oxidation rates following birth in the newborn rabbit. *Circulation Research* 1997; 80: 482-489.
  187. Marsin AS, Bertrand L, Rider MH, Deprez J, Beauloye C, Vincent MF, et al. Phosphorylation and activation of heart PFK-2 by AMPK has a role in the stimulation of glycolysis during ischemia. *Current Biology* 2000; 10: 1247-1255.

188. Marsin AS, Bertrand L, Rider MH, Deprez J, Beauloye C, Vincent MF, Van den Berghe G, Carling D, Hue L. Phosphorylation and activation of heart PFK-2 by AMPK has a role in the stimulation of glycolysis during ischaemia. *Current Biology* 2000; 10: 1247-1255.
189. Masuyama N, Oishi K, Mori Y, Ueno T, Takahama Y, Gotoh Y. Akt inhibits the orphan nuclear receptor Nur77 and T-cell apoptosis. *Journal of Biological Chemistry* 2001; 276: 32799-32805.
190. Matthews FS. The structure, function and evolution of cytochromes. *Progress in Biophysics and Molecular Biology* 1985; 45: 1-56.
191. Maulik N, Kagan EV, Das DK. Translocation of phosphatidylserine and phosphatidylethanolamine precedes apoptosis in ischemic reperfused heart. *American Journal of Physiology* 1998; 274: H242-H248. (b)
192. Maulik N, Yoshida T, Das DK. Oxidative stress developed during reperfusion of ischemic myocardium induces apoptosis in rat heart. *Free Radical Biology and Medicine* 1998; 24: 869-875. (a)
193. McFarlane SI, Banerji M, Sowers JR. Insulin resistance and cardiovascular disease. *The Journal of Clinical Endocrinology and Metabolism* 2001; 86:713-718.
194. McGarry JD, Woeltje KF, Kuwajima M, Foster DW. Regulation of ketogenesis and the renaissance of carnitine palmitoyltransferase. *Diabetes Metabolism Reviews* 1989; 5: 271-284.
195. McLellan F. Obesity rising to alarming levels around the world. *Lancet* 2002; 359: 1412.
196. McVeigh JJ, Lopaschuk GD. Dichloroacetate stimulation of glucose oxidation improves recovery of ischemic rat hearts. *American Journal of Physiology* 1990; 259: H1079-H1085.
197. Mitchell P, Moyle J. Chemiosmotic hypothesis of oxidative phosphorylation. *Nature* 1967; 213: 137-139.
198. Miura T, Suzuki W, Ishihara E, Arai I, Ishida H, Seino Y, Tanigawa K. Impairment of insulin-stimulated GLUT4 translocation in skeletal muscle and adipose tissue in the Tsumura Suzuki obese diabetic mouse: a new

- genetic animal model of type 2 diabetes. *European Journal of Endocrinology* 2001; 145: 785-790.
199. Mocanu MM, Field DC, Yellon DM. A potential role for PTEN in the diabetic heart. *Cardiovascular Drugs and Therapy* 2006; 20: 319-321.
  200. Morris DI, Robbins JD, Ruoho AE, Sutkowski EM, Seamon KB. Forskolin photoaffinity labels with specificity for adenylyl cyclase and the glucose transporter. *Journal of Biological Chemistry* 1991; 266: 13377-13384.
  201. Morrow DA, Givertz MM. Modulation of myocardial energetics: emerging evidence for a therapeutic target in cardiovascular disease. *Circulation* 2005; 112: 3218-3221.
  202. Mueckler M, Weng W, Kruse M. Glutamine 161 of Glut1 glucose transporter is critical for transport activity and exofacial ligand binding. *Journal of Biological Chemistry* 1994; 269: 20533-20538.
  203. National Center of Health Statistics. Deaths and percentage of total death for the 10 leading causes of death: United States (2002-2003).
  204. Neitzel AS, Carley AN, Severson DL. Chylomicron and palmitate metabolism by perfused hearts from diabetic mice. *American Journal of Physiology Endocrinology and Metabolism* 2003; 284: E357-E365.
  205. Norton GR, Majane OH, Libhaber E, Maseko S, Libhaber C, Woodiwiss AJ. The relationship between blood pressure and left ventricular mass index depends on an excess adiposity. *Journal of Hypertension* 2009; 27: 1873-1883.
  206. Okada T, Kawano Y, Sakakibara R, Hazeki O, Ui M. Essential role of phosphatidylinositol 3-kinase in insulin-induced glucose transport and antilipolysis in rat adipocytes. Studies with a selective inhibitor wortmannin. *Journal of Biological Chemistry* 1994; 269: 3568-3573.
  207. Oudit GY, Kassiri Z, Zhou J, Liu QC, Liu PP, Backx PH et al. Loss of PTEN attenuates the development of pathological hypertrophy and heart failure in response to biomechanical stress. *Cardiovascular Research* 2008; 78(3): 505-514.

208. Oudit GY, Penninger JM. Cardiac regulation by phosphoinositide 3-kinases and PTEN. *Cardiovascular Research* 2009; 82: 250-260.
209. Oudit GY, Sun H, Kerfant BG, Crackower MA, Penninger JM, Backx PH. The role of phosphoinositide-3 kinase and PTEN in cardiovascular physiology and disease. *Journal of Molecular and Cellular Cardiology* 2004; 449-471.
210. Ozes ON, Mayo LD, Gustin JA, Pfeffer SR, Pfeffer LM, Donner DB. NF- $\kappa$ B activation by tumour necrosis factor requires the Akt serine-threonine kinase. *Nature* 1999; 401: 82-85.
211. Palmer JW, Tandler B, Hoppel CL. Biochemical properties of subsarcolemmal and interfibrillar mitochondria isolated from rat cardiac muscle. *Journal of Biological Chemistry* 1977; 252: 8731-8739.
212. Paradis S, Ailion M, Toker A, Thomas JH, Ruvkun G. A PDK 1 homolog is necessary and sufficient to transducer AGE-1 Pi3 kinase signals that regulate diapauses in *Caenorhabditis elegans*. *Genes and Development* 1999; 13: 1438-1452.
213. Paradis S, Ruvkun G. *Caenorhabditis elegans* Akt/PKB transduces insulin receptor-like signals from AGE-1 PI 3 kinase to the DAF-16 transcription factor. *Genes and Development* 1998; 12: 2488-2498.
214. Park SH, Gammon SR, Knippers JD, Paulsen SR, Rubink DS, Winder WW. Phosphorylation-activity relationships of AMPK and acetyl-CoA carboxylase in muscle. *Journal of Applied Physiology* 2002; 92: 2475-2482.
215. Patel S, Doble B, Woodgett JR. Glycogen synthase kinase-3 insulin and Wnt signaling: a double-edged sword? *Biochemical Society Transactions* 2004; 32: 803-808.
216. Pekarsky Y, Hallas C, Palamarchuk A, Koval A, Bullrich F, Hirata Y, Bichi R, Letofsky J, Croce CM. Akt phosphorylates and regulates the orphan nuclear receptor Nur77. *Proceedings of the National Academy of Sciences. U.S.A* 2001; 98: 3690-3694.



217. Pessin J, Saltiel A. Signaling pathways in insulin action: molecular targets of insulin resistance. *The Journal of Clinical Investigation* 2000; 106: 165-169.
218. Peyton RB, Jones RN, Attarian D, Sink JD, Van Trigt P, Currie WD, Wechsler AS. Depressed high-energy phosphate content in hypertrophied ventricles of animal and man: the biologic basis for increased sensitivity to ischemic injury. *Annals of Surgery* 1982; 196: 278-284.
219. Pickavance LC, Tadayyon M, Widdowson PS, Buckingham RE, Wilding JP. Therapeutic index for resoglitazone in dietary obese rats: separation of efficacy and haemodilution. *British Journal of Pharmacology* 1999; 128 (7): 1570-1576.
220. Ponticos M, Lu QL, Morgan JE, Hardie DG, Partridge TA, Carling D. Dual regulation of the AMP-activated protein kinase provides a novel mechanism for the control of creatine kinase in skeletal muscle. *EMBO Journal* 1998; 17: 1688-1699.
221. Poulliot M, Poulliot C, et al. Visceral obesity in men. *Diabetes* 1992; 41: 826-834.
222. Puigserver P, Wu Z, Park CW, Graves R, Wright M, Spiegelman BM. A cold-inducible coactivator of nuclear receptors linked to adaptive thermogenesis. *Cell* 1998; 92: 829-839.
223. Qatanani M, Lazar MA. Mechanisms of obesity-associated insulin resistance: many choices on the menu. *Genes and Development* 2007; 21: 1443-1455.
224. Quon MJ. Limitations of the fasting glucose to insulin ratio as an index of insulin sensitivity. *Journal of Clinical Endocrinology and Metabolism* 2001; 85: 4615-4617.
225. Randle P, Sugden P, Kerbey A, et al. Regulation of pyruvate oxidation and the conservation of glucose. *Biochemical Society Symposia* 1978; 43: 47-67.
226. Reaven G, Abbasi F, McLaughlin T. Obesity, insulin resistance, and cardiovascular disease. *The Endocrine Society* 2004; 59: 207-223.

227. Reaven GM. Pathophysiology of insulin resistance in human disease. *Physiology Review* 1995; 75: 473-486.
228. Reddy KS, Yusuf S. Emerging epidemic of cardio-vascular diseases in developing countries. *Circulation* 1998; 97: 569-601.
229. Rena G, Guo S, Cichy SC, Unterman TG, Cohen P. Phosphorylation of the transcription factor forkhead family member FKHR by protein kinase B. *Journal of Biological Chemistry* 1999; 274: 17179-17183.
230. Reszko AE, Kasumov T, Comte B, Pierce BA, David F, Bederman IR, Deutsch J, Des Rosiers C, Brunengraber H. Assay of the concentration and <sup>13</sup>C-isotopic enrichment of malonyl-coenzyme A by gas chromatography-mass spectrometry. *Analytical Biochemistry* 2001; 298: 69-75.
231. Richter C. Pro-oxidants and mitochondrial Ca<sup>2+</sup>: Their relationship to apoptosis and oncogenesis. *Letters of the Federation of American Societies for Experimental Biology* 1993; 325: 104-107.
232. Roche TE, Baker JC, Yan X, Hiromasa Y, Gong X, Peng T, Dong J, Turkan A, Kasten SA. Distinct regulatory properties of pyruvate dehydrogenase kinase and phosphatase isoforms. *Progress in Nucleic Acid Research and Molecular Biology* 2001; 70: 33-75.
233. Roduit R, Morin J, Masse F, Segall L, Roche E, Newgard CB, Assimacopoulos-Jeannet F, Prentki M. Glucose down-regulates the expression of the peroxisome proliferator-activated receptor- $\alpha$  gene in the pancreatic beta-cell. *Journal of Biological Chemistry* 2000; 275: 35799-35806.
234. Rossetti L, Smith D, Shulman GI, Papachristou D, DeFronzo RA. Correction of hyperglycemia with phlorizin normalizes tissue sensitivity to insulin in diabetic rats. *Journal of Clinical Investigation* 1987; 79: 1510-1515.
235. Rouslin W. Mitochondrial complexes I, II, III, IV and V in myocardial ischemia and autolysis. *American Journal of Physiology Heart Circulatory Physiology* 1983; 224: 743-748.

236. Russel RR 3<sup>rd</sup>, Bergeron R, Shulman GI, Young LH. Translocation of myocardial GLUT 4 and increased glucose uptake through activation of AMPK by AICAR. *American Journal of Physiology* 1999; 277: H643-H649.
237. Saddik M, Gamble J, Witters LA, Lopaschuk GD. Carnitine Palmitoyl Transferase I and the Control of  $\beta$ -Oxidation in Heart Mitochondria. *Biology and Chemistry* 1993; 268: 25836-25845.
238. Saddik M, Lopaschuk GD. Triacylglycerol turnover in isolated working hearts of acutely diabetic rats. *Canadian Journal of Physiology and Pharmacology* 1994; 72: 1110-1119.
239. Sakamoto J, Barr RL, Kavanagh KM, Lopaschuk GD. Contribution of malonyl-CoA decarboxylase to the high fatty acid oxidation rates seen in the diabetic heart. *American Journal of Physiology Heart and Circulatory Physiology* 2000; 278: H1196-H1204.
240. Saltiel AR, Kahn CR. Insulin signaling and the regulation of glucose and lipid metabolism. *Nature* 2001; 414: 799-806.
241. Sambandam N, Lopaschuk G.D. AMP-activated protein kinase (AMPK) control of fatty acid and glucose metabolism in the ischemic heart. *Progress in Lipid Research* 2003; 42: 238-256.
242. Sansal I, Sellers WR. The biology and clinical relevance of the PTEN tumor suppressor pathway. *Journal of Clinical Oncology* 2004; 22: 2954-2963.
243. Savagner F, Mirebeau D, Jacques C, Guyetant S, Morgan C, Franc B, Reynier P, Malthiery Y. PGC-1-related coactivator and targets are upregulated in thyroid oncocyoma. *Biochemical and Biophysical Research Communications* 2003; 310: 779-784.
244. Scarpulla RC. Nuclear activators and coactivators in mammalian mitochondrial biogenesis. *Biochimica et Biophysica Acta* 2002; 1576: 1-14.
245. Schreiber SN, Knutti D, Brogli K, Uhlmann T and Kralli A. The transcriptional coactivator PGC-1 regulates the expression and activity of the orphan nuclear receptor estrogen-related receptor  $\alpha$  (ERR $\alpha$ ). *Journal of Biological Chemistry* 2003; 278: 9013-9018.

246. Schultz BE, Chan SI. Structures and proton-pumping strategies of mitochondrial respiratory enzymes. *Annual Review of Biophysics and Biomolecular Structure* 2001; 30: 23-65.
247. Schummer CM, Werner U, Tennagels N, Schmoll D, Haschke G, Juretschke HP, Patel MS, Gerl M, Kramer W, Herling AW. Dysregulated pyruvate dehydrogenase complex in Zucker diabetic fatty rats. *American Journal of Physiology Endocrinology Metabolism* 2008; 294: E88-E96.
248. Shimizu H, Hupp TR. Intrasteric regulation of MDM2. *Trends in Biochemical Sciences* 2003; 28: 346-349.
249. Shiojima I, Walsh K. Regulation of cardiac growth and coronary angiogenesis by the Akt/PKB signaling pathway. *Genes and Development* 2006; 20: 3347-3365.
250. South African National Standard: The care and use of experimental animals standards SA. SANS 10386: 200X – latest version 2008.
251. Stanley WC, Lopaschuk GD, McCormack JG. Regulation of energy substrate metabolism in the diabetic heart. *Cardiovascular Research* 1997; 34: 25-33.
252. Stanley WC, Recchia FA, Lopaschuk GD. Myocardial substrate metabolism in the normal and failing heart. *Physiological Reviews* 2005; 85: 1093-1129.
253. Steinbeck K, Caterson ID, Turtle JR. The activity of the pyruvate dehydrogenase complex in heart muscle in the previously obese mouse model. *Bioscience Reports* 1986; 6: 1071-1075.
254. Stephens LR, Jackson TR, Hawkins PT. Agonist-stimulated synthesis of phosphatidylinositol (3,4,5)-triphosphate: a new intracellular signaling system? *Biochimica et Biophysica Acta* 1993; 1179: 27-75.
255. St-Pierre J et al. Bioenergetic analysis of peroxisome proliferator-activated  $\gamma$  coactivators 1 $\alpha$  and 1 $\beta$  (PGC-1  $\alpha$  and PGC-1 $\beta$ ) in muscle cells. *Journal of Biological Chemistry* 2003; 278: 26597-26603.
256. Stump CS, Short KR, Bigelow ML, Schmitz JM, Nair KS. Effect of insulin on human skeletal muscle mitochondrial ATP production, protein synthesis,

- and mRNA transcripts. The proceedings of the National Academy of Sciences U.S.A. 2003; 100: 7996-8001.
257. Sugden MC, Bulmer K, Holness MJ. Fuel-sensing mechanism integrating lipid and carbohydrate utilization. *Biochemical Society Transactions* 2001; 29: 272-278.
258. Sugden MC, Langdown ML, Harris RA, Holness MJ. Expression and regulation of pyruvate dehydrogenase kinase isoforms in the developing rat heart and in adulthood: role of thyroid hormone status and lipid supply. *Biochemistry Journal* 2000; 352: 731-738.
259. Sugden MC, Orfali KA, Holness MJ. The pyruvate dehydrogenase complex: nutrient control and the pathogenesis of insulin resistance. *The Journal of Nutrition* 1995: 1746S-1752S.
260. Sugden PH, Clerk A. Cellular mechanisms of cardiac hypertrophy. *Journal of Molecular Medicine* 1998; 76: 725-746.
261. Suwa M, Nakano H, Kumagai S. Effects of chronic AICAR treatment on fiber composition, enzyme activity, UCP3, and PGC-1 in rat muscles. *Journal of Applied Physiology* 2003; 95: 960-968.
262. Tahiliani AG, McNeil JH. Effects of insulin perfusion and altered glucose concentrations on heart function in 3-day and 6-week diabetic rats. *Canadian Journal of Physiology and Pharmacology* 1986; 64: 188-192.
263. Tchernof A, Lamarchi B, Prud'homme A. The dense LDL phenotype: association with plasma lipoprotein levels, visceral obesity, and hyperinsulinemia in men. *Diabetes Care* 1996; 19: 629-637.
264. Terada S, Goto M, Kato M, Kawanaka K, Shimokawa T, Tabata I. Effects of low-intensity prolonged exercise on PGC-1 mRNA expression in rat epitrochlearis muscle. *Biochemical and Biophysical Research Communications* 2002; 296: 350-354.
265. Tian Q, Barger P. Deranged energy substrate metabolism in the failing heart. *Current Science Incorporated* 2006; 8: 465-471.
266. Toker A, Cantley LC. Signalling through the lipid products of phosphoinositide-3-OH kinase. *Nature* 1997; 387: 673-676.

267. Trencia A, Perfetti A, Cassese A, Vigliotta G, Miele C, Oriente F, Santopietro S, Giacco F, Condorelli G, Formisano P, Beguinot F. Protein kinase B/Akt binds and phosphorylates PED/PEA-15, stabilizing its antiapoptotic action. *Molecular and Cellular Biology* 2003; 23: 4511-4521.
268. Uldry M, Ibberson M, Hosokawa M, Thorens B. GLUT 2 is a high affinity glucosamine transporter. *FEBS Letters* 2002; 524: 199-203.
269. Uldry M, Thorens B. The SLC2 family of facilitated hexose and polyol transporters. *Pflugers Archive – European Journal of Physiology* 2004;447: 480-489.
270. Unger RH, Orci L. Diseases of liporegulation: new perspective on obesity and related disorders. *Journal of the Federation of American Societies for Experimental Biology* 2001; 15: 312-332.
271. Ussher JR, Lopaschuk GD. Metabolic profile in heart disease. *Heart and Metabolism* 2006; 32: 36-38.
272. Vague J. The degree of masculine differentiation of obesities: a factor determining predisposition to diabetes, atherosclerosis, gout, and uric calculous disease. *American Journal of Clinical Nutrition* 1956; 4: 20-34.
273. Van den Brom C, Huisman M, Vlasblom R, Boontje N, Duijst S, Lubberink M, Molthoff C, Lammertsma A, van der Velden J, Boer C, Ouwens D, Diamant M. Altered myocardial substrate metabolism is associated with myocardial dysfunction in early diabetic cardiomyopathy in rats: studies using positron emission tomography. *Cardiovascular Diabetology* 2009; 8: 1-12.
274. Van der Vusse GJ, Glatz JF, Stam HC, Reneman RS. Fatty acid homeostasis in the normoxic and ischemic heart. *Physiology Review* 1992; 72: 881-940.
275. Vega RB, Huss JM, Kelly DP. The coactivator PGC-1 cooperates with peroxisome proliferator-activated receptor  $\alpha$  in transcriptional control of nuclear genes encoding mitochondrial fatty acid oxidation enzymes. *Molecular and Cellular Biology* 2000; 20: 1868-1876.

276. Victor T, Jordaan AM, Bester AJ, Lochner A. A sensitive and rapid method for separating adenine nucleotides and creatine phosphate by ion-pair reversed-phase high-performance liquid chromatography. *Journal of Chromatography* 1987; 389: 339-344.
277. Virbasius CA, Virbasius JV, Scarpulla RC. NRF-1, an activator involved in nuclear-mitochondrial interactions, utilizes a new DNA-binding domain conserved in a family of developmental regulators. *Genes Dev* 1993; 7: 2431-2445.
278. Wall ST, Lopaschuk GD. Glucose oxidation rates in fatty acid perfused isolated working hearts from diabetic rat. *Biochimica et Biophysica Acta* 1989; 1006: 97-103.
279. Wallhaus TR, Taylor M, DeGrado TR, Russell DC, Stanko P, Nickles RJ & Stone CK. Myocardial free fatty acid and glucose used after carvedilol treatment in patients with congestive heart failure. *Circulation* 2001; 103: 2441-2446.
280. Wang H, Hiatt WR, Barstow TJ, Brass EP. Relationships between muscle mitochondrial DNA content, mitochondrial enzyme activity and oxidative capacity in man: alteration with disease. *European Journal of Applied Physiological and Occupational Physiology* 1999; 80: 22-27.
281. Waselle L, Gerona R, Vitale N, Martin T, Bader M, Regazzi R. Role of phosphoinositide signaling in the control of insulin exocytosis. *Molecular Endocrinology* 2005; 19: 3097-3106.
282. Watson R, Pessin J. Intracellular organization of insulin signaling and GLUT4 translocation. *Recent Progress in Hormone Research* 2001; 56: 175-194.
283. Welsh GI, Proud CG. Glycogen synthase kinase-3 is rapidly inactivated in response to insulin and phosphorylates eukaryotic initiation factor eIF-2B. *Biochemistry Journal* 1993; 294: 625-629.
284. WHO. World Health Report (2002).

285. Wilfinger WW, Mackey M, Chomczynski P. Effect of pH and ionic strength on the spectrophotometric assessment of nucleic acid purity. *Bio Techniques* 1997; 22: 474.
286. Woldegiorgis G, Shi J, Zhu H, Arvidson DN. Functional characterization of mammalian mitochondrial carnitine palmitoyltransferases I and II expressed in the yeast *Pichia pastoris*. *American Society for Nutritional Sciences* 2000: 310S-314S.
287. Wolfe RR, Jahoor F. Recovery of labeled CO<sub>2</sub> during the infusion of C-1- vs C-2-labeled acetate: implications for tracer studies of substrate oxidation. *American Journal of Clinical Nutrition* 1990; 51: 248-252.
288. Wolfrum C, Besser D, Luca E, Stoffel M. Insulin regulates the activity of forkhead transcription factor Hnf-3 $\beta$ /Foxa-2 by Akt-mediated phosphorylation and nuclear/cytosolic localization. *Proceedings of the National Academy of Sciences. U.S.A* 2003; 100: 11624-11629.
289. Woods A, Johnstone SR, Dickerson K, Leiper FC, Fryer LG, Neumann D, Schlattner U, Wallimann T, Carlson M, Carling D. LKB1 is the upstream kinase in the AMP-activated protein kinase cascade. *Current Biology* 2003; 13: 2004-2008.
290. Wu A, Boss O. Targeting PGC-1  $\alpha$  to control energy homeostasis. *Expert Opinion on Therapeutic Targets* 2007; 11: 1329-1338.
291. Wu H, Kanatous SB, Thurmond FA, Gallardo T, Isotani E, Bassel-Duby R, Williams RS. Regulation of mitochondrial biogenesis in skeletal muscle by CaMK. *Science* 2002; 296: 349-352.
292. Wu P, Inskeep K, Bowker-Kinley M, et al. Mechanism responsible for inactivation of skeletal muscle pyruvate dehydrogenase complex in starvation and diabetes. *Diabetes* 1999; 48: 1593-1599. (a)
293. Wu P, Sato J, Zhao Y, Jaskiewicz J, Popov KM, Harris RA. Starvation and diabetes increase the amount of pyruvate dehydrogenase kinase isoenzyme 4 in rat heart. *Biochemistry Journal* 1998; 329: 197-201.



294. Wu Z, Puigserver P, Andersson U, Zhang C, Adelmant G, et al. Mechanisms controlling mitochondrial biogenesis and respiration through the thermogenic coactivator PGC-1. *Cell* 1999; 98: 115-124. (b)
295. Yao M, Keogh A, Spratt P, dos Remedios CG, KieBling PC. Elevated Dnase I levels in human idiopathic dilated Cardiomyopathy: An indicator of apoptosis? *Journal of Molecular and Cellular Cardiology* 1996; 28: 95-101.
296. Yellon DM, Baxter GF. Reperfusion injury revisited: is there a role for growth factor signaling in limiting lethal reperfusion injury? *Trends Cardiovascular Medicine* 1999 9: 245-249.
297. Young ME, Goodwin GW, Ying J, Guthrie P, Wilson CR, Laws FA, Taegtmeyer H. Regulation of cardiac and skeletal muscle malonyl-CoA decarboxylase by fatty acids. *American Journal of Physiology Heart and Circulatory Physiology* 2001; 280: E471-479.
298. Young ME, Patil S, Ying J, et al. Uncoupling protein 3 transcription is regulated by peroxisome proliferator-activated receptor (alpha) in the adult rodent heart. *Federation of American Societies for Experimental Biology Journal* 2001; 15: 833-845.
299. Zhao Z-P, Nakamura M, Wang N-P et al. Reperfusion induces myocardial apoptotic cell death. *Cardiovascular Research* (2000) 45: 651-660.
300. Zhou BP, Liao Y, Xia W, Spohn B, Lee MH, Hung MC. Cytoplasmic localization of p21Cip1/WAF1 by Akt-induced phosphorylation in HER-2/neu-overexpressing cells. *Nature and Cellular Biology* 2001; 3: 245-252.
301. Zhou L, Salem JE, Saidel GM, Stanley WC, Cabrera ME. Mechanistic model of cardiac energy metabolism predicts localization of glycolysis to cytosolic subdomain during ischemia. *American Journal of Physiology Heart and Circulatory Physiology* 2005; 288: H2400-H2411.
302. Zhu H, Shi J, de Vries Y, Arvidson DN, Cregg JM, Woldegiorgis G. Functional studies of yeast expressed human heart muscle carnitine palmitoyltransferase I. *Archives of Biochemistry and Biophysics* 1997; 347: 53-61.